CONVENTIONAL AND PROBABILISTIC SEISMIC SAFETY ANALYSIS OF RIGID RETAINING WALLS

by

D.A. Grivas and V.J. Vlavianos

Report No. CE-82-7

Department of Civil Engineering
Rensselaer Polytechnic Institute
Troy, New York 12181

Sponsored by the Earthquake Hazard Mitigation Program of the National Science Foundation under Grant No. PFR-7905500

July 1982

TABLE OF CONTENTS

Page

LIST OF TABLES

LIST OF FIGURES

Page

LIST OF SYMBOLS

English Characters

a_h	Horizontal ground acceleration
a_v	Vertical component of the maximum ground acceleration
B	Width of the base of retaining wall
b	Width of the top of retaining wall
b_i	Regional parameters entering the expression for the attenuation of the maximum horizontal acceleration
C	Capacity of a structure (Resistance)
c	Cohesion (random variable)
D	Demand on a structure (Loading)
D_f	Depth of embedment of a retaining wall
e	Eccentricity of the load on the base of a retaining wall
f( )	Probability density function of the quantity in parenthesis
F( )	Cumulative distribution of the quantity in parenthesis
FS	Factor of safety
g	Acceleration of gravity
H	Height of the retaining wall
h_A	Distance from bottom of retaining wall to the point of application of the total force
i	Slope of ground surface behind the wall
k	Constant
K_A	Active earth pressure coefficient
K_{AE}	Active earth pressure coefficient (under seismic conditions)
k_P	Passive earth pressure coefficient
ℓ	Length

m	Earthquake magnitude (random variable)
m_0	Lower limit of earthquake magnitude
m_1	Upper limit of earthquake magnitude
n	Number of earthquakes
n_m	Number of earthquakes with a magnitude larger than m
N_γ, N_q, N_c	Bearing capacity factors
p	Probability
P_A	Active force on retaining wall
P_P	Passive force on retaining wall
p_f	Probability of failure
P[ ]	Probability of the event in brackets
$p(z)$	Pressure in a depth z from the top of retaining wall
R	Reliability of retaining wall
SM	Safety margin
Var( )	Variance of the random variable in parenthesis
z	Depth from top of retaining wall

Greek Characters

β	Angle between the back side of a retaining wall and the vertical direction
γ	Unit weight of the soil material
γ_c	Unit weight of concrete
δ	Angle of friction between a wall and the backfill material
θ	Angle between failure surface and horizontal
λ	Mean earthquake occurrence rate
ρ	Correlation coefficient
σ	Standard deviation of a random variable

ϕ Angle of internal friction of a soil material (random variable)

$\psi(z)$ Angle between the failure plane passing through a point of depth z and the horizontal direction (in Dubrova's method)

PREFACE

This is the first in a series of reports on the research project entitled "Reliability of Soil Retaining Structures during Earthquakes". This study is sponsored by the Earthquake Hazard Mitigation Program of the National Science Foundation under Grant No. PFR-7905500, and is directed jointly by Dr. Dimitri A. Grivas, Associate Professor of Civil Engineering, Rensselaer Polytechnic Institute, and Dr. Milton E. Harr, Professor of Civil Engineering, Purdue University. Drs. Ralph B. Peck and Neville C. Donovan serve as advisors to the project of which Dr. Michael Gaus is the Earthquake Hazard Mitigation Program Manager.

The authors are thankful to the National Science Foundation for sponsoring this research. Special thanks are also extended to Mrs. Diana Rogers and Mrs. Jo Ann Grega for their typing of this report.

ABSTRACT

The two main objectives of the present study are (a) to review and compare through a case study currently available methods for the analysis of earth retaining structures, and (b) to provide an alternative, probabilistic approach to the assessment of the safety of such structures when subjected to a seismic loading. The latter objective is achieved through a quasi-static stability analysis that accounts for the movement experienced by the wall during loading. The resulting distribution of the lateral pressure along the structure is parabolic-like (rather than the customarily assumed linear variation) and, thus, it is in closer agreement with experimental and field observations. Four modes of possible failure are considered in the analysis (i.e., overturning, base sliding, bearing capacity of the foundation and overall sliding) and the probability of failure in each mode is determined.

The examined conventional methods and the new probabilistic approach are applied in a case study involving the safety of a gravity wall during an earthquake and the obtained results are presented and discussed. It is concluded that the provided probabilistic analysis is an improved alternative to conventional procedures because it accounts for the uncertainties associated with important material and seismic parameters while, at the same time, it takes into consideration the movement experienced by the wall during the ground shaking.

CHAPTER 1

INTRODUCTION

Damage of earth retaining structures, resulting from movements and increased lateral pressures induced by earthquakes, is a common phenomenon. As a consequence, special efforts must be undertaken by geotechnical engineers in order to describe the loading conditions and secure the safe design of such structures when subjected to a seismic environment.

Historically, the earliest method of determining the seismic effect on the force acting on a retaining wall was developed by Okabe (1926) and Mononobe (1929). This method, commonly referred to as the Mononobe-Okabe procedure, is basically the Coulomb sliding wedge approach in which two additional forces are included: the horizontal and vertical components of the seismic inertia of the backfill material. A simplified version of the Mononobe-Okabe procedure was proposed by Seed (Seed, 1969; Seed and Whitman, 1970), while Prakash and Basavanna (1969) attempted to improve upon the procedure through an analysis that would satisfy the additional condition of equilibrium of moments on the sliding wedge.

In the Mononobe-Okabe procedure, the movement of a retaining wall is not considered as a factor with an explicit influence on the pressure distribution along the wall. This is in contrast to an earlier recognition (Meem, 1910) that, for example, the difference between the earth pressures along rigid and flexible walls is a function of the difference in the movements that occur along these two types of structures.

Terzaghi (1936) interpreted lateral earth pressure measurements in terms of the associated deformations while Ohde (1938) attempted a mathematical formulation of the relationship between the two quantities.

A simple, analytical procedure for the determination of the pressure distribution along retaining walls that is also capable of accounting for the wall movement was proposed by Dubrova (1963). Although it was initially developed for static conditions, the Dubrova method was easily extended to provide the analytical expression for pressure distributions that result from the occurences of earthquakes (e.g., Saran and Prakash, 1977).

1.1 Scope of the Present Study

In all the above methods, the safety of retaining walls during earthquakes is measured in terms of the customary factor of safety. In order to overcome the shortcomings associated with this measure of safety (e.g., A-Grivas, 1977, etc.) and, also, to account for the uncertainties that are involved in material parameters, loading conditions, analytical procedures, etc., geotechnical engineers have suggested the use of a more rational approach to design, i.e., one based on probability theory and reliability analysis (e.g., Wu et. al., 1970; Hoeg and Murarka, 1974; Vanmarcke, 1977; Harr, 1977, etc.). It is the objective of this endeavor to provide such an approach to the analysis and design of soil retaining structures during earthquakes.

A detailed presentation of the procedures capable of determining the active earth pressures against retaining walls under static and seismic conditions is given in Chapter 2. Chapter 3 presents a probabilistic description of the seismic loading while the reliability analysis of retaining walls is given in Chapter 4. The conventional and probabilistic approaches are applied in a case study, a detailed description of which is given in Chapter 5. Finally, Chapter 6 presents the results of a parametric study which explores the effect of important material and loading parameters on the pressure distribution along retaining walls and the corresponding safety measure.

CHAPTER 2

REVIEW OF AVAILABLE PROCEDURES

In this chapter, a review is presented of the procedures currently available for the determination of the pressure system behind earth retaining structures and of the associated safety measures.

2.1 Procedures Used Under Static Conditions

2.1.1 The Coulomb Method. The Coulomb method (Coulomb, 1773) is based on the notion that failure of a retaining wall is accompanied by a sliding of the soil mass located behind the wall.

The soil sliding is assumed to occur along a plane surface and the expression for the thrust on the wall is obtained by considering the equilibrium of the forces acting on the sliding soil mass.

In Fig. 2.1a is shown schematically a Coulomb type trial wedge that consists of cohensionless soil with horizontal free surface and is in contact with a vertical retaining wall. If, for the moment, the shearing forces at the back of the wall are assumed to be zero and the possibility of cracking in the tension zone is ignored, then the force system on the wedge consists of its weight W; the force P between the wedge and the wall; and the force F along the sliding surface (with normal component N and shearing component T). This is shown in Fig. 2.1a while the polygon of forces appears in Fig. 2.1.b.

The weight W of the wedge is known in both magnitude and direction. The resultant forces P and F have known directions but unknown magnitudes. The equations of equilibrium along the vertical and

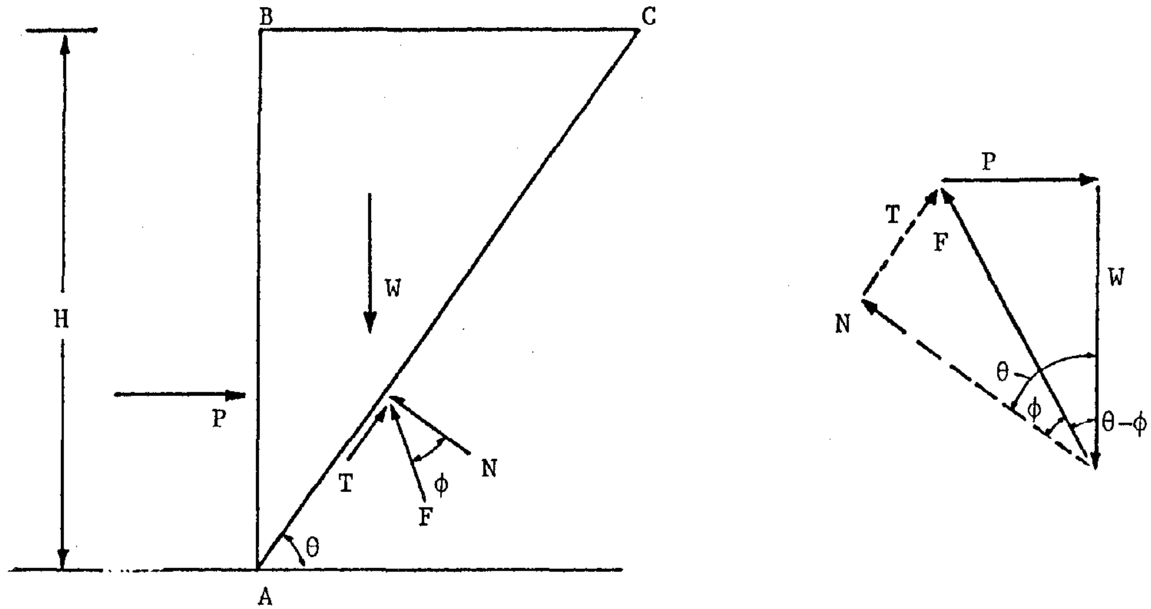

(a) Trial Wedge

(b) Polygon of Forces

Figure 2.1 Equilibrium of Forces on a Trial Wedge for Simple Retaining Wall (active case) horizontal direction produce the following expressions for P and F, respectively:

$$\Sigma H = 0 \quad : \quad P = W \tan(\theta-\phi)$$
$$\Sigma V = 0 \quad : \quad F = \frac{W}{\cos(\theta-\phi)} \tag{2-1}$$

Replacing in the first of the expressions above the weight W by its equal $(1/2)\gamma H\cot\theta$, where γ is the unit weight of the material, H is the height of the wall and θ is the inclination with respect to the horizontal of the sliding surface, one has

$$P = \frac{1}{2}\gamma H^2 \cot\theta \tan(\theta-\phi)$$

In order to determine the critical value θ_{cr} of θ that produces the maximum value of the thrust P, one has to consider the derivative of P with respect to θ; i.e.,

$$\frac{\partial P}{\partial \theta} = \frac{1}{2}\gamma H^2 \frac{\sin\phi \cos(2\theta-\phi)}{[\sin\theta \cos(\theta-\phi)]^2} \tag{2-2}$$

The derivative $\frac{\partial P}{\partial \theta}$ becomes zero when $\cos(2\theta_{cr}-\phi) = 0$, or $2\theta_{cr}-\phi = 90°$, or $\theta_{cr} = 45° + \frac{\phi}{2}$. The corresponding value for the thrust, i.e. the active force P_A on the wall, is expressed as

$$P_A = \frac{1}{2}\gamma H^2 K_A \tag{2-3}$$

in which

$$K_A = \left[\frac{1}{(1/\cos\phi) + (\tan^2\phi + \tan\phi)^{1/2}}\right]^2$$

The minimum value of the thrust, i.e., the passive force P_p on the wall, is expressed as

$$P_P = \frac{1}{2}\gamma H^2 K_P \qquad (2\text{-}4)$$

in which

$$K_P = \left[\frac{1}{(1/\cos\phi) - \{\tan^2\phi + (\tan\phi)\}^{1/2}}\right]^2$$

The above expressions can be found similarly for the general case where the backfill forms an angle i with the horizontal and there exists a friction angle δ between wall and soil. These conditions are illustrated in Fig. 2.2. Thus, one has

$$P_{A/P} = \frac{1}{2}\gamma H^2 K_{A/P} \qquad (2\text{-}5)$$

in which

$$K_{A/P} = \left[\frac{\csc\beta \sin(\beta-\phi)}{\{\sin(\beta+\delta)\}^{1/2} \pm \{\sin(\phi+\delta) \sin(\phi-i)/\sin(\beta-i)\}^{1/2}}\right]^2$$

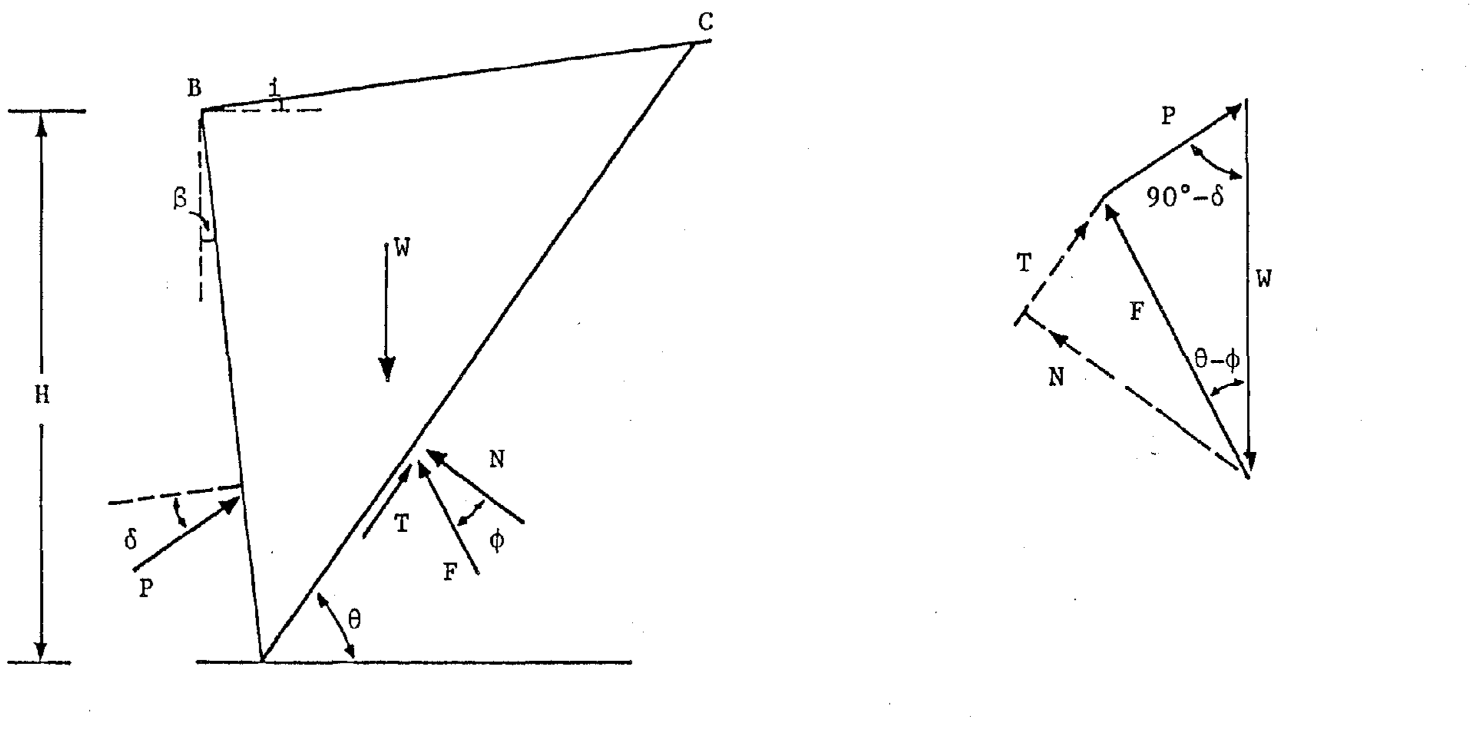

(a) Trial Wedge

(b) Polygon of Forces

Figure 2.2 Equilibrium of Forces on a Trial Wedge for Simple Retaining Wall (active case) where the positive sign in the denominator of the above expression corresponds to the active and the negative to the passive case.

2.1.2 The Dubrova Method. Coulomb provided no analytical basis for the distribution of earth pressure against a wall. He simply assumed the pressure distributions to be quasi-hydrostatic and considered the resultant earth force to act at a distance above the base of the wall equal to one third of its height. Results, however, of large-scale model tests by Terzaghi (1943) and Tschebotarioff (1951) have demonstrated the validity of this distribution for very rigid retaining walls with sand backfills. For other modes of motion, such as a rotation about the top or center of a wall or translational movements, test results indicate a parabolic-like distribution of pressures.

A procedure that appears to have considerable merit for determining the pressure distribution behind retaining walls is the one proposed by Dubrova (1963). This is based on the method of redistribution of pressure and is illustrated in Fig. 2.3.

For the wall movement shown in Fig. 2.3, Dubrova assumed that force F, acting on the failure plane passing through the bottom of the wall, is inclined at an angle $+\phi$ to the normal; while the angle between force F and the normal to the failure plane passing through the top of the wall is equal to $-\phi$. The wall may rotate around any point 'O' along its height and, therefore, distance h_1 (Fig. 2.3) can receive any value between 0 and H. Dubrova further assumed that the angle between the force and the normal to any failure line, denoted by ψ, is linearly distributed over the depth receiving values between $-\phi$ and $+\phi$.

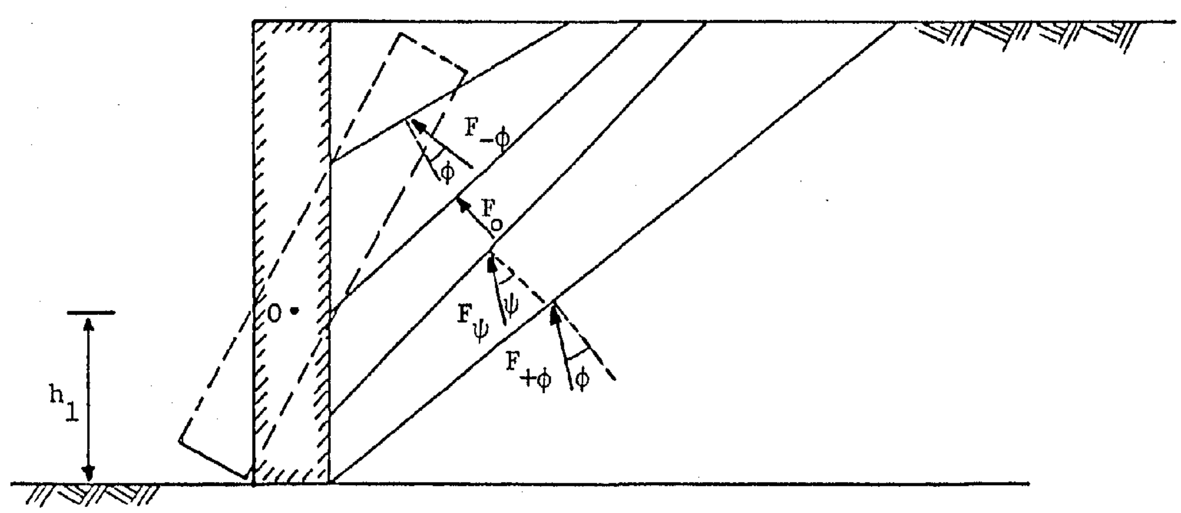

Figure 2.3 Variation of ψ-parameter along the wall in the Dubrova Method

Thus, for example, in the case of a wall rotating around its mid-point, ψ is equal to

$$\psi = \psi(z) = 2\phi \frac{z}{H} - \phi \qquad (2\text{-}6)$$

in which

z is the particular value of the depth,

H is the height of the wall, and

ϕ is the strength parameter of the backfill material.

The corresponding value of the force P at any depth z along the wall has an expression similar to that provided by Coulomb, the only difference being that ϕ is replaced by ψ and H by z. That is,

$$P = \frac{1}{2}\gamma \left[\frac{z\cos\psi}{(\cos\delta)^{1/2} + \{\sin(\psi+\delta)\sin\psi\}^{1/2}}\right]^2 \qquad (2\text{-}7)$$

or,

$$P = \frac{\gamma}{2\cos\delta}\left[\frac{z}{(1/\cos\psi) + \{\tan\psi(\tan\psi + \tan\delta)\}^{1/2}}\right]^2 \qquad (2\text{-}8)$$

In Table 2.1 are given the expressions for $\psi = \psi(z)$ for various points of rotation along the height of the wall.

The corresponding pressure distributions are shown in Fig. 2.4.

Table 2.1 Expressions of Function $\psi = \psi(z)$ for Various Points of Rotation of a Retaining Wall.

Case	Point of Rotation	$\psi = \psi(z)$
a	Top (outwards)	$\psi = \frac{\phi z}{H}$
b	Top (inwards)	$\psi = -\frac{\phi z}{H}$
c	Toe (outwards)	$\psi = \phi - \frac{\phi z}{H}$
d	Toe (inwards)	$\psi = \frac{\phi z}{H} - \phi$
e	Center (upper half inwards)	$\psi = \frac{2\phi z}{H} - \phi$

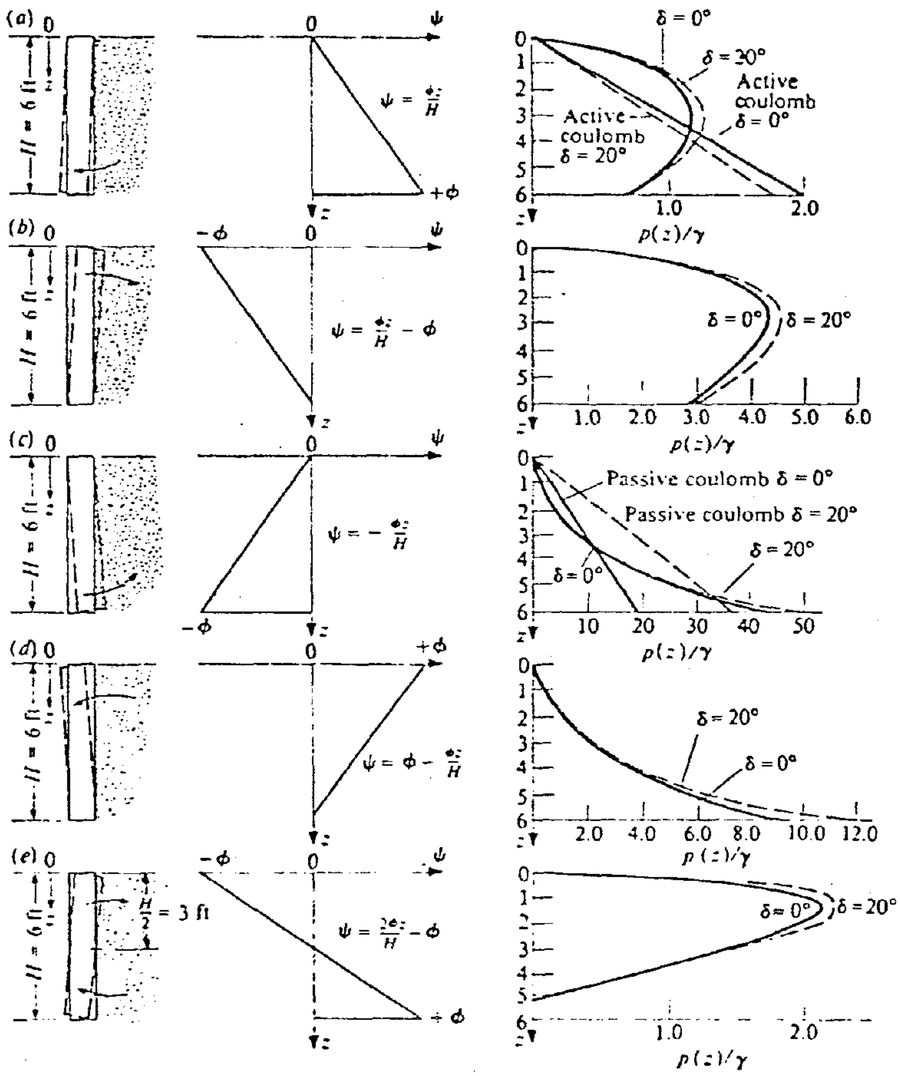

Figure 2.4 Examples of Pressure Distribution for Various Centers of Rotation of a Retaining Wall (after Harr, 1977)

The Dubrova method has been verified by Scott et al. (1972), on the basis of results obtained through field measurements. These are shown in Figs. 2.5, 2.6 and 2.7. Following Scott et al. (1972), the expression for the horizontal component of the active force P_A on the wall is given as

$$P_A = \frac{\gamma}{2} \left[\frac{z}{(1/\cos\psi) + (\tan^2\psi + \tan\psi \tan\delta)^{1/2}} \right]^2 \qquad (2\text{-}9)$$

2.2 Procedures Used Under Seismic Conditions

2.2.1 The Mononobe-Okabe Method. The earliest procedure that aimed to describe the lateral pressures on earth retaining structures under seismic conditions was proposed by Okabe (1926) and Mononobe (1929). Applicable only for the case of backfills consisting of dry cohesionless soils, the Mononobe-Okabe procedure was based on the following additional assumptions (Seed and Whitman, 1970):

(1) The wall yields sufficiently during an earthquake to produce minimum active pressures.

(2) When the minimum active pressure is attained, a soil wedge behind the wall is at the point of incipient failure and the maximum shear strength is mobilized along the potential sliding surface.

(3) The backfill behaves as a rigid body and therefore, the acceleration field is uniform throughout the soil mass.

The effect of the ground motion on the wall-backfill system is introduced in this procedure in terms of two additional inertia forces acting at the center of gravity of the sliding soil mass: a horizontal force,

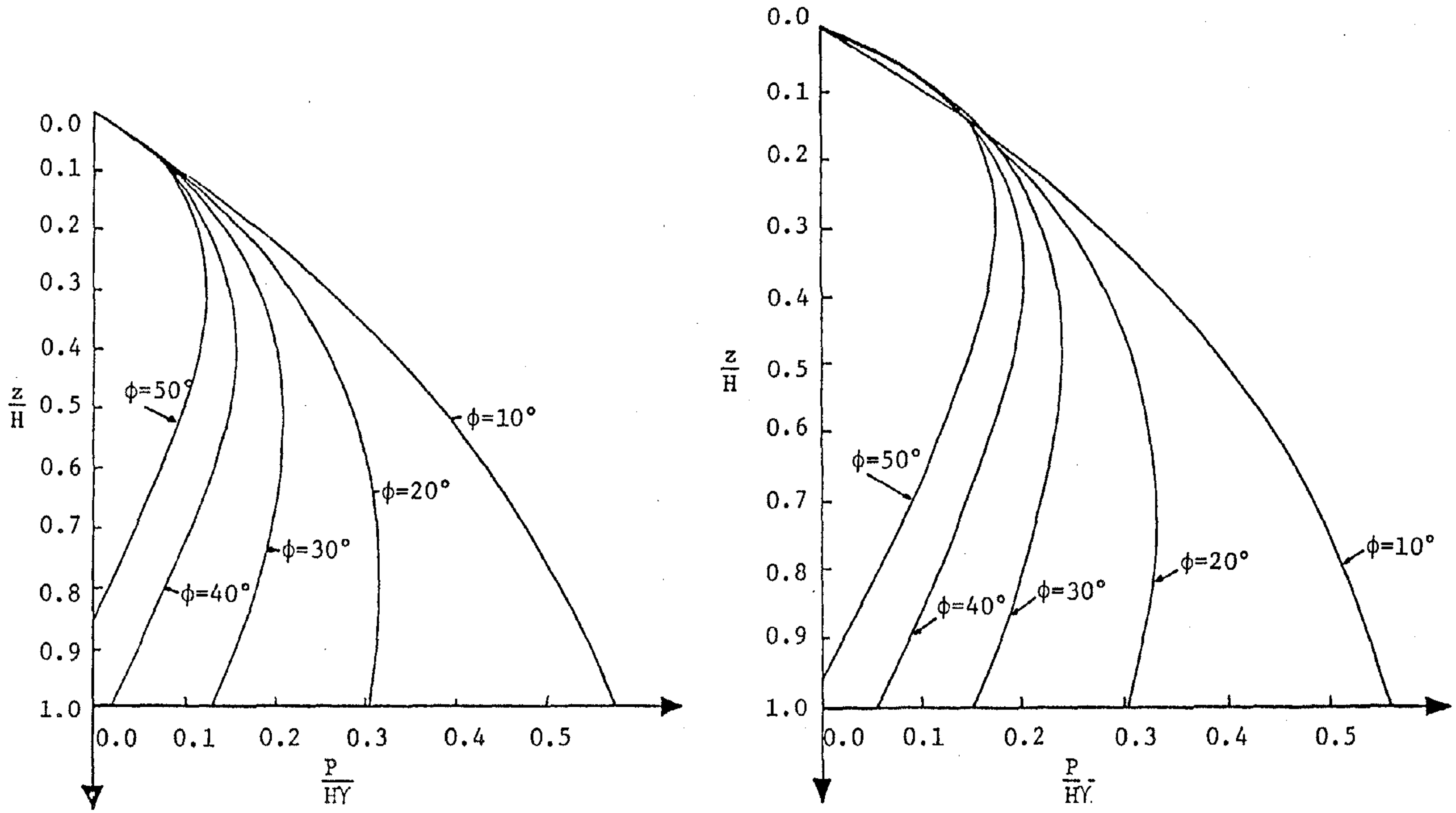

(a) wall rotating about top

(b) wall rotating about H/4

Figure 2.5 Pressure Distributions along a Wall for Various Centers of Rotation

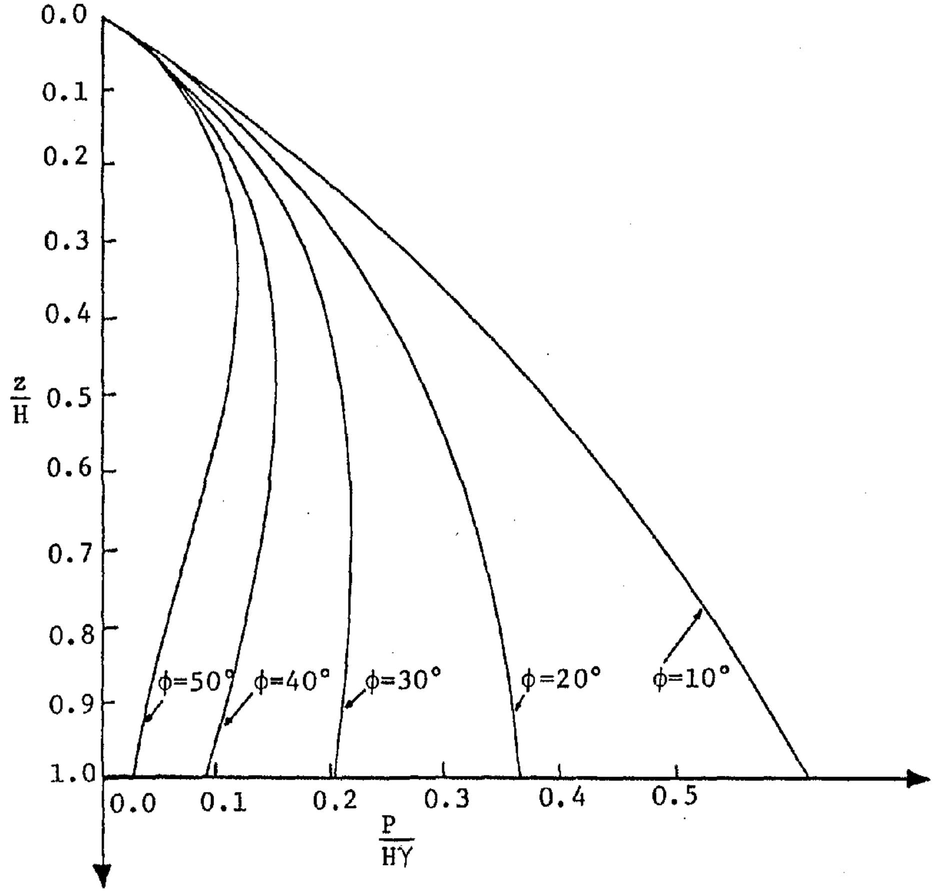

Figure 2.6 Pressure Distribution along a Wall Rotating about H/4 and Moving out Laterally

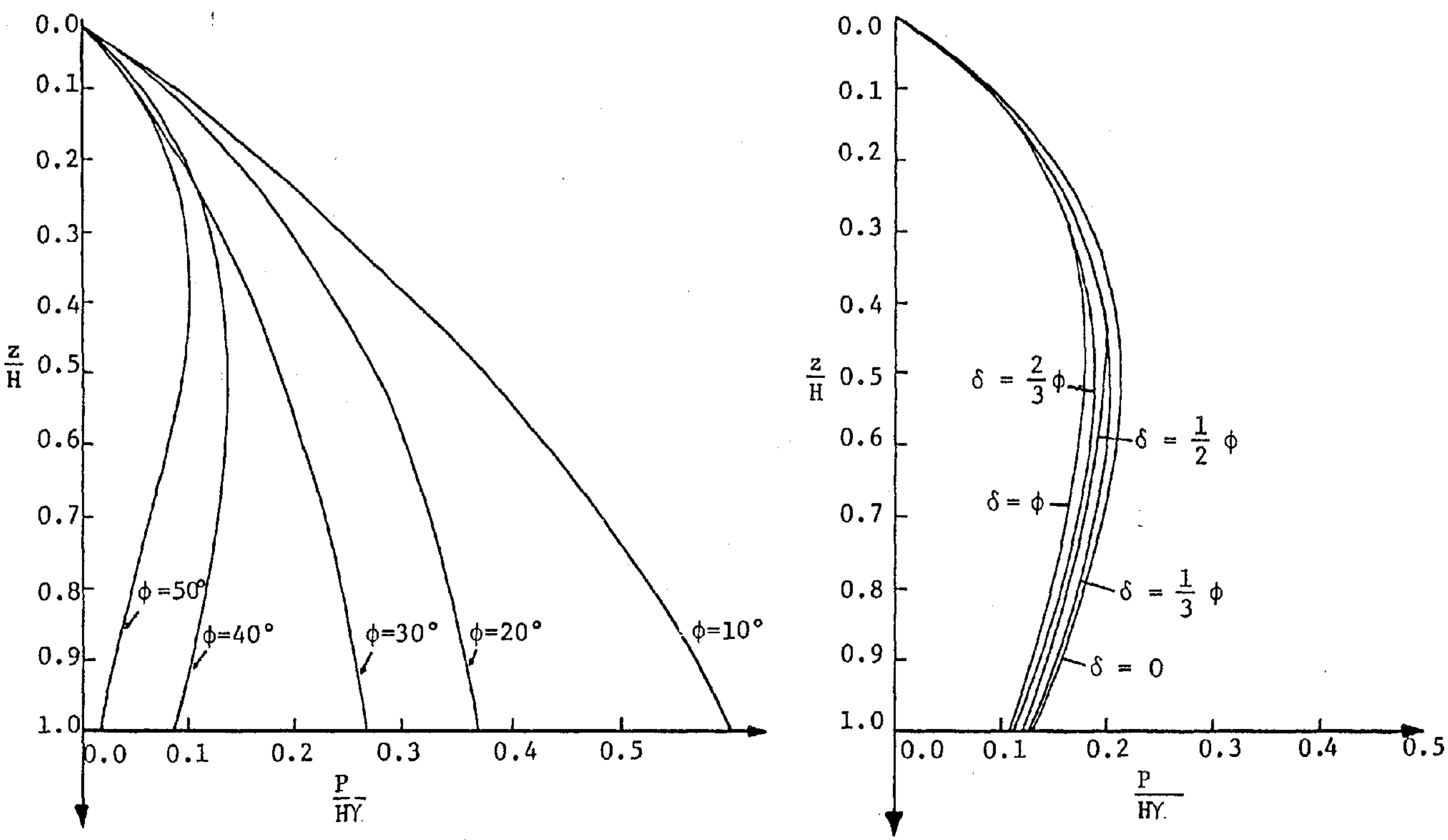

(a) Wall rotating about top and moving out laterally

(b) Wall rotating about top

Figure 2.7 Pressure Distribution Along a Wall for Various Centers of Rotation denoted as $k_h W$, and a vertical force, denoted as $k_v W$, where W is the weight of the sliding soil mass. Quantities k_h and k_v are the horizontal and vertical earth pressure coefficients, respectively. This is shown schematically in Fig. 2.8.

The active force P_{AE} on a wall during an earthquake is determined using Coulomb's method in which the additional forces $k_h W$ and $k_v W$ are considered. The critical sliding surface is also that of the Coulomb method. The expression for the active force against the wall is given as (Seed and Whitman, 1970)

$$P_{AE} = \frac{1}{2}\gamma H^2 (1-k_v) K_{AE} \qquad (2\text{-}10)$$

in which K_{AE} is the earth pressure coefficient for the active case and is equal to

$$K_{AE} = \frac{\cos^2(\phi-\theta-\beta)}{\cos\theta \cos^2\beta \cos(\delta+\beta+\theta)\left[1 + \left\{\frac{\sin(\phi+\delta)\sin(\phi-\theta-i)}{\cos(\delta+\beta+\theta)\cos(i-\beta)}\right\}^{1/2}\right]^2}$$

and

$\theta = \tan^{-1}\left(\frac{k_h}{1-k_v}\right)$,

γ = the unit weight of soil,

H = the height of the retaining structure,

ϕ = the angle of internal friction of the soil mass,

δ = the angle of wall-soil friction,

i = the inclination of the backfill,

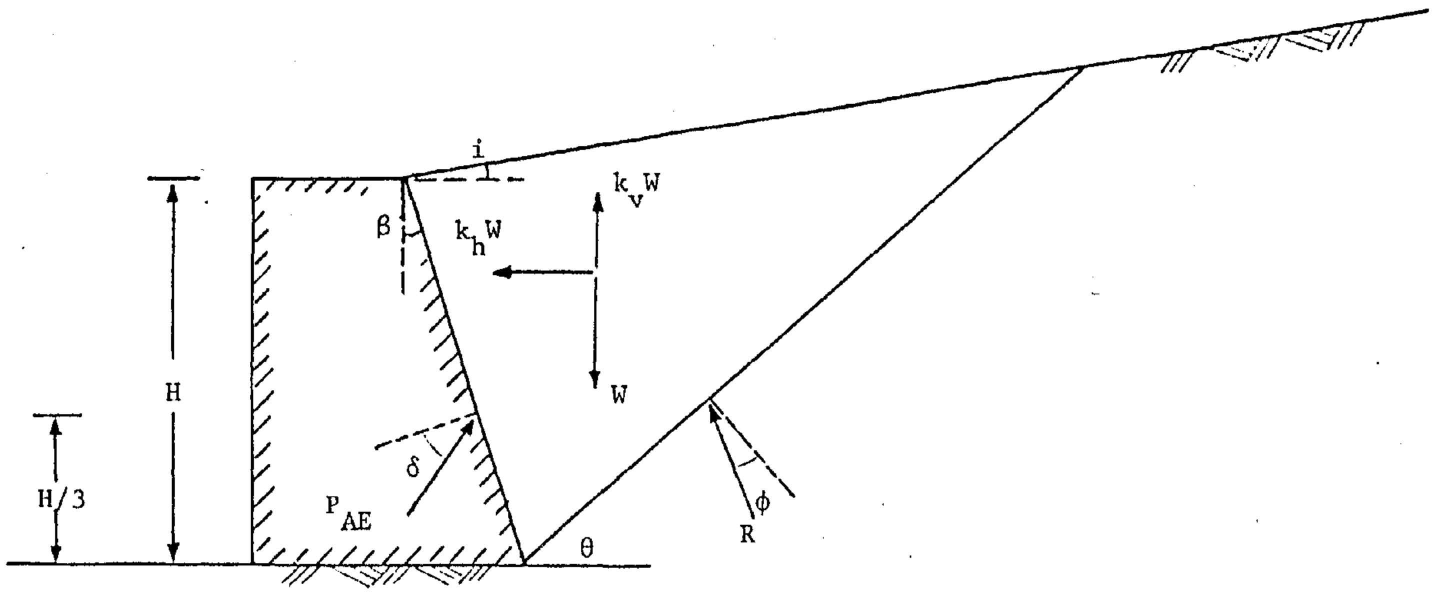

Figure 2.8 The Force System on the Sliding Soil Mass in Accordance with the Mononobe-Okabe Method.

β = the angle between the back side of wall and the vertical,

k_h = coefficient of horizontal ground acceleration in g's, and

k_v = coefficient of vertical ground acceleration in g's.

The horizontal component P_{AE_h} of the active force P_{AE} is equal to

$$P_{AE_h} = P_{AE} \cos (\delta+\beta) \tag{2-11}$$

or,

$$P_{AE_h} = \frac{1}{2}\gamma H^2 (1-k_v) K_{AE} \cos (\delta+\beta)$$

For the special case of a wall with a vertical back side (i.e., β=0), Eqn. (2-11) is reduced to

$$P_{AE_h} = \frac{1}{2}\gamma H^2 (1-k_v) K_{AE} \cos\delta \tag{2-12}$$

The total force determined by the Mononobe-Okabe approach is considered to act at a height equal to H/3 above the base of the wall. Thus, the resulting pressure distribution along the wall is linear with depth.

The passive force that corresponds to the Mononobe-Okabe method is obtained in a manner similar to the one described above and may be expressed as (Kapila, 1962)

$$P_p = \frac{1}{2}\gamma H^2 \ (1-k_v)K_{PE} \tag{2-13}$$

in which

$$K_{PE} = \frac{\cos^2(\phi+\beta-\theta)}{\cos\theta\cos^2\beta\cos(\delta-\beta+\theta)\ [\ 1-\ \{\frac{\sin(\phi-\delta)\sin(\phi+i-\theta)}{\cos(i-\beta)\cos(\delta-\beta+\theta)}\}^{1/2}\ ]^2}$$

and all parameters entering the above expression are given in Eqn. (2-10).

The validity of the Mononobe-Okabe method was investigated in a study by Ishii, et al. (1960).

The approach taken by the authors provided a magnitude for the maximum lateral force against a retaining wall that was approximately equal to that determined using Mononobe-Okabe procedure while its point of application was found to lie between 0.33H to 0.4H above the base of the wall.

2.2.2 The Simplified M-O Method. For the simple but commonly encountered cases of vertical walls retaining horizontal dry backfills, Seed (1969) proposed a simplified procedure for determining the Mononobe-Okabe earth pressure. This is based on the notion that the total maximum seismic active force P_{AE} may be considered to consist of two terms: one, the initial static force P_s and, another, the seismic force increment ΔP_{AE}; i.e.,

$$P_{AE} = P_s + \Delta P_{AE} \tag{2.14}$$

in which

$$P_s = \frac{1}{2} K_A \gamma H^2,$$

K_A = the coefficient of active earth pressure,

γ = the unit weight of the backfill material, and

H = the height of the wall.

For the case where the friction angle of the backfill material is about 35° (ϕ=35°), the seismic force increment ΔP_{AE} is found to be approximately equal to the inertia force on a soil wedge extending a distance 0.75 H behind the crest of the wall. This is shown schematically in Fig. 2.9. Thus,

$$\Delta P_{AE} \simeq \frac{1}{2}\, 0.75 \quad k_h \,\gamma\, H^2 \tag{2-15}$$

in which k_h is the horizontal seismic coefficient.

Introducing the expressions for P_s and ΔP_{AE} into Eqn. (2-14) one has that the total maximum active force P_{AE} is approximately equal to

$$P_{AE} \simeq \frac{1}{2}\,\gamma\, H^2\, (K_A + 0.75\, k_h) \tag{2-16}$$

A comparison of the numerical values of K_{AE}, found from the M-O analysis, and the coefficient $K_A + 0.75k_h$, appearing in Eqn. (2-16), has shown that the simplified method is adequate for a wide range of values

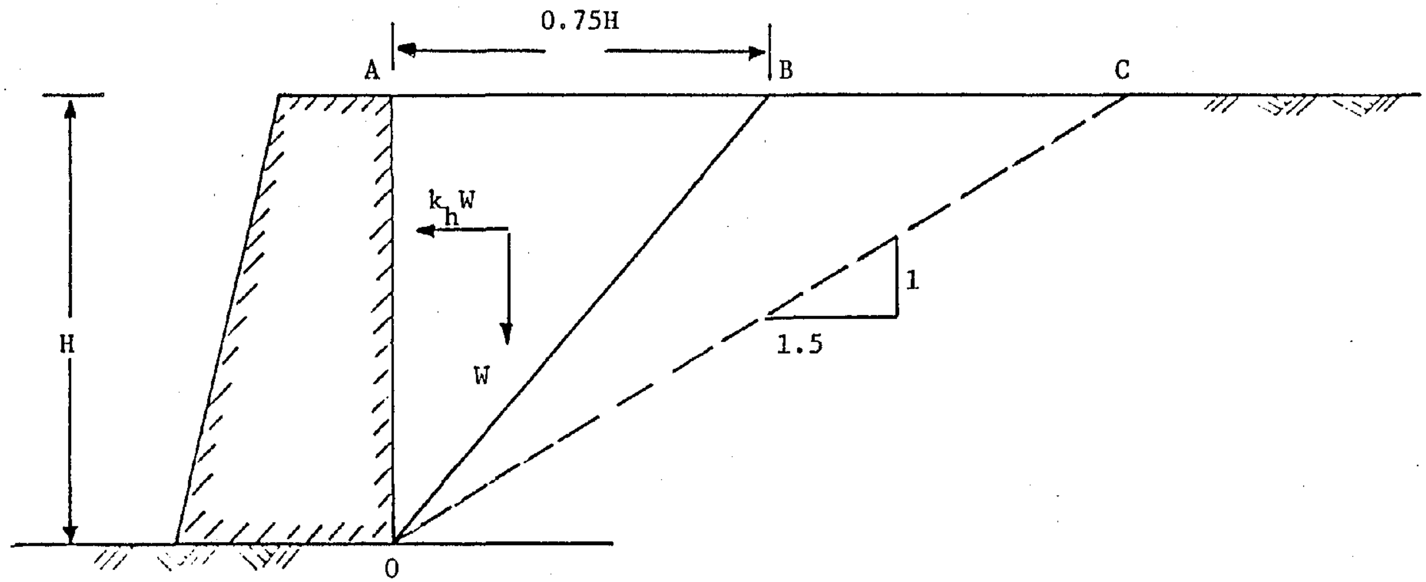

Figure 2.9 Soil Wedge Required to Determine the Seismic Force Increment (after Seed and Whitman, 1970).

of k_h.

The seismic force increment ΔP_{AE}, found in accordance with the above simple rule, is assumed to act at a height 0.6H above the base of the wall.

Finally, Seed (1969) recommended that the critical failure surface (which depends on the magnitude of the horizontal seismic coefficient k_h) be taken to lie anywhere within the region OBC, shown in Fig. 2.9.

2.2.3 The Prakash and Basavanna Method. Experimental observations on the force system behind retaining walls have indicated that, even under static conditions, pressure distributions are different from hydrostatic. Furthermore, Terzaghi (1936,1941) has shown that, if the earth pressure distribution is assumed to be hydrostatic, the forces acting on the sliding wedge do not satisfy the condition of equilibrium of moments. Thus, the M-O analysis based on Coulomb's theory and therefore on a hydrostatic-like distribution of pressures, violates both experimental evidence and the conditions of static equilibrium.

Prakash and Basavanna (1969) attempted to improve upon the M-O procedure through an analysis that would satisfy the conditions of equilibrium of moments. Their approach is based on the following assumptions:

(a) the backfill material consists of cohesionless soil,

(b) the failure surface is a plane along which shear resistance is fully mobilized,

(c) vertical pressures along planes parallel to the ground surface (which may be inclined) are constant, and

(d) the principle of superposition of forces is valid.

In Fig. 2.10 is shown schematically the use of the principle of superposition of forces as employed by Prakash and Basavanna (1969). Figure 2.10 (b) shows the force system on the sliding wedge for only horizontal body forces and Fig. 2.10 (c) for only vertical body forces. From the condition of equilibrium of moments around point A of the base of the wall, Fig. 2.10 (a), the following expression was obtained for the active force P_A:

$$P_A = \frac{\gamma H^2 \sin^2(\beta_1 + i)[\cot(\beta_1 + i) + \cot(\theta - i)}{2 \sin \beta_1 \sin(\beta_1 + i - \delta)} [$$

$$\frac{\{(1 + a_v)\sin i + a_h \cos i\} \tan(\beta_1 + i - \delta)}{\tan(\beta_1 + i - \delta) + \tan(\theta - i - \phi)} +$$

$$+ \frac{(1 + a_v)\cos i + a_h \sin i}{\cot(\beta_1 + i - \delta) + \cot(\theta - i - \phi)}] \qquad (2\text{-}17)$$

in which

$$\beta_1 = \frac{\pi}{2} - \beta.$$

The distance of the point of application of P_A from the base of the wall was found using the expressions of the moment M_A of the force system around point A (Fig. 2.10) and of the active force P_A, as given in Eqn. (2-17).

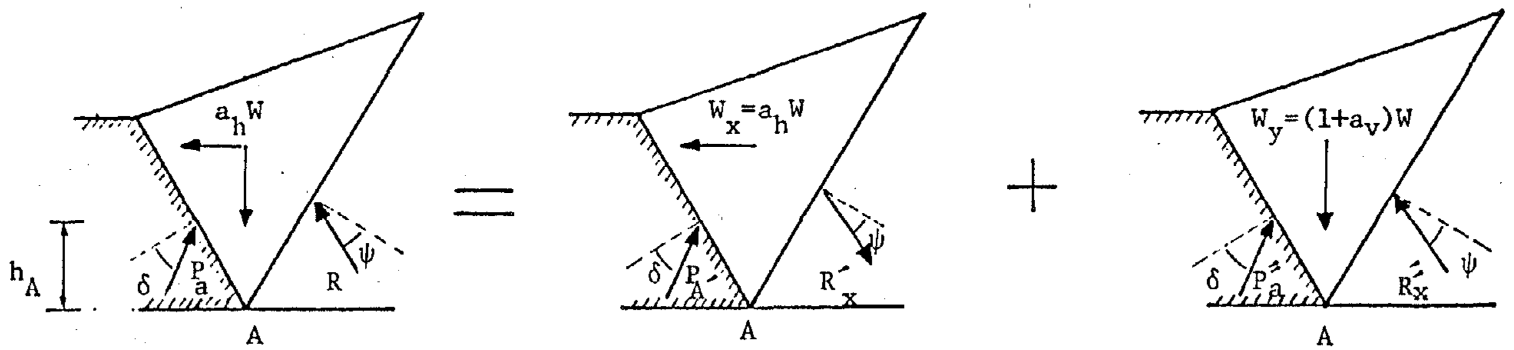

(a) Forces on Sliding Wedge

(b) Only Horizontal Body Forces

(c) Only Vertical Body Forces

Figure 2.10 Superposition of Forces Acting on the Sliding Wedge (after Prakash and Basavanna, 1969)

Finally, Prakash and Basavanna (1969) assumed that the active seismic pressure $p(z)$ at a depth z along the wall has the form

$$p(z) = Kz^{m}$$

in which K and m are constants determined from the conditions of equilibrium of the wall.

2.2.4 The Richard and Elms Method. The previously described methods of analysis of retaining walls under seismic conditions were concerned exclusively with the change in the intertia of the sliding soil mass during an earthquake. In a more recent study, Richard and Elms (1979) noted that, for the displacement-governed gravity walls, a force increase, in addition to that predicted by the Mononobe-Okabe analysis may occur because of the inertia effects of the wall itself. This was attributed to the fact that it is the weight of gravity wall that provides most of the resistance to the wall movement that is caused by the ground shaking. Thus, a procedure was developed by the authors that calculates the weight of the wall required to prevent motion greater than any specified value.

The needed design relationship for gravity walls that may fail in sliding was derived by Richard and Elms (1979) by considering the force system appearing in Fig. 2.11. From the conditions of force equilibrium of the wall along the vertical and horizontal directions, it is found that (Fig. 2.11)

$$N = (1-k_v)\ W_w + E_{AE}\ \sin\ (\delta+\beta) \qquad (2\text{-}18)$$

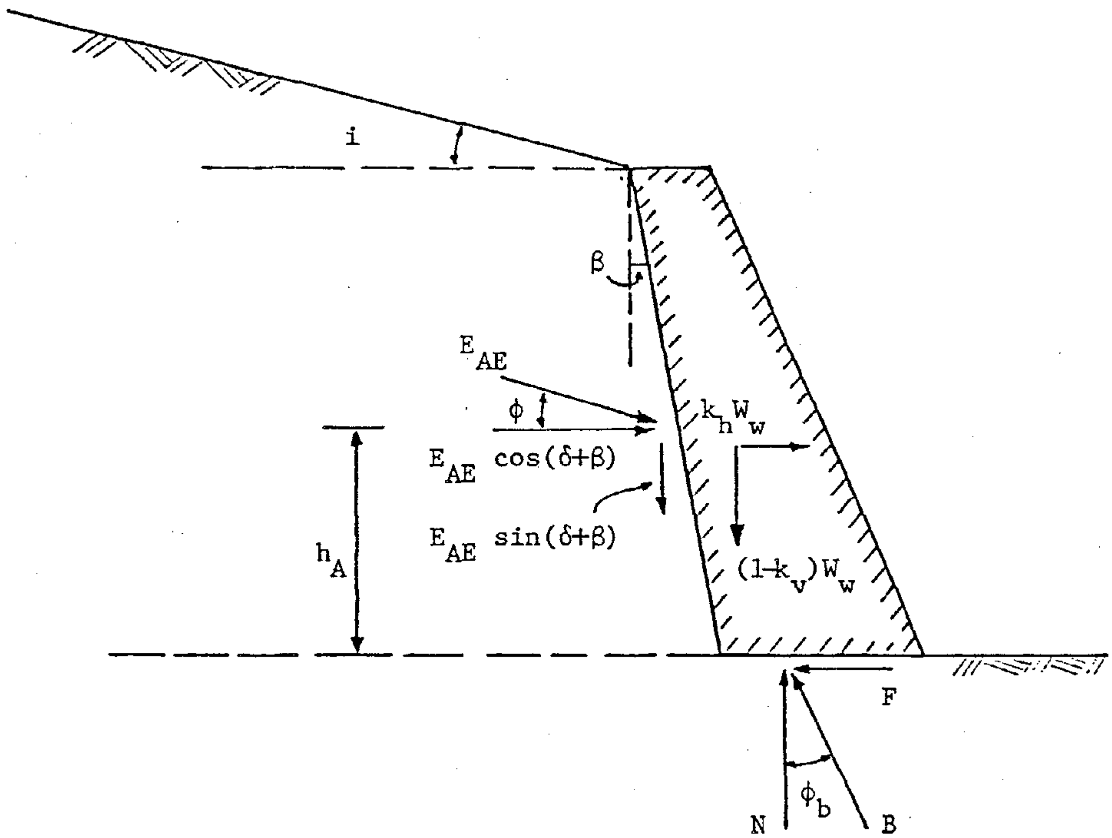

Figure 2.11 Forces Acting on a Retaining Wall in the Richard and Elms Method

$$F = E_{AE} \cos(\delta+\beta) + k_h W_w \tag{2-19}$$

in which,

W_w = the weight of the wall,

E_{AE} = the total active thrust,

k_h = coefficient of horizontal ground acceleration in g's,

k_v = coefficient of vertical ground acceleration in g's,

β = the angle between the back side of wall and the vertical, and

δ = the angle of wall-soil friction.

From the above equations, the expression for the weight of the wall is found as

$$W_w = C_{IE} E_{AE} \tag{2-20}$$

in which,

$$C_{IE} = \frac{\cos(\delta+\beta)-\sin(\delta+\beta)\tan\phi_b}{(1-k_v)(\tan\phi_b-\tan\theta)}$$

$$E_{AE} = \frac{1}{2}\gamma H^2 (1-k_v) K_{AE}$$

and

K_{AE} = the earth pressure coefficient (Eqn. (2-10)),

ϕ_b = the angle of internal friction at the base of the wall, and

$\theta = \tan^{-1}\dfrac{k_h}{1-k_v}$

In this form, the weight W_w of the wall is essentially the seismic thrust K_{AE}, as computed by the Mononobe-Okabe method, multiplied by a wall inertia factor C_{IE}. Thus, Eqn. (2-20) incorporates in the same expression the increase in the driving force due to both the increase in the inertia force of the sliding wedge and the increase in the inertia of the wall itself.

In order to examine the relative importance of the two seismic effects, Richard and Elms (1979) introduced two normalized quantities, namely, a soil thrust factor (F_T) and a wall inertia factor (F_I) defined as

$$F_T = \frac{K_{AE}(1-k_v)}{K_A} \qquad (2\text{-}21)$$

$$F_I = \frac{C_{IE}}{C_I} \qquad (2\text{-}22)$$

in which,

$$K_A = \frac{\cos^2(\phi-\beta)}{\cos^2\beta\cos(\delta+\beta)\left[1+\left\{\frac{\sin(\delta+\phi)\sin(\phi-i)}{\cos(\delta+\beta)\cos(\beta-i)}\right\}^{1/2}\right]^2}$$

and

$$C_I = \frac{\cos(\delta+\beta)-\sin(\delta+\beta)\tan\phi_b}{\tan\phi_b}$$

The safety factor F_w with respect to the weight of the wall that accounts for soil pressure and wall inertia was defined as the product of F_T and F_I; i.e.,

$$F_w = F_T F_I \tag{2-23a}$$

or,

$$F_w = \frac{W_w}{W} \tag{2-23b}$$

in which

W = the weight of the wall required for equilibrium under static conditions.

The design procedure for walls that can sustain a specified but limited displacement was derived using a progressive failure model based on the observations that: (a) the total displacement of a wall due to an earthquake takes place in a series of smaller displacements; and (b) a more critical loading is due to earthquakes with high velocity, rather than acceleration, peaks. The specific stages of the design procedure are as follows:

1. Decide upon an acceptable maximum displacement d. If wall connections are present, they have to be capable of allowing for this displacement.
2. Obtain the value of k_h that corresponds to the maximum displacement d. In locations within the United States, the value of k_h may be obtained in terms of the Effective Peak Acceleration (A_a) and Effective Peak Velocity (A_v) as follows:

$$k_h = A_a\left(\frac{0.2A_v^2}{A_a d}\right)^{1/4} \tag{2-24}$$

in which A_a and A_v have values that can be found in the draft-code location maps of the Applied Technology Council (ATC) and d is measured in inches.

3. Use Eqn. (2-20) to obtain the required wall weight W_w.
4. Apply a suitable safety factor, say 1.5, to determine W_w.

2.2.5 <u>The Dubrova Method Including Seismic Effects</u>. The Dubrova method, described in Section 2.1.2, can be easily extended to provide the lateral earth pressure distribution along a retaining wall under seismic conditions.

Thus, Saran and Prakash (1977) expressed the total active (P_A) and passive (P_P) forces against a retaining wall of a height H (Fig. 2.12) as

$$P_{A/P} = \frac{1}{2}\gamma H^2 \quad \frac{(1 \pm a_v)\cos^2(\psi - \lambda_1 \mp \beta)}{\cos\lambda_1 \cos^2\beta \cos(m\psi \pm \beta + \lambda_1)} \left[\frac{1}{1 \pm \left\{ \frac{\sin(\psi + m\psi)\sin(\psi \mp i - \lambda_1)}{\cos(\beta - i)\cos(m\psi \pm \beta + \lambda_1)} \right\}^{1/2}} \right]^2 \tag{2-25}$$

in which,

P_A = the total active earth pressure (taking upper sign of the expression).

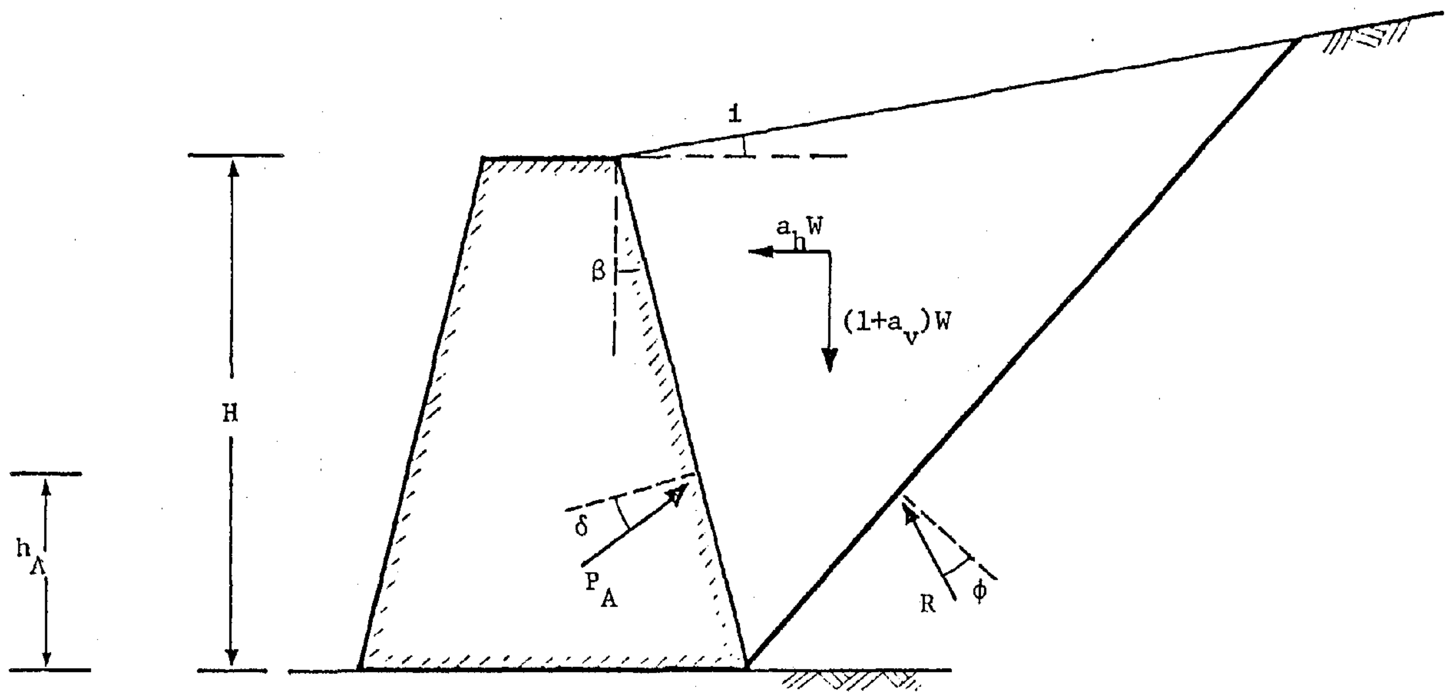

Figure 2.12 The Force System on the Sliding Soil Mass in Accordance with the Saran-Prakash Method.

P_P = the total passive earth pressure (taking lower sign of the expression),

δ = the angle of wall-soil friction,

i = the inclination of the backfill,

β = the angle between the back side of the wall and the vertical,

$\lambda_1 = \tan^{-1}\left(\frac{a_h}{1+a_v}\right)$,

γ = the unit weight of the soil,

a_h = coefficient of horizontal ground acceleration in g's,

a_v = coefficient of vertical ground acceleration in g's, and

m = a factor less than unity.

The expression for the ψ parameter depends on the mode of movement expected to be experienced by the wall. Thus, for the active case and for a rotation about the base of the wall, ψ is equal to $\psi = \phi - \frac{\phi z}{H}$, in which ϕ is the angle of internal friction of the soil mass, z is the particular value of the depth, and H is the height of the wall. For a rotation around the top of the wall, ψ becomes equal to $\psi = \frac{\phi z}{H}$. For the passive case and for a rotation about the base of the wall, ψ is equal to $\psi = -\frac{\phi z}{H}$ while, for a rotation around the top, $\psi = \frac{\phi z}{H} - \phi$.

The pressure distribution is obtained by forming the derivative of the expression for total force ($P_{A/P}$) with respect to z; i.e.,

$$p_{A/P}(z) = \frac{\partial P_{A/P}}{\partial z} \tag{2-26}$$

The point of application of the total pressure from the base of the wall is given as

$$h_{A/P} = H - \frac{\int_{o}^{H} \left(\frac{\partial P_{A/P}}{\partial z}\right) dz}{P_{A/P}} \qquad (2\text{-}27)$$

A modified version of Dubrova's method was also used by A-Grivas (1978) for the assessment of the reliability of retaining structures during earthquakes. In Fig. 2.13 is shown the polygon of forces that was employed in the analysis. The total force (Q) is inclined at an angle β with respect to the vertical direction and has a magnitude equal to

$$Q = W\,[(1-a_v)^2 + a_h^2]^{1/2} = W(1-a_v)/\cos\beta \qquad (2\text{-}28)$$

where a_h and a_v are the horizontal and vertical ground accelerations, respectively. The derived expression for force P_{AE} against the wall as a function of the ψ parameter has the form

$$P_{AE} = \frac{\gamma(1-a_v)z^2}{\cos\beta} \left[\frac{\sin(45 - \frac{\psi}{2} + \beta)}{\tan(45 + \frac{\psi}{2})\sin(45 + \delta + \frac{\psi}{2})} \right] \qquad (2\text{-}29)$$

while the distribution of the lateral pressure $p_{AE}(z)$ with depth z, found by forming the derivative of Eqn. (2-29) with respect to z, is equal to

$$p_{AE}(z) = \frac{\gamma(1-a_v)}{\cos\beta} \left[\frac{n(\psi)}{\tan^2(45 + \frac{\psi}{2})\sin(45+\delta+\frac{\psi}{2})} \right] \qquad (2\text{-}30)$$

in which

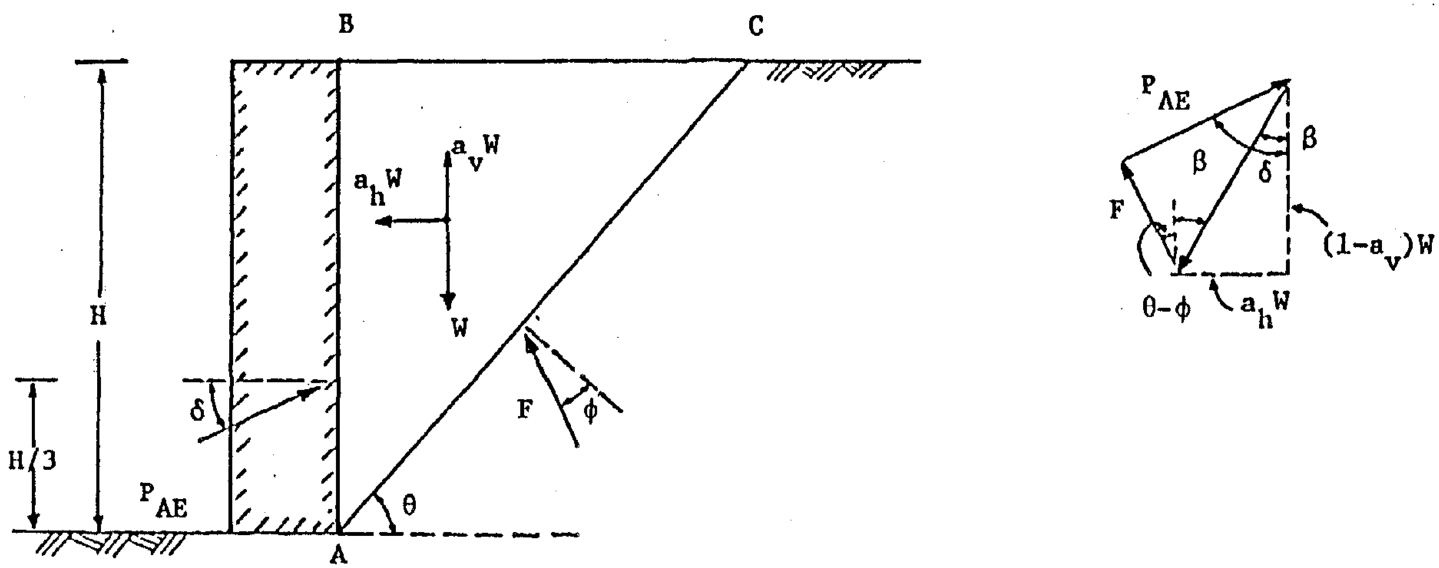

(a) (b)

Figure 2.13 (a) Trial Wedge for Dynamic Lateral Force
(b) Polygon of Forces

$$n(\psi) = \tan(u)\ \sin(v)\left[2z\sin(w) - \frac{z^2}{2}\cos(w)\ \left(\frac{\partial\psi}{\partial z}\right)\right] -$$

$$- \frac{z^2}{2}\ \sin(w)\left[\tan(v)\cos(w) + \sin(w)\ \sec^2(u)\right]\ \left(\frac{\partial\psi}{\partial z}\right),$$

$$u = 45° + \frac{\psi}{2},$$

$$v = 45 + \delta + \frac{\psi}{2}, \text{ and}$$

$$w = 45 - \frac{\psi}{2} + \beta$$

2.3 Comparison of Procedures

Common to all the procedures described in the previous section are the following characteristics:

1. two dimensional conditions;
2. the backfill material is a rigid body; and
3. soil sliding occurs along a plane surface.

In Table 2.2 is given a summary of the important additional assumptions made in each method. Finally, Table 2.3 provides a comparison of the various procedures with respect to their consideration of wall movement, ground motion parameter used, point of application of thrust, shape of pressure distribution, and conditions of equilibrium satisfied.

Table 2.2 Summary of Important Assumptions Made in Each Method.

METHODS	ASSUMPTIONS
Mononobe-Okabe	1. The wall yields sufficiently during an earthquake to produce minimum active pressures. 2. When the minimum active pressure is attained, the maximum shear strength is mobilized along the potential sliding surface. 3. It satisfies the equations of equilibrium of forces (horizontal and vertical) but does not satisfy equilibrium of moments. 4. The total maximum seismic force P_{AE} acts at a height H/3 from the base of the wall.
Simplified [illegible]	The total maximum seismic active force P_{AE} consists of two terms: the initial static force P_s, acting at H/3; the seismic force increment ΔP_{AE}, acting at 0.6H from the base of the wall.
Prakash-Bas[illegible]	1. The shear resistance along the plane rupture surface is fully mobilized. 2. The vertical pressure on planes parallel to the groun surface is constant. 3. The principal of superposition holds true. 4. Satisfies of three equations of equilibrium
Richard-E[illegible]	1. It is based on deformation limits. 2. It accounts for the change of the inertia of the wall during earthquakes. The mass of the wall is considered to provide most of the resistance to movement caused by an earthquake (gravity walls). 3. The total displacement of the wall occurs in series of smaller displacements.
Dubrova Including Seismic Effects	1. The magnitude and distribution of the force against the wall depends on the type of movement experienced by the wall. 2. During an earthquake the wall may rotate around any point.

Table 2.3 Comparison of Procedures

METHOD	CONDITION				
	Considers wall Movement	Ground Motion Parameters	Point of Application	Shape of Pressure distribution	Condition of Equilibrium
Mononobe - Okabe (M-O)	No	Peak Acceleration	H/3	Linear	Horizontal and Vertical Forces
Simplified (M-O)	No	Peak Acceleration	Static Component: $\frac{H}{3}$ Dynamic Component: 0.6H	Linear	Horizontal and Vertical Forces
Prakash-Basavanna	No	Peak Acceleration	From equilibrium of moments around the toe of the wall	Linear	Horizontal and Vertical Forces and Equilibrium of Moments
Richard-Elms	Yes	Peak Acceleration Peak Velocity Maximum Dis-placement	H/3	Linear	Horizontal and Vertical Forces
Dubrova including Seismic effects	Yes	Peak Acceleration	From equilibrium of moments around the toe of the wall	Non-linear (depends on the type of wall movement)	Horizontal and Vertical Forces

CHAPTER 3

DESCRIPTION OF THE SEISMIC LOADING

3.1 Probabilistic Description of the Earthquake Magnitude

The empirical formula most commonly employed to yield the number of earthquakes n_m exceeding a certain magnitude m is Richter's log-linear relationship expressed in the form

$$\log n_m = a - bm \tag{3-1}$$

where a and b are regional constants. If m_0 and m_1 denote the lower and upper limits of m, respectively, Eqn. (3-1) becomes

$$\log n_m = a - b(m-m_0), \quad m_0 \leq m \leq m_1 \tag{3-2}$$

or,

$$n_m = 10^a \exp\left[-\beta(m-m_0)\right]$$

where

$$\beta = b \ln 10$$

From Eqn. (3-2), one has that the expected number of earthquakes (n_{m_0}) with magnitude greater than the assumed lower bound (m_0) is equal to

$$n_{m_0} = 10^a \exp(-\beta m_0)$$

The ratio of n_m over n_{m_0} signifies the probability with which the earthquake magnitude M is greater than m. Thus,

$$P[M > m] = \frac{n_m}{n_{m_0}} = \frac{10^a \exp(-\beta m)}{10^a \exp(-\beta m_0)}$$

or,

$$P[M > m] = \exp[-\beta(m-m_0)], \quad m_0 \le m \le m_1, \tag{3-3}$$

The cumulative density function F(m) of the earthquake magnitude m is equal to

$$F(m) = P[M \le m] = 1 - P[M > m]$$

Introducing Eqn. (3-3) into the above expression, it is found that

$$F(m) = 1 - \exp[-\beta(m-m_0)] \tag{3-4}$$

A normalizing factor is required so that F(m) becomes unity when m receives maximum value m_1. If this factor is denoted by k, from Eqn. (3-4) one has

$$F(m_1) = k\,\{1-\exp[-\beta(m,-m_0)]\} = 1 \tag{3-5}$$

from which

$$k = \{1-\exp\,[-\beta(m_1 - m_0)]\}^{-1}$$

Thus, F(m) may be written as

$$F\,(m) = \begin{cases} 0 & m < m_1 \\ k\ \{1-\exp[-\beta(m-m_0)] & m_0 \leq m \leq m_1 \\ 1 & m_1 < m \end{cases} \tag{3-6}$$

The probability density function f(m) of the magnitude m can be found by forming the derivative of Eqn. (3-6) with respect to m. Thus,

$$F(m) = \begin{cases} 0 & m < m_0 \\ \beta\ k\ \exp\ [-\beta(m-m_0)], & m_0 \leq m \leq m_1 \\ 0 & m_1 \leq m \end{cases} \tag{3-7}$$

The mean value $\bar{m}$ and variance Var(m) of the earthquake magnitude m can be found from Eqn (3-7) as

$$\begin{aligned} \bar{m} &= \int_{m_0}^{m_1} mf\,(m)\,dm \\ \mathrm{Var}(m) &= \int_{m_0}^{m_1} (m-\bar{m})^2 f(m)\,dm \end{aligned} \tag{3-8}$$

where f(m) is the probability density function of m, given in Eqn. (3-7). Substituting the latter into Eqns. (3-8) and performing the indicated integrations, one has

$$\bar{m} = k \{m_0 + \frac{1}{\beta} - (m_1 + \frac{1}{\beta}) \exp [-\beta(m_1 - m_0)]\}$$

$$\mathrm{Var}(m) = k \{m_0^2 - m_1^2 \exp [-\beta(m_1 - m_0)]\} + \frac{2\bar{m}}{\beta} - \bar{m}^2 \quad (3\text{-}9)$$

3.2 Attenuation Relationship for Maximum Horizontal Ground Acceleration

The attenuation relationship for maximum horizontal ground acceleration a_{max} is commonly expressed in the form (A-Grivas, 1979)

$$a_{max} = b_1 e^{b_2 m} (R + b_4)^{-b_3} \quad (3\text{-}10)$$

where a_{max} is measured in cm/sec^2, m is the earthquake magnitude, R is the distance between source and site (in km) and b_1, b_2, b_3, b_4 are regional parameters.

Comparisons made between observed and computed values of the ground motion parameters have indicated that their ratio follows closely a log-normally distributed random variable. Denoting the latter by ε and introducing it into Eqn. (3-10), the latter becomes

$$a_{max} = b_1 e^{b_2 m} (R + b_4)^{-b_3} \varepsilon \quad (3\text{-}11)$$

where ε is log-normally distributed variable with median equal to one and standard deviation varying between 0.5 and 1.0.

3.3 Types of Earthquake Sources

The construction of a model for the earthquake source is an attempt to represent, using only a few parameters, the complex movements that take place within the crust of the earth. The simplest possible model of an earthquake source requires the specification of only two parameters: the location of the hypocenter and the magnitude of the earthquake. A more complex model requires the additional specification of the fault surface and the directions along the latter of the slip that occurs during the seismic activity. An even more complex model would also include the length and width of the slip area and the time required for each point along the slip to reach its maximum offset. Thus, as the model becomes more realistic, the number of the required parameters increases and so does the complexity of the task associated with the representation of the seismic source.

In engineering applications, the most commonly employed representation of the earthquake source is that provided by Cornell (1968). Three types of seismic sources are distinguished in Cornell's model, namely, (a) a point source, (b) a line source (or, fault), and (c) an area source.

A point source, shown schematically in Fig. 3.1, represents the fundamental source model that has been used in studies aiming at the determination of the seismic hazard of a region. It may be used in cases where the seismic activity is concentrated in an area that is small compared to the distance between the source and the site of interest.

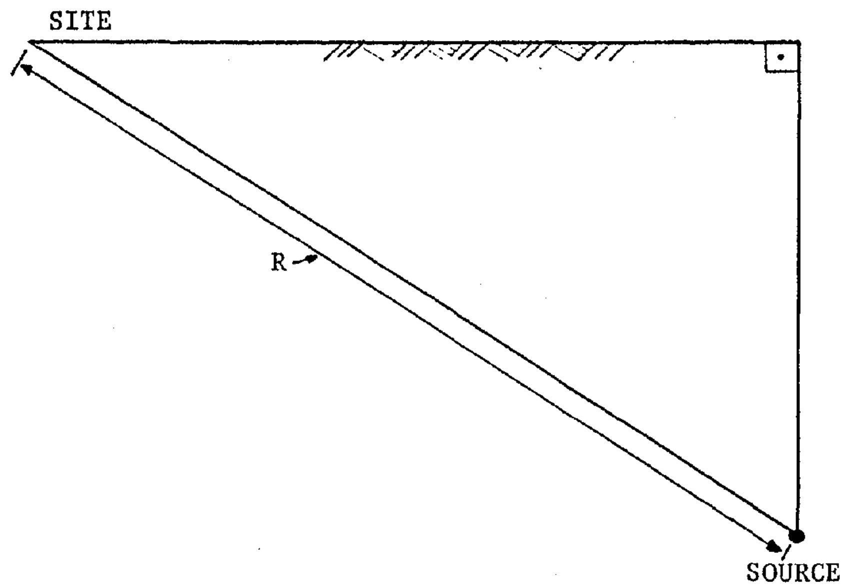

Figure 3.1 Point Source

A line (or, fault) source, shown schematically in Fig. 3.2, is used in cases where earthquakes are associated with clearly identified faults, or if a string of earthquakes have occurred over a period of time along a well defined line. When this is not the case, or when historical data and other information available on the seismicity of a region are very limited, a description of the earthquake source as an area source may be considered. This is shown schematically in Fig. 3.3.

3.4 Probabilistic Description of Maximum Horizontal Ground Acceleration.

3.4.1 Case of Point Source. Using the concept of transformation of variables (Harr, 1977), the probability density function of the maximum horizontal ground acceleration a_{max} can be obtained from Eqn. (3-9) as

$$f(a_{max}) = \frac{f_m(m)}{\left| \frac{\partial a_{max}(m)}{\partial m} \right|} \tag{3-12}$$

where $f_m(m)$ is the probability density function of the earthquake magnitude, and $\frac{\partial a_{max}(m)}{\partial m}$ is the absolute value of the derivative of a_{max} with respect to m. The latter is found from Eqn. (3-10) to be equal to

$$\frac{\partial a_{max}(m)}{\partial m} = b_1 b_2 \, e^{b_2 m} \, (R + b_4)^{-b_3} = b_2 \, a_{max} \tag{3-13}$$

Combining Eqns. (3-7), (3-12) and (3-13), it is found that

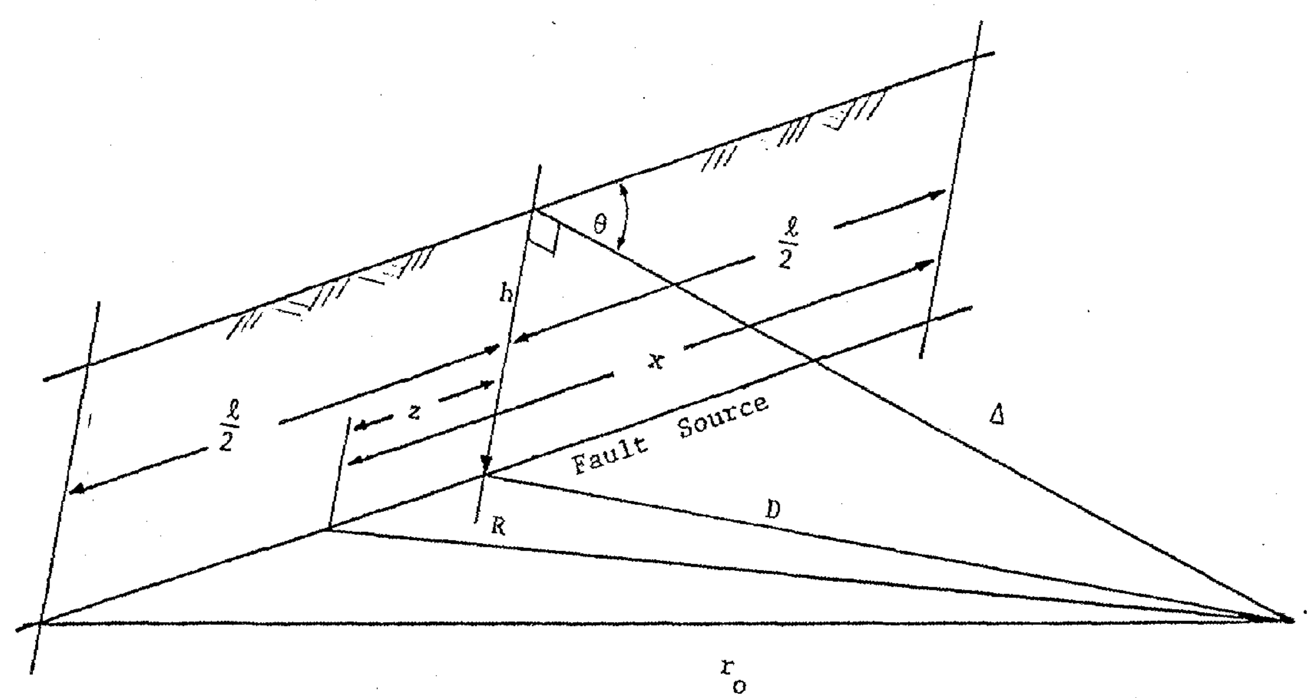

Figure 3.2 Line Source (perspective)

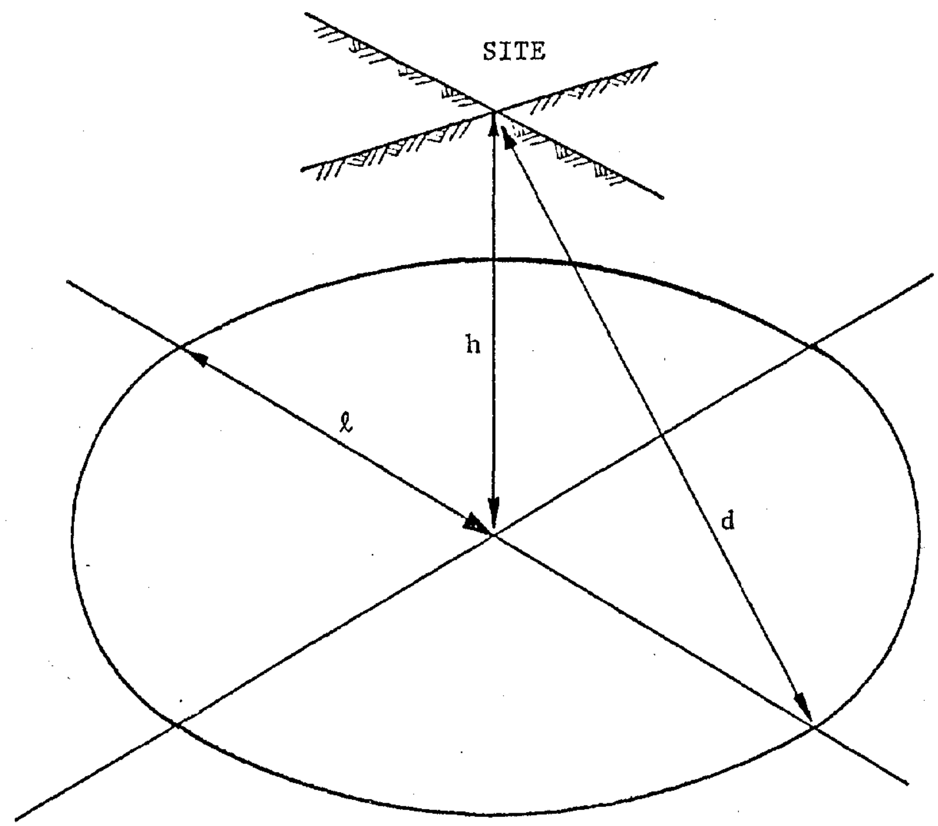

Figure 3.3 Area Source (perspective)

$$f(a_{max}) = \frac{k}{b_2} \frac{1}{a_{max}} \exp \; [-\beta(m-m_0)] \qquad (3\text{-}14)$$

Solving Eqn. (3-10) for m and substituting into the Eqn. (3-14), the probability density function of a_{max} is obtained as

$$f(a_{max}) = \frac{k}{b_2} \frac{1}{a_{max}} \exp \; [-\beta(\frac{1}{b_2} \ln \frac{a_{max}}{b_1(R+b_4)^{-b_3}} - m_0)] \qquad (3\text{-}15)$$

The range of variation of a_{max} can be found by introducing the lower and upper limits of magnitude m into Eqn. (3-10). Thus,

$$b_1 \, e^{b_2 m_0} \, (R + b_4)^{-b_3} \leq a_{max} \leq b_1 e^{b_2 m_1} \, (R + b_4)^{-b_3} \qquad (3\text{-}16)$$

The cumulative distribution $F(a_{max})$ of a_{max} can be obtained through an integration of Eqn. (3-14) with respect to a_{max}. The resulting expression is

$$F(a_{max}) = k \; \{1-\exp[-\beta(\frac{1}{b_2} \ln \frac{a_{max}(R + b_4)^{b_3}}{b_1} - m_0)]\} \qquad (3\text{-}17)$$

3.4.2 Case of Line (or, Fault) Source. The cumulative distribution $F(a_{max})$ of the maximum acceleration a_{max} when $\theta = 90°$ (Fig.3.2) has the form (Grivas and Howland, 1979)

$$F(a_{max}) = 1-[(1-k) + k \exp \; (\beta m_0) \; (\frac{a_{max}}{b_1})^{-\frac{\beta}{b_2}} \; I \;] \qquad (3\text{-}18)$$

where k, β, m_0, b_1 b_2, b_3 were defined above and I is the integral

$$I = \int_D^{r_o} \frac{2R}{\ell(R^2-D^2)^{1/2}} (R)^{\frac{-b_3\beta}{b_2}} dR \qquad (3\text{-}19)$$

in which R, r_o, D and ℓ are shown in Fig. 3.2.

The probability density function of a_{max}, found by forming the derivative of Eqn. (3-18) with respect to a_{max}, has the following expressions:

$$f(a_{max}) = \frac{k}{b_1} \frac{\beta}{b_2} I (\beta m_0) \left(\frac{a_{max}}{b_1}\right)^{-\left(\frac{\beta}{b_2}+1\right)} \qquad (3\text{-}20)$$

3.4.3 Case of Area Source. In this case, the probability with which the maximum acceleration A_{max} receives values larger than a_{max} is equal to (Tong, 1975),

$$P[A_{max} > a_{max}] = (1-k) + \frac{2}{d^2-h^2} k [\exp(\beta m_0)] b_1^{\beta/b_2} H a_{max}^{-\beta/b_2} \qquad (3\text{-}21)$$

where

$$H = \frac{h^{\frac{-b_3}{2}\beta+2} \left[1 - \left(\frac{d}{h}\right)^{\frac{-b_3}{b_2}\beta+2}\right]}{\frac{b_3}{b_2}\beta-2} \qquad (3\text{-}22)$$

(3-22)

The cumulative distribution $F(a_{max})$ of a_{max} can be obtained as the complement of the above expression; i.e.,

$$F(a_{max}) = 1 - [(1-k) + \frac{2}{d^2-h^2} \text{kexp } (\beta m_0) b_1^{\beta/b_2} H\, a_{max}^{-\beta/b_2}] \qquad (3\text{-}23)$$

The frequency distribution $f(a_{max})$ of a_{max} is found from Eqn. (3-23) by forming the derivative of $F(a_{max})$ with respect to a_{max}, or

$$f(a_{max}) = \frac{2k}{d^2-h^2} \frac{\beta}{b_2} b^{\beta/b_2} H \exp (\beta m_0) a_{max}^{-(\frac{\beta}{b_2}+1)} \qquad (3\text{-}24)$$

3.4.4 Statistical Values of Maximum Horizontal Ground Acceleration (Point Source.) The exact expressions for the mean value $\bar{a}_{max}$ and variance $Var(a_{max})$ of the maximum horizontal acceleration can be obtained using the probability density function $f(a_{max})$ of a_{max} as follows:

$$\bar{a}_{max} = \int a_{max} f(a_{max})\, da_{max}$$

$$Var(a_{max}) = \int (a_{max} - \bar{a}_{max})^2 f(a_{max}) da_{max} \qquad (3\text{-}25)$$

where $f(a_{max})$ is given in Eqn. (3-15) and the limits of the integration (minimum and maximum values of a_{max}) are given is Eqn. (3-16).

An alternative convenient way to obtain estimates of the mean value $\bar{a}_{max}$ and variance $Var(a_{max})$ of a_{max} is to apply a Taylor series expansion of the function $a_{max}(m)$ around the value $a_{max}(\bar{m})$, where $\bar{m}$ is the mean value of the magnitude m. The resulting estimates of $\bar{a}_{max}$ and $Var(a_{max})$ are then equal to (Grivas and Howland, 1979)

$$\bar{a}_{max} = a_{max}(\bar{m}) + \frac{1}{2} \frac{\partial^2 \bar{a}_{max}}{\partial m^2} Var(m) \qquad (3\text{-}26)$$

$$Var(a_{max}) = \left(\frac{\partial \bar{a}_{max}}{\partial m}\right)^2 \quad Var(m) \tag{3-26}$$

Introducing into the above expressions derivatives of a_{max} with respect to m, obtained from Eqn. (3-10), one has

$$\bar{a}_{max} = \frac{b_1 e^{b_2 \bar{m}}}{(R + b_4)^{b_3}} \left[1 + \frac{1}{2} b_2^2 \; Var(m) \right]$$

$$Var(a_{max}) = \left[\frac{b_1 b_2 e^{b_2 \bar{m}}}{(R + b_4)^{b_3}}\right]^2 \; Var\;(m) \tag{3-27}$$

where the mean value $\bar{m}$ and variance Var(m) of the magnitude m are given in Eqns. (3-9)

3.5 Other Strong Ground Motion Parameters.

With the exception of the method developed by Richard and Elms (1979), all other procedures presented in Chapter 2 and which are currently employed for the determination of the force on retaining walls during earthquakes introduce the seismic effect in terms of the maximum ground acceleration.

In the method provided by Richard and Elms (1979), the maximum horizontal ground acceleration k_h is obtained using an empirical relationship between k_h and the maximum ground displacement d (Franklin and Chang, 1977). This was given in Eqn. (2-24) as

$$K_h = A_a \left(\frac{0.2\, A_v^2}{A_a d}\right)^{1/4}$$

in which A_a and A_v are effective peak acceleration (EPA) and effective peak velocity (EPV), respectively, as provided in the provisions of the Applied Technology Council (ATC 3-06, 1978).

It should be noted that parameters A_a and A_v do not have a precise definition in terms of their physical meaning. They should be considered as normalizing factors used for the construction of smooth elastic response spectra for ground motions of normal duration (Newmark and Hall, 1969). Thus, A_a and A_v are related to the peak ground acceleration and peak ground velocity, respectively, but are not necessarily the same with or even proportional to these quantities.

Finally, it has been observed (McGuire, 1975) that, if very high frequencies are present in the ground motion, A_a may be significantly less than the peak acceleration ; and that A_v will generally be greater than the peak velocity at large distances from the epicenter of a major earthquake.

CHAPTER 4

PROBABILISTIC SAFETY ANALYSIS OF EARTH RETAINING STRUCTURES

4.1 Definition of Failure

In general, the stability of any soil structure is conventionally measured in terms of a factor of safety (FS), defined as the ratio of two point estimates: one, for the capacity C_o of the structure (its available resistance against failure) and, another, for the demand D_o on the structure (the applied loading). That is,

$$FS = \frac{C_o}{D_o} \tag{4-1}$$

In many practical geotechnical situations, however, both the capacity C and the demand D of a structure exhibit a considerable degree of variation. This observation has led to a consideration of C and D as random variables (A-Grivas and Harrop-Williams, 1978), and their analytical description through their probability density functions, $f_C(C)$ and $f_D(D)$, respectively. This is shown schematically in Fig. 4.1.

The difference between the capacity C and the demand D is also a random variable which, in probabilistic parlance, is called the "safety margin SM"; i.e.,

$$SM = C - D \tag{4-2}$$

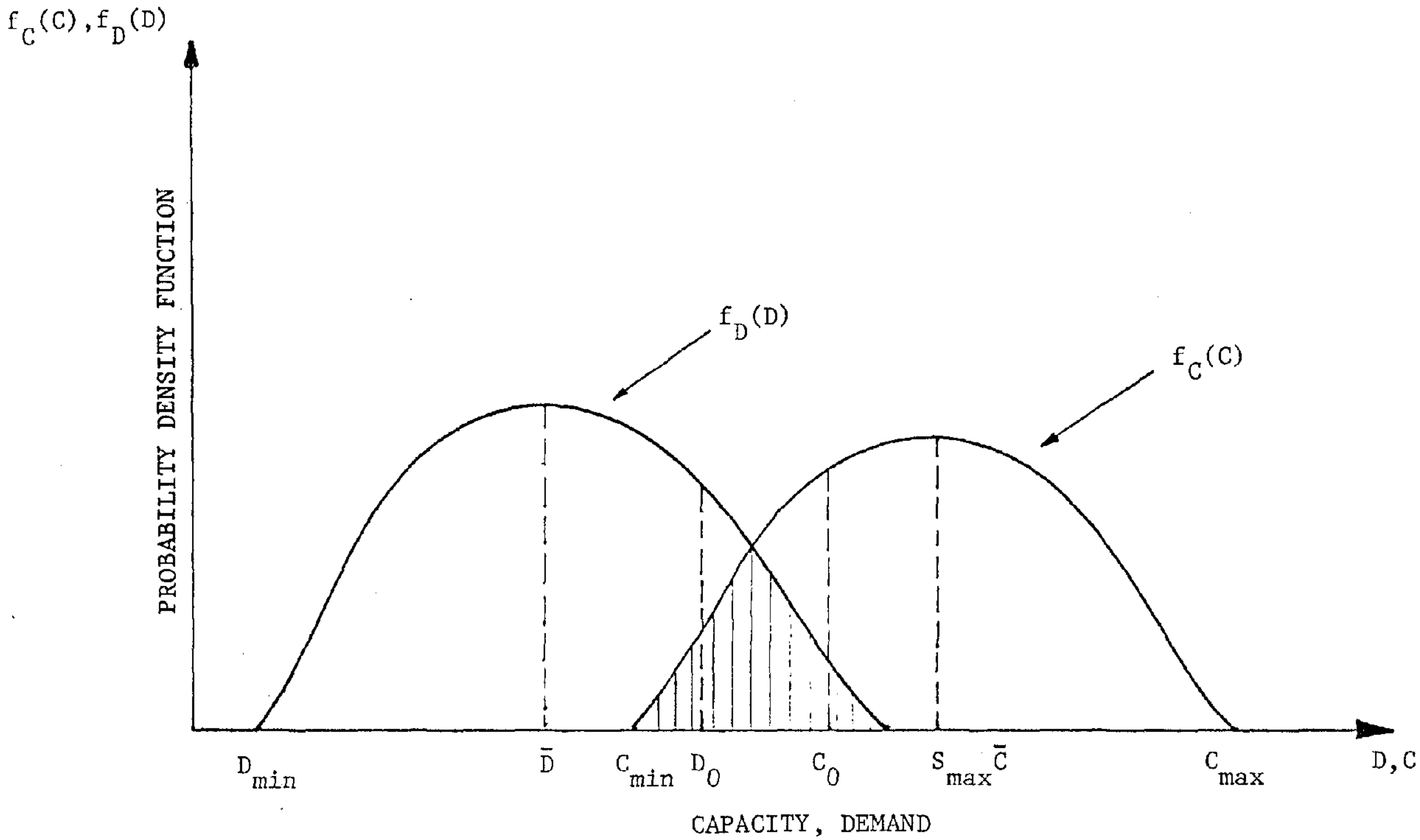

Figure 4.1 Probability Density Function of the Capacity (C) and Demand (D)

If the statistical values (e.g., mean values, standard deviations, etc.) of the capacity C and demand D were known, then from Eqn. (4-2) one could easily obtain the corresponding statistical values of the safety margin SM. Thus, if $\bar{C}$, $\bar{D}$ and σ_C, σ_D denote the mean values and standard deviations of C and D, respectively, the mean value $\overline{SM}$ and standard deviation σ_{SM} of SM are equal to (Harr, 1977)

$$\overline{SM} = \bar{C} - \bar{D}$$

$$\sigma_{SM} = (\sigma_C^2 + \sigma_D^2)^{1/2} \tag{4-3}$$

Failure of a structures is defined as the event whereby its safety margin SM receives a value smaller than or equal to zero; i.e.,

$$\text{"Failure"} = [SM \leq 0] = [C-D \leq 0] \tag{4-4}$$

The possibility for failure exists if the lower limit of the capacity (C_{min}) becomes smaller than the upper limit of the demand (D_{max}). Thus, the interval (C_{min},D_{max}), shown in Fig. 4.1 as shaded area, defines the region where it is possible for the capacity C to receive a value smaller than that of the demand D ($C < D$).

4.2 Possible Modes of Failure.

A retaining wall, like the one shown schematically in Fig. 4.2, may fail in any of the following four modes:

(1) overturing around any point on the plane of the wall;

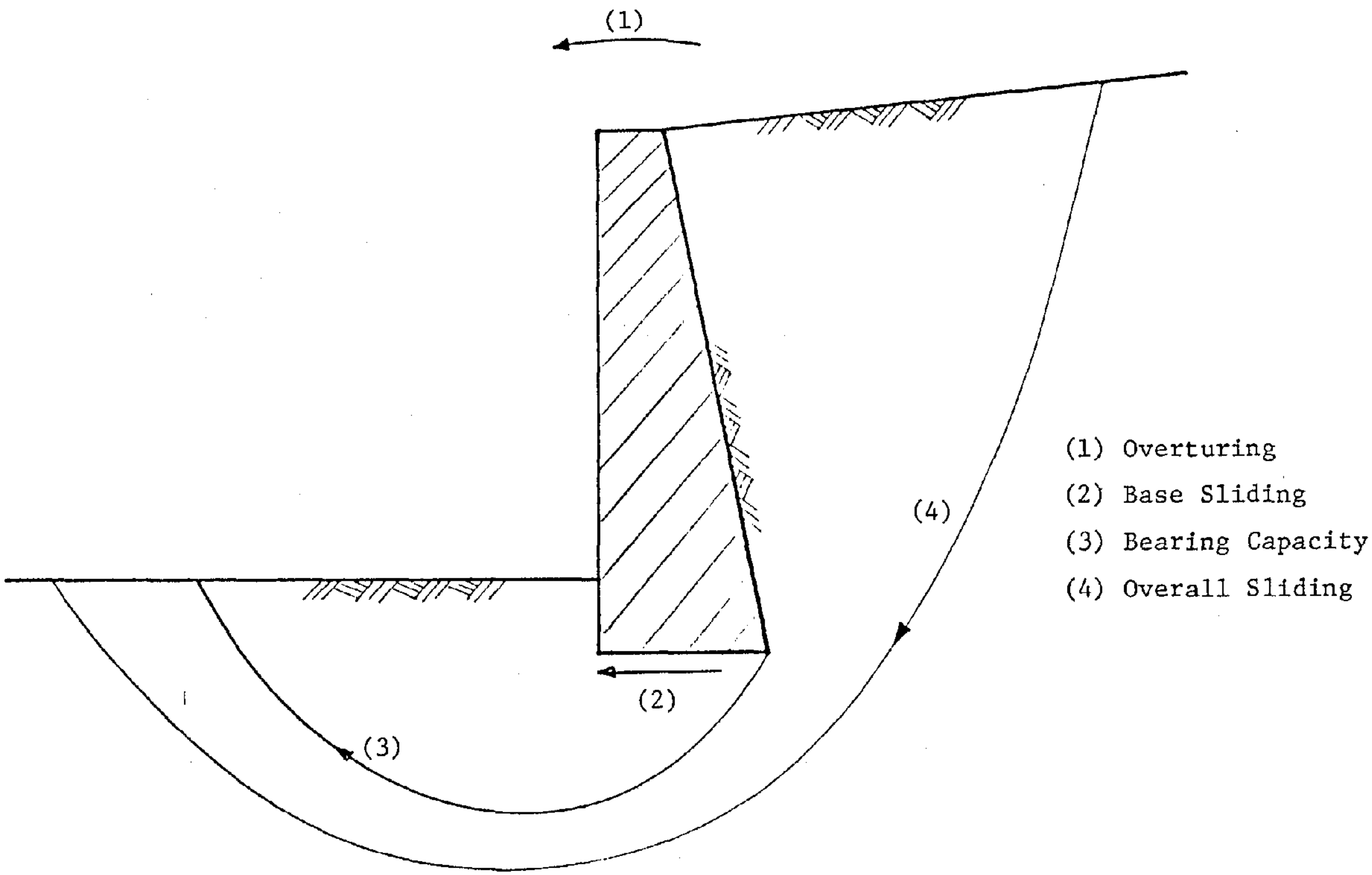

Figure 4.2 The Four Modes of Failure of a Retaining Wall

(2) bearing capacity of the foundation of the wall;

(3) sliding along the base of the wall; and

(4) overall sliding of the wall and the backfill material.

In Table 4.1 are provided the capacity C and demand D of the above four modes of failure. Their analytical expressions are given below in Section 4.3.

4.3 Probability of Failure of an Earth Retaining Structure.

Let $SM_i = C_i - D_i$, $i = 1, \ldots, 4$, denote the safety margin of any mode i of possible failure of a retaining wall. The capacity C_i and demand D_i, $i = 1, \ldots, 4$ are given in Table 4.1. From Eqn. (4-4), one has that failure along the i-th mode is defined as the event whereby SM_i receives a value smaller than or, at most, equal to zero, i.e., $[SM_i \leq 0]$.

The probability of the occurence of this event is equal to the probability of failure p_{f_i} of the wall along mode i. Thus,

$$p_{f_i} = P[SM_i \leq 0], \quad i = 1, \ldots 4 \tag{4-5}$$

where P [ ] denotes the probability of the event in brackets.

Furthermore, let $f_{SM_i}(SM_i)$ represent the probability density function of the safety margin SM_i along mode i. As the area under $f_{SM_i}(SM_i)$ up to a particular value provides the probability with which SM_i is smaller than or at most equal to that value, one has that p_{f_i} is the area under $f_{SM_i}(SM_i)$ and in front of zero. This is shown schematically as the shaded region in Fig. 4.3. Recalling the definition of

Table 4.1 Capacity and Demand of the Various Modes of Failure

MODE OF FAILURE	CAPACITY C	DEMAND D
Overtruning	Moment of resisting forces around center of rotation	Moment of forces causing rotation around same point
Bearing Capacity	Bearing capacity formula for the foundation of the wall	Force acting on the wall plus weight of wall
Base Sliding	Vertical component of the demand in bearing capacity times friction coefficient	Horizontal components of the demand in bearing capacity
Overall Sliding (Slope Type)	Resisting forces along failure surface	Driving forces along failure surface

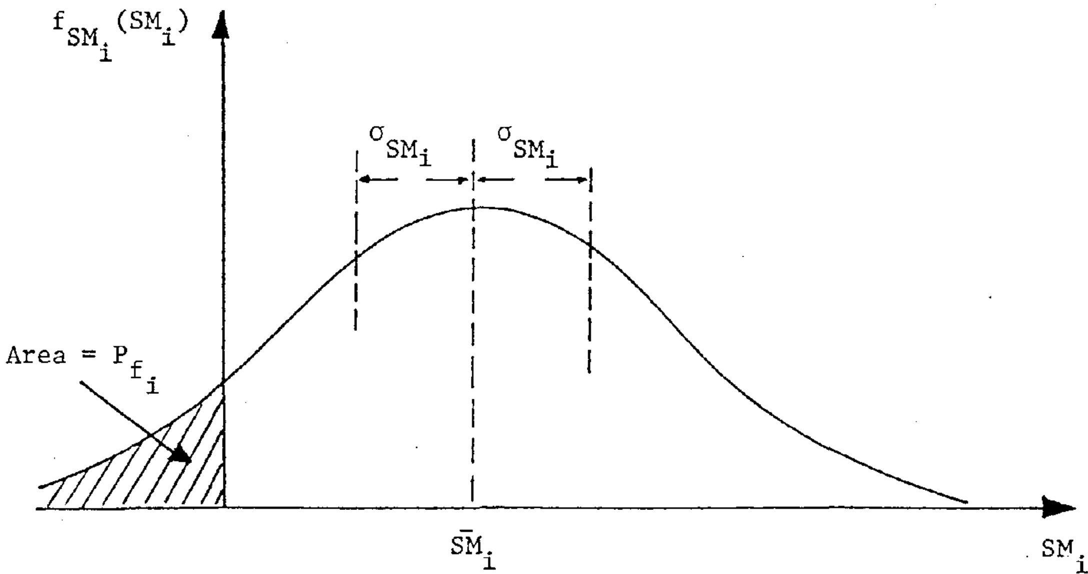

(a) Probability Density Function of SM_i

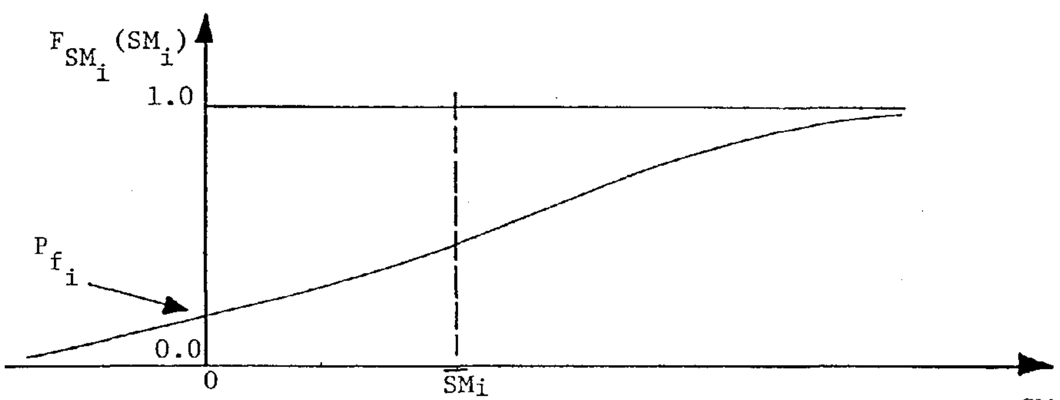

(b) Cumulative Distribution of SM_i

Figure 4.3 Schematic Representation of Probability Density Function $f_{SM_i}(SM_i)$ and Cumulative Distribution $F_{SM_i}(SM_i)$ of SM_i.

the cumulative distribution $F_{SM_i}(SM_i)$ of SM_i as

$$F_{SM_i}(SM_i) = \int_{-\infty}^{SM_i} f_{SM_i}(SM_i)\ d(SM_i) \tag{4-6}$$

one has that p_{f_i} is equal to $F_{SM_i}(SM_i)$ for $SM_i = 0$; or

$$p_{f_i} = F_{SM_i}(0) \tag{4-7}$$

The complement of the probability of failure p_{f_i} (i.e., the probability of success) is defined as the reliability R_i of the wall in mode i ; i.e.,

$$R_i = 1 - p_{f_i} \quad , \quad i - 1, \ldots 4, \tag{4-8}$$

To obtain a measure for the total probability of failure p_f of a retaining wall, the latter may be considered as a "system" with four modes of failure. As failure in any element (mode) will cause failure of the entire system (wall), elements 1, 2, 3 and 4 are said to form a configuration in-series. If, furthermore, the four modes of failure are independent, then the total probability of failure p_f of the wall is equal to (Harr, 1977)

$$p_f = 1 - \prod_{i=1}^{4} (1-p_{f_i}) \quad (4\text{-}9)$$

Finally, the complement of p_f is the total reliability of the wall and is equal to

$$R = 1-p_f$$

or,

$$R = \prod_{i=1}^{4} R_i \quad (4\text{-}10)$$

4.3.1 Overturning. In the case of failure of the wall in overturing, from Table 4.1 one has that the capacity C is equal to the moment of resisting forces around the center of rotation while the demand D is given by the moment of the forces causing rotation around the same point. A typical wall cross-section including the applied forces is shown schematically in Fig. 4.4.

The expressions for the capacity and the demand in this case are

C = Moment of Resisting Forces Around Point O

or,

$$C = (1 + a_v)\, W_w \ell + P_A\, B \sin\delta \quad (4\text{-}11)$$

D = Moment of Forces Causing Rotation Around O

or,

$$D = P_A h_A \cos\delta + a_h W_w h \quad (4\text{-}12)$$

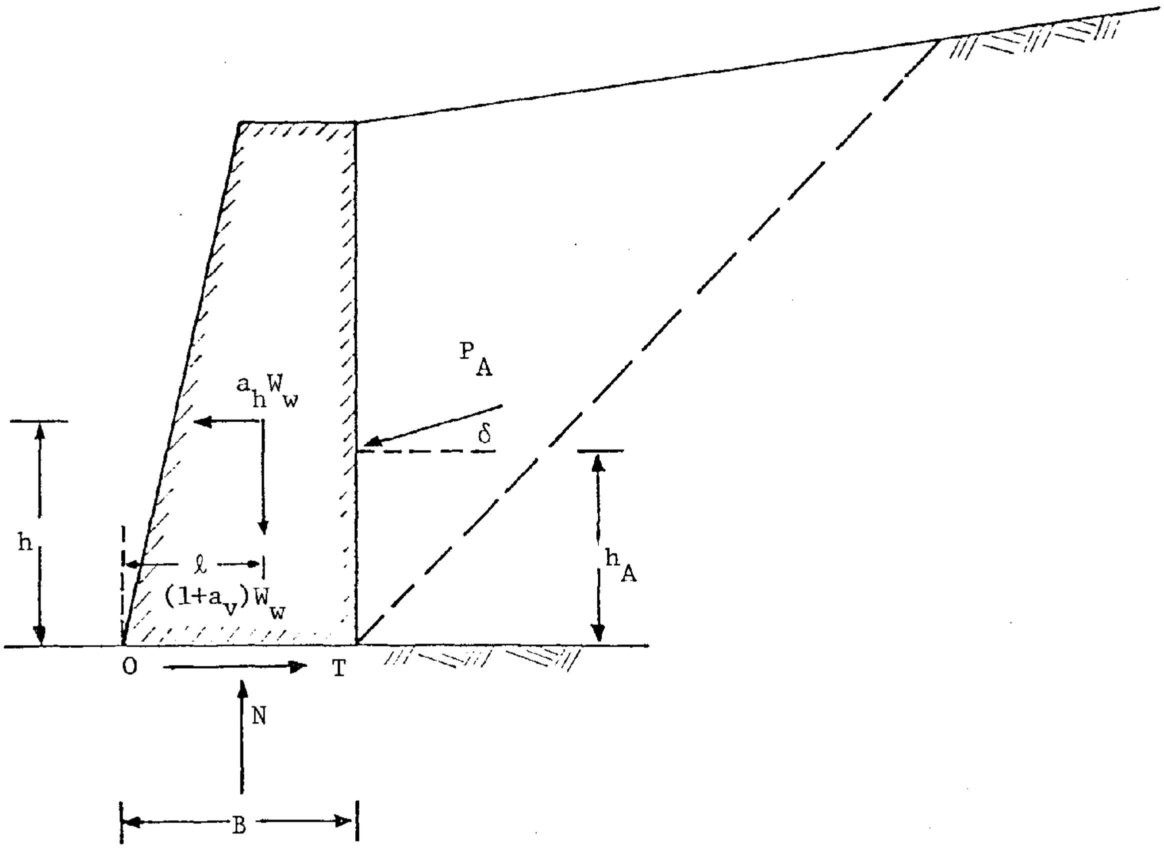

Figure 4.4 Forces on the wall for Overturning and Base Sliding Failure

in which

P_A = the total forces on the wall,

W_w = the weight of the wall, and

γ = the unit weight of the backfill material.

4.3.2 Bearing Capacity. In this case, from Table 4.1 one has that the capacity of the wall is given as the bearing capacity of its footing while the demand is equal to the sum of the external forces acting on the back of the wall plus the weight of the wall itself. A typical cross-section of the wall together with the forces acting on it are shown schematically in Fig. 4.5.

Following Meyerhof (1953), the expressions for the capacity C and the demand D are given as

$$C = \frac{1}{2}\gamma B'^2 N_\gamma + \gamma D_f B' N_q + N_c B_c' c \tag{4-13}$$

$$D = (D_v^2 + D_H^2)^{1/2} \tag{4-14}$$

in which

$Nq = \tan^2(45 + \frac{\phi}{2}) e^{\pi \tan\phi}$,

$N_\gamma = (N_q - 1)\tan(1.4\phi)$,

$N_c = (N_q - 1)\cot\phi$,

$B' = B\,(1 - \frac{2e}{B})$,

$D_H = P_A \cos\delta + W_w a_h$, and

$D_v = P_A \sin\delta + W_w(1 + a_v)$

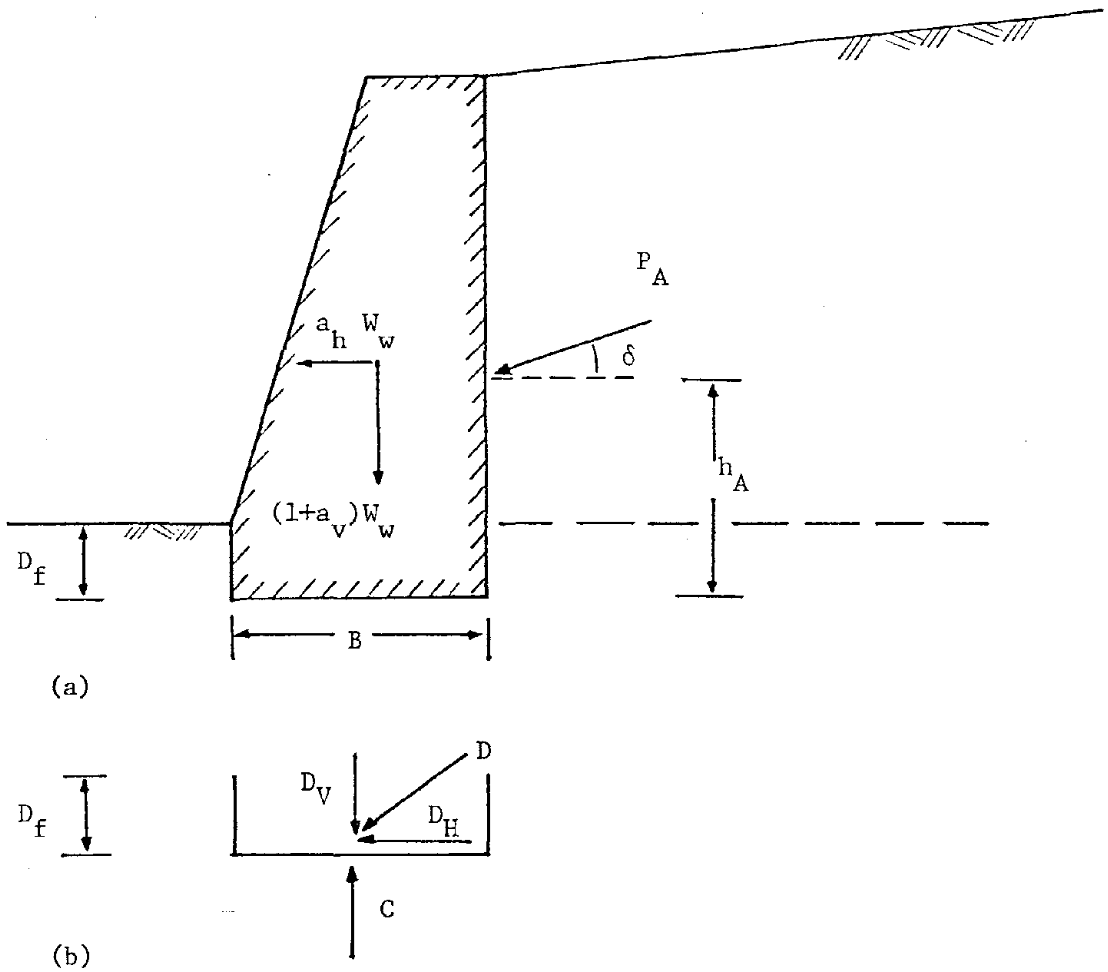

Figure 4.5 Bearing Capacity Failure

(a) Forces on Wall
(b) Forces on Footing

4.3.3 Base Sliding. In this case (Table 4.1), the capacity of the wall is equal to the vertical component D_V of the demand D, as given in Eqn. (4-14), multiplied by the footing-soil friction coefficient. The demand is equal to the horizontal companent D_H, given in Eqn. (4-14).

A typical cross-section of the wall together with the forces acting on it are shown schematically in Fig. 4.4.

The expressions for the capacity C and the demand D of the wall for the case of base sliding are

$$C = [P_A \sin\delta + W_w(1 + a_v)] \tan\phi \tag{4-15}$$

$$D = P_A \cos\delta + W_w a_h \tag{4-16}$$

in which,

P_A = the total force on the wall, and
W_w = the weight of the wall.

4.3.4 Overall Sliding.

This is a slope type failure that may occur if the sloping backfill slides and takes the wall along with it. From Table 4.1, one has that the expressions for the capacity and the demand are given as the resisting and driving forces (or, moments), respectively, along the surface of failure.

Any method of seismic slope stability analysis can be used for the assesment of the safety of the wall-backfill system in overall sliding. In Fig. 4.6 are shown schematically the conditions corresponding to the simple method of slices. The effect of the earthquake is introduced by considering additional horizontal and vertical components of the inertia forces. Thus, from Fig. 4.6 one has that the expression for the capacity C and the demand D are equal to

$$C = R \sum_{i=1}^{i=n} \{ c\Delta\ell_i + [W_i(1+a_v)] \tan\phi\cos\theta_i \} \qquad (4\text{-}17)$$

$$D = R\left(\sum_{i=1}^{i=n} W_i \sin\theta_i \right) (1+a_v) + \left(\sum_{i=1}^{i=n} W_i a_h y_i \right) + P_A\, y_A \qquad (4\text{-}18)$$

in which

$N_i = W_i \cos\theta_i = [W_i(1+a_v)] \cos\theta_i$,

R = the radius of the circle of failure,

y_A = the vertical distance of P_A from the center of the failure circle, and

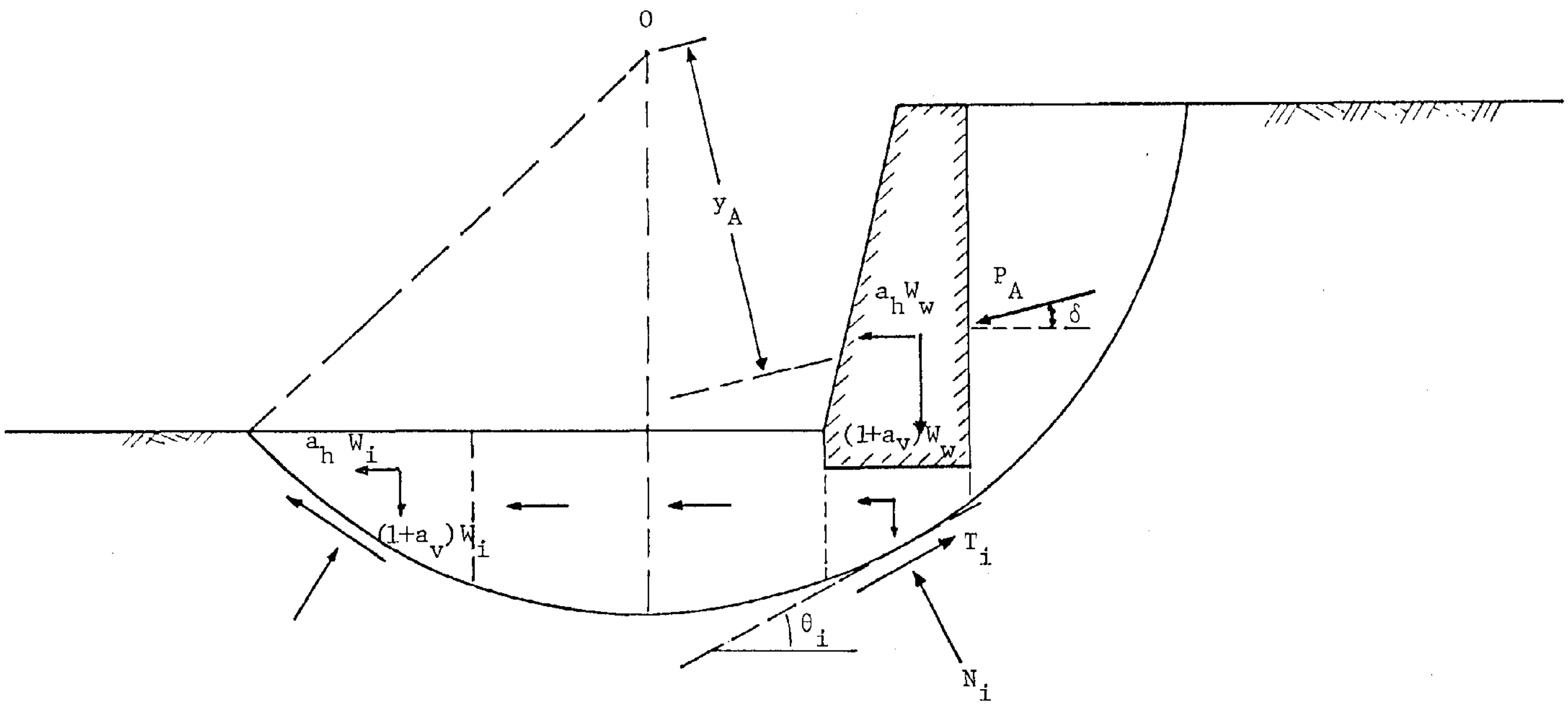

Figure 4.6 Forces on the Wall and on the Failure Surface for Overall Sliding.

Y_i = the distance between the center of gravity of the i-th slice and the vertical line that passes through the center of the failure circle.

CHAPTER 5

CASE STUDIES

The procedures reviewed in Chapter 2 and the probabilistic approach described in Chapter 4 are applied in a case study in order to determine: (a) the magnitude and distribution of the pressures behind a wall, as provided by each procedure, and (b) the corresponding values of the safety measure.

The wall under examination is shown schematically in Fig. 5.1. It has a height H = 16 ft (4.8m), average thickness 5.7 ft (1.73m) and retains a horizontal backfill consisting of granular soil. The back side of the wall is inclined at an angle $\beta = -5°$ with respect to the vertical direction. The backfill material has a ϕ parameter of strength equal to 34° ($\phi = 34°$) while the wall-soil friction angle is 15.5° ($\delta = 15.5°$). The unit weights of the soil and concrete are $\gamma = 100$ pcf (15.7 kN/m^3) and $\gamma_c = 150$ pcf (23.55 kN/m^3), respectively.

5.1 Static Condition.

5.1.1 The Coulomb Method.

The expression for the active thrust against the wall provided by the Coulomb analysis was given in Eqn. (2-3) as

$$P_A = \frac{1}{2}\gamma H^2 K_A$$

in which

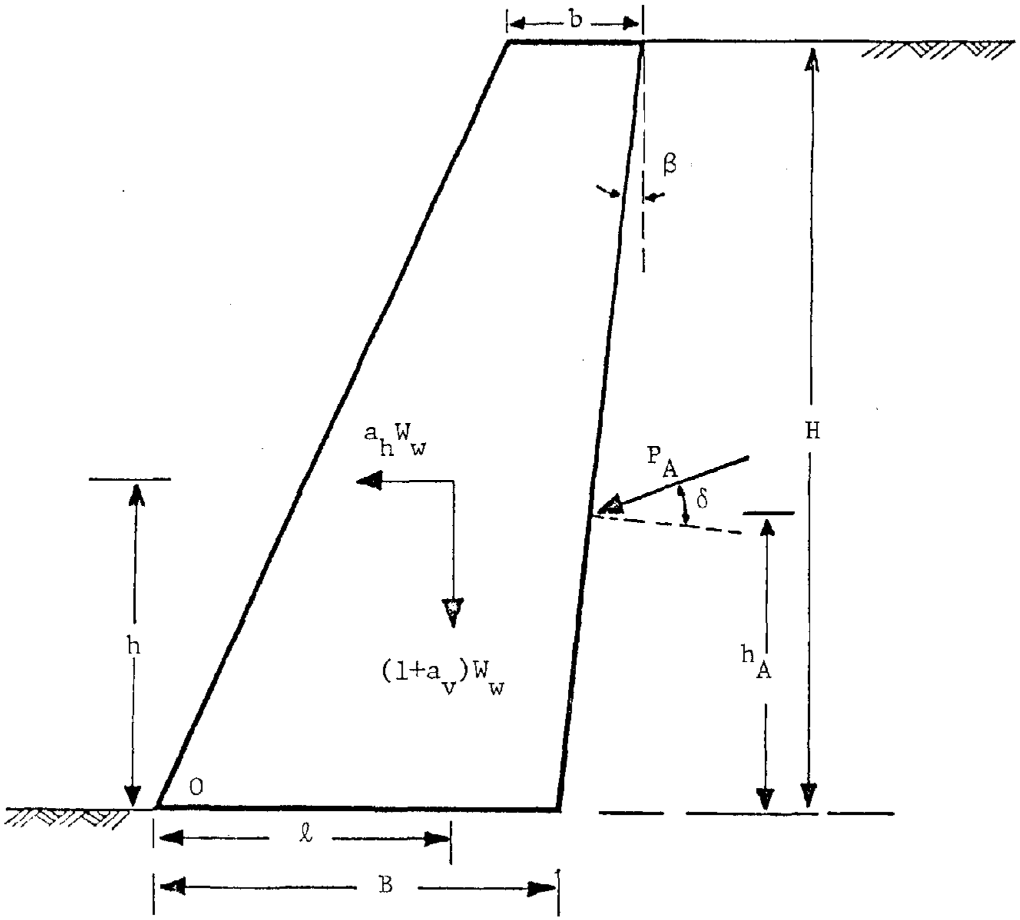

Geometry:

$H = 16$ ft (4.8m)
$B = 8.55$ ft (2.6m)
$b = 2.85$ ft (0.87m)
$h = 6.7$ ft (2.04m)
$\ell = 6.2$ ft (1.9m)
$\beta = -5°$
$i = 0°$

Material Parameters:

$\phi = 34°$
$\delta = 15.5°$
$\gamma = 100$ lb/ft^3 (15.7kN/m^3)
$\gamma_c = 150$ lb/ft^3 (23.5kN/m^3)

Figure 5.1 Geometry and Material Parameters of the Retaining Wall Used in the Case Study

$$K_A = \frac{\cos^2(\phi-\beta)}{\cos^2\beta\cos(\delta + \beta)[1 + \{\frac{\sin(\delta+\phi)\sin(\phi-i)}{\cos(\delta+\beta)\cos(\beta-i)}\}^{1/2}]^2},$$

$\gamma =$ the unit weight of soil, and

$H =$ the height of the wall.

For the geometry and material parameters of the wall under examination, Fig. 5.1, one has that $H = 16$ ft (4.87 m), $\phi = 34°$, $\beta = -5°$, $\delta = 15.5°$, $i = 0°$. Substituting these values into the expression for K_A, it is found that $K_A = 0.224$ and the total force P_A against the wall is

$$P_A = (\frac{1}{2})\ (100)(256)(0.224) = 2867 \text{ lb/ft } (40.15 \text{ kN/m})$$

The point of application of P_A is at $h_A = \frac{H}{3} = 5.33$ ft (1.62m) above the base of the wall. The resulting pressure distribution is shown in Fig. 5.2.

The value of the factor of safety FS of the wall is determined for two possible modes of failure, namely, (a) overturning and (b) base sliding.

(a) The expression of FS in overturning (FS_o) is

$$FS_o = \frac{C}{D} \tag{5-1}$$

in which C is the moment around the base of the wall of the forces resisting failure and D the moment of the forces causing failure. From Fig. 5.1, one has that

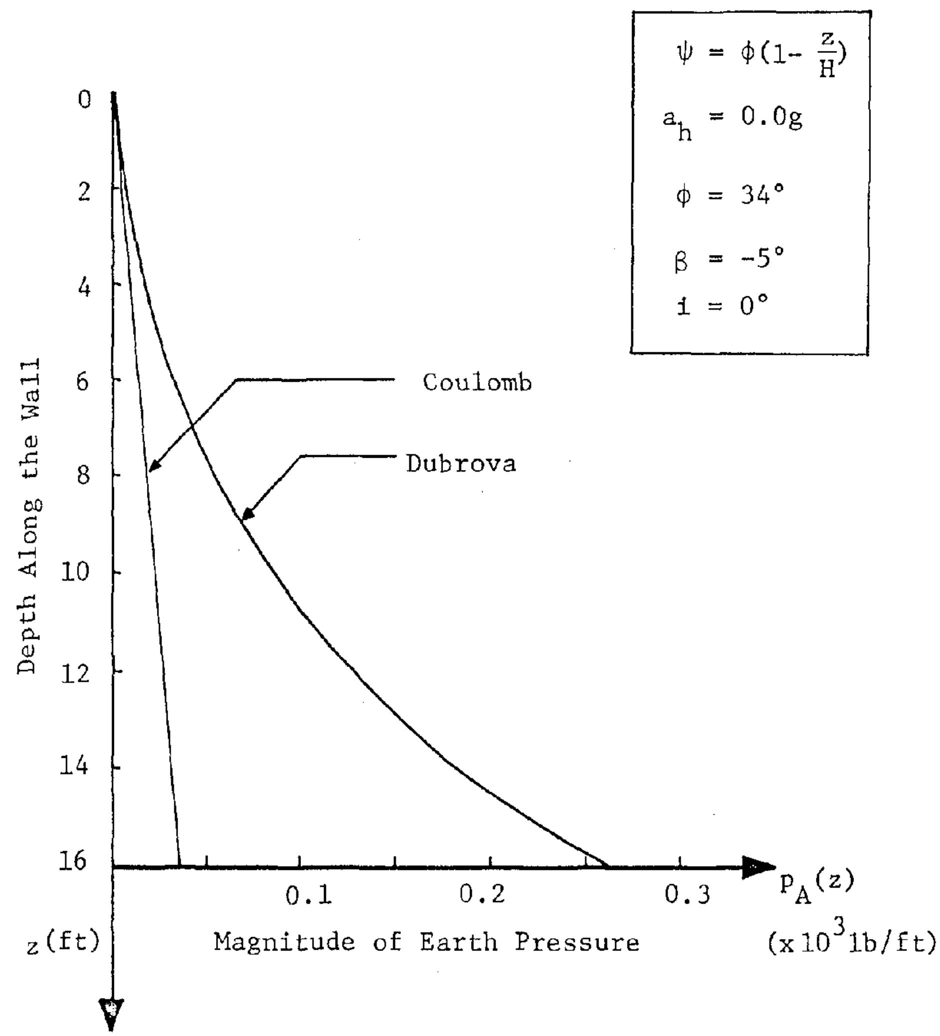

Figure 5.2 Pressure Distributions Along Wall in Accordance with the Coulomb and Dubrova Methods.

$$C = W_w \ell + P_A B \sin (\delta+\beta)$$

$$D = P_A h_A \cos (\delta+\beta) \tag{5-2}$$

where W_w = the weight of the wall,

ℓ = the horizontal distance of the center of gravity to the point of rotation O, and

B = the width of the base of the wall.

Introducing the numerical values of the geometry and material parameters shown in Fig. 5.1 into Eqn. (5-2), it is found that

C = 89277.3 lbs-ft/ft (401.7kN-m/m)

D = 15021.33 lbs - ft/ft (67.6 kN-m/m).

From Eqn. (5-1), one has

$$FS_0 = \frac{89277.33 \text{ lbs-ft/ft}(40.17\text{kN-m/m})}{15021.33 \text{ lbs-ft/ft}(67.6\text{kN-m/m})} = 5.9$$

(b) Similarly, the factor of safety against sliding (FS_s) at the wall along its base is given as

$$FS_s = \frac{C}{D}$$

in which C and D are given in Eqns. (4-15) and 4-16) for $a_h = a_v = 0$. That is

$$C = [P_A \sin(\delta+\beta) + W_w] \tan\phi$$

$$D = P_A \cos(\delta+\beta) \tag{5-3}$$

Introducing the numerical values of the geometry and material parameters into the above expressions, it is found that

$$FS_s = \frac{9572.01 \text{ lbs - ft/ft } (43.07\text{kN-m/m})}{2818.26 \text{ lbs - ft/ft } (12.68\text{kN-m/m})} = 3.39$$

5.1.2 The Dubrova Method. For the active case, with rotation of the wall around its base, the expression for the pressure distribution along the wall if found by forming the derivative of Eqn.(2-7) with respect to z. Thus,

$$\frac{p(z)}{\gamma} = \frac{z\cos\psi}{(1+1.2\sin\psi^2\cos\delta} \left[\cos\psi - z\left(\frac{d\psi}{dz}\right) \right] \qquad (5\text{-}4)$$

in which $\psi = \phi\ (1-\frac{z}{H})$.

Introducing into Eqn. (5-4) the numerical values of the geometry and material parameters shown in Fig. 5.1, the pressure distribution along the wall becomes

$$\frac{p(z)}{\gamma} = \frac{z\cos(0.59 - 0.0362)}{[(1+1.2\sin(0.59-0.036z)]^2\ 0.963} \left[\cos(0.59-0.036z)-0.036z \right]\text{ft}$$

This is shown in Fig. 5.2. The total force P_A behind the wall is found from Eqn. (2-7) to be equal to

P_A = 12,314 lb/ft (179kN/m)

The point of application of P_A is found from equilibrium of moments around point 0 (Fig. 5.1) to be h_A = 3.96 ft (1.20m).

The value of the safety measure as provided by the Dubrova method is determined for the overturning and base sliding modes of failure as follows:

(a) The expression for the factor of safety in overturning (FS_o) is given by Eqn. (5-1) in which the capacity C and demand D are equal to

$$C = W_w \ell + P_A B \sin\delta$$
$$D = P_A h_a \cos\delta \qquad (5\text{-}5)$$

Introducing the numerical values of the geometry and material parameters, shown in Fig. 5.1, into Eqns. (5-5), it is found that

$$C = 114{,}094.55 \text{ lb - ft/ft } (513\text{kN-m/m})$$
$$D = 48{,}897.92 \text{ lb - ft/ft } (220\text{kN-m/m}).$$

Thus,

$$FS_o = \frac{114{,}094.55 \text{ lb - ft/ft}}{48{,}897.92 \text{ lb - ft/ft}} = 2.33$$

(b) Similarly, the factor of safety against sliding (FS_s) of the wall along its base is given by Eqn. (5-2a) in which C and D are equal to

$$C = (P_A \sin\delta + W_w) \tan\phi$$
$$D = P_A \cos\delta \qquad (5\text{-}6)$$

Introducing the numerical values of the geometry and the material parameters into the above expressions, it is found that

$$FS_s = \frac{11,534.56 \text{ lb - ft/ft } (51.9 \text{ kN-m/m})}{12,334.6 \text{ lb - ft/ft } (55.5 \text{kN-m/m})} = 0.93$$

5.2 Seismic Conditions.

In the conventional methods of the seismic analysis of the safety of the retaining wall shown in Fig. 5.1, the effect of the earthquake is expressed in terms of the maximum horizontal and vertical ground accelerations (a_h and a_v, respectively) expected to be experienced at the site of the wall. For the purpose of this case study, the maximum ground acceleration is assumed to be equal to 24% of the acceleration of gravity g ($a_h = 0.24g$) while the value of the vertical maximum ground acceleration a_v is assumed to be equal to two-thirds that of the horizontal; i.e., $a_v = \frac{2}{3} a_h = 0.16g$.

5.2.1 The Mononobe-Okabe (M-O) Method.

The expression for the active thrust against the wall provided by the Mononobe-Okabe analysis is given in Eqn. (2-10) as

$$P_{AE} = \frac{1}{2} \gamma H^2 (1-k_v) \; K_{AE}$$

in which

$$K_{AE} = \frac{\cos^2(\phi-\theta-\beta)}{\cos\theta\cos^2\beta\cos(\delta+\beta+\theta)\left[1+\left\{\frac{\sin(\phi+\delta)\sin(\phi-\theta-i)}{\cos(\delta+\beta+\theta)\cos(i-\beta)}\right\}^{1/2}\right]^2}$$

k_h = the coefficient of horizontal ground acceleration

$(k_h = a_h = 0.24g)$

k_v = the coefficient of vertical ground acceleration

$(k_v = a_v - 0.16g)$.

Introducing the values of the geometry and material parameters of the wall under examination, Fig. 5.1, one has that the resulting value of K_{AE} is

$$K_{AE} = 0.432$$

The value of the total force P_{AE} against the wall is then equal to

$$P_{AE} = (\frac{1}{2})\ (100)\ (256)\ (0.84)\ (0.432) = 4{,}644.8 \text{ lb/ft } (65.02\text{kNm})$$

while its point of application is at $h_A = \frac{H}{3} = 5.33$ ft (1.62m) above the base of the wall.

In Fig. 5.3 is shown the pressure distribution along the wall as provided by the Mononobe-Okabe method.

The value of the factor of safety of the wall is found for the overturning and sliding modes of failure

(a) The expression for FS in overturning (FS_o) is given by Eqn. (5-1), in which C and D are equal to

$$C = (1+k_v)\ W_w.\ell + P_A B \sin(\delta+\beta)$$
$$D = P_A h_A \cos(\delta+\beta) \quad + k_h W_w h \qquad (5\text{-}7)$$

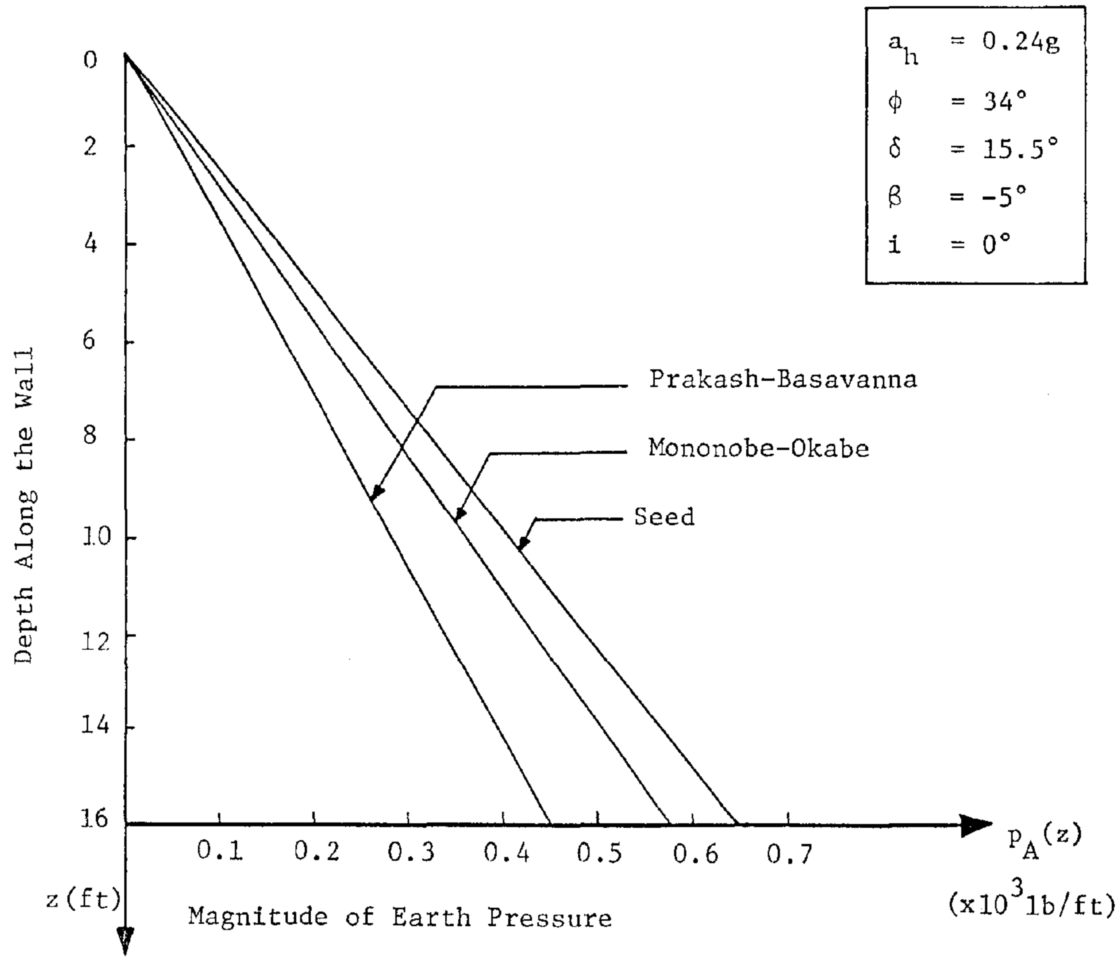

Figure 5.3 Comparison of the Pressure Distribution Obtained Through Currently Available Procedures.

Introducing the numerical values of the geometry and the material parameters into the above expressions, it is found that

$$C = 105{,}934.46 \text{ lb-ft/ft } (476\text{kN-m/m}),$$

$$D = 46{,}140.54 \text{ lb-ft/ft } (207.63\text{kN}).$$

Thus,

$$FS_o = \frac{105{,}934.46 \text{ lb-ft/ft}}{46{,}140.54 \text{ lb-ft/ft}} = 2.29$$

(b) Similarly, the factor of safety against sliding (FS_s) of the wall along its base is given by Eqn. (5-2a) in which C and D are equal to

$$\begin{aligned} C &= [P_A \sin(\delta+\beta) + W_w (1+k_v)]\tan\phi \\ D &= P_A \cos(\delta+\beta) + W_w k_h \end{aligned} \qquad (5\text{-}8)$$

Introducing the numerical values of the geometry and the material parameters into the above expression, it is found that

$$FS_s = \frac{11{,}260.82 \text{lb - ft/ft } (50.67\text{kN-m/m})}{7{,}812.864 \text{lb - ft/ft } (35.15\text{kN-m/m})} = 1.44$$

5.2.2 The Simplified M-O Method. From Eqn. (2-16), one has that for the simpliefied M-O method, the expression for the active thrust against the wall is

$$P_{AE} = \frac{1}{2} \gamma H^2 \left(K_A + \frac{3}{4} k_h\right)$$

in which,

K_A = the active thrust coefficient, given in Eqn. (2.5), and

k_h = the horizontal ground acceleration, assumed to be equal to 0.24g.

Introducing the numerical values of the goemetry and material parameters shown in Fig. 5.1 into the above expression, one has

$$P_{AE} = (\frac{1}{2})\ (100)\ (256)\ (0.224 + \frac{3}{4}\ 0.24) = 5171\ \text{lb/ft}\ (72.4\text{kN/m})$$

The point of application of P_{AE} is at $h_A = \frac{H}{3} = 5.33$ ft (1.62m) above the base of the wall.

In Fig. 5.3 is shown the pressure distribution along the wall as provided by the simplified M-O method.

The factor of safety of the wall is determined for the overturning and base sliding modes of failure as follows:

(a) The expression for FS in overturning (PS_o) is given by Eqn. (5-1). Introducing the numerical values of the geometry and material parameters (shown in Fig. 5.1) into Eqn. (5-7), it is found that

$$C = 106866.65\ \text{lb-ft/ft}\ (480.9\text{kN - m/m})$$

$$D = 49090.72\ \text{lb-ft/ft}\ (220.9\text{kN - m/m})$$

and, thus,

$$FS_o = \frac{106,866.65 \text{ lb-ft/ft}}{49,090.72 \text{ lb-ft/ft}} = 2.17$$

(b) The factor of safety against sliding (FS_s) of the wall along its base is given by Eqn. (5-2a). Introducing the numerical values of the various parameters (Fig. 5.1), it is found that

$$FS_s = \frac{11,329.88 \text{ lb-ft/ft } (50.98\text{kN - m/m})}{8,367.61 \text{ lb-ft/ft } (37.65\text{kN - m/m})} = 1.35$$

5.2.3 <u>The Prakash and Basavanna Method</u>. In Eqn. (2-17) is given the active thrust P_A against the wall as provided by the Prakash and Basavanna method. For the conditions shown in Fig. 5.1 (i = 0), Eqn. (2-17) becomes

$$P_A = \frac{1}{2}\gamma H^2 \frac{\sin^2(90°-\beta)[\cot(90°-\beta) + \cot\theta]}{\sin(90-\beta)\sin(90-\beta-\delta)} \{$$

$$\frac{a_h \tan(90°-\beta-\delta)}{\tan(90°-\beta-\delta) + \tan(\theta-\phi)} + \frac{1 + a_v}{\cot(90°-\beta-\delta) + \cot(\theta-\phi)}\}$$

Introducing into the above expression the numerical values of the geometry and material parameters (Fig. 5.1) and letting $\theta = 45° + \frac{\phi}{2}$, it is found that P_A is equal to

$$P_A = \left(\frac{1}{2}\right)(100)(256)(0.35) = 4480 \text{ lb/ft } (62.72\text{kN/m})$$

The point of application of P_A is at $h_A = \frac{H}{3} = 5.33$ ft (1.62m) above the base of the wall. The corresponding pressure distribution is shown in Fig. 5.3.

The factor of safety of the wall is determined for the overturning and sliding modes of failure as follows:

(a) The expression of the factor of safety is given by Eqn. (5-1) and the capacity and demand D by Eqns.(5-7).

Introducing the numerical values of the geometry and material parameters, shown in Fig. 5.1, into Eqns. (5-7), it is found that

$$C = 105357.89 \text{ lb - ft/ft } (474.1 \text{ kN - m/m})$$

$$D = 45469.9 \text{ lb - ft/ft } (204.6 \text{ kN - m/m})$$

and, thus,

$$FS_o = \frac{105357.89 \text{ lb - ft/ft}}{45469.9 \text{ lb - ft/ft}} = 2.31$$

(b) The factor of safety against sliding (FS_s) of the wall along its base is given in Eqn. (5-2a) and the expressions of the capacity C and demand D in Eqns. (5-8). Introducing the numerical values of the various parameters (Fig. 5.1), it is found that

$$FS_s = \frac{11{,}245.12 \text{ lb - ft/ft } (50.6\text{kN - m/m})}{7{,}687.04 \text{ lb - ft/ft } (34.59\text{kN- m/m})} = 1.46$$

5.2.4 <u>The Richard and Elms Method.</u>

The expression for the active thrust against the wall used in this method is given by Eqn. (2-20) as

$$P_{AE} = \frac{1}{2}\gamma H^2 \ (1-k_v)K_{AE}$$

in which

$$K_{AE} = \frac{\cos^2(\phi+\theta+\beta)}{\cos\theta\cos^2\beta\cos(\delta+\beta+\theta)\left[1+\left\{\frac{\sin(\phi+\delta)\sin(\phi-\theta-i)}{\cos(\delta+\beta+\theta)\cos(i-\beta)}\right\}^{1/2}\right]^2}$$

k_h = the coefficient of horizontal ground acceleration and

k_v = the coefficient of vertical ground acceleration

Letting $k_h = a_h = 0.24g$ and $k_v = a_v = \frac{2}{3}\,a_h = 0.16g$, and introducing into the expression for K_{AE} the values of the geometry and material parameters of the retaining wall under examination (Fig. 5.1), the resulting value of K_{AE} is $K_{AE} = 0.432$ and the value of the total force P_{AE} against the wall is equal to

$$P_{AE} = (\tfrac{1}{2})\ (100)\ (256)\ (0.84)\ (0.432) = 4{,}644.8 \text{ lb/ft } (65.02\text{kN/m})$$

The point of application of P_{AE} is at $h_A = \frac{H}{3} = 5.33$ ft (1.62m) above the base of the wall. The corresponding pressure distribution is shown in Fig. 5.2. The corresponding pressure distribution is shown in Fig. 5.2.

Introducing the value of $k_h = 0.24g$ into Eqn. (2-24) and assuming $A_a = A_v = 0.2$, one has that the resulting magnitude of the maximum displacement d between the wall and the backfill, given in Eqn. (2-24), is equal to

$$d = \frac{0.2A_v^{\;2}}{A_a} \left(\frac{A_a}{k_h}\right)^4$$

or,

$$d = \frac{0.2^3}{0.2} \left(\frac{0.2}{0.24}\right)^4 = 0.02 \text{ in (5mm)}$$

That is, for the examined conditions, the magnitude of the maximum displacement d is very small (approximately equal to zero). Thus, the Richard and Elms method provides the same results as the Mononobe-Okabe procedure ($FS_o = 2.29$ and $FS_s = 1.44$).

5.2.5 <u>The Extended Dubrova Method</u>. In Eqn. (2-25) is given the expression for the active thrust against the wall provided by Saran and Prakash (1977) as

$$P_A = \frac{1}{2}\gamma H^2 \; \frac{(1 + a_v)\cos^2(\psi-\lambda_1-\beta)}{\cos\lambda_1\cos^2\beta\cos(\delta+\beta+\lambda_1)} \left[1 + \frac{1}{\left\{\frac{\sin(\psi+\delta)\sin(\psi-\lambda_1)}{\cos\beta\cos(\delta+\beta+\lambda_1)}\right\}^{1/2}}\right]^2 \tag{5.9}$$

in which $\psi = \phi(1 - \frac{z}{H})$. This corresponds to the case where the wall rotates around point 0 (Fig. 5.1). Introducing the numerical values of the geometry and material parameters shown in Fig. 5.1, it is found that

$$P_A = 16{,}995 \text{ lb/ft } (237.93\text{kN/m})$$

The point of application P_A is found from equilibrium of moments around point 0 (Fig. 5.1) to be at h_A = 3.85 ft (1.17m) above its base.

The pressure distribution is obtained by forming the derivative of the above expression with respect to z; i.e.,

$$P_A(z) = \frac{dP_A}{dz} \tag{5-10}$$

The factor of safety of the wall is determined for the overturning and base sliding modes of failure as follows:

(a) The expression for FS in overturning (FS_o) is given by Eqn. (5-1) in which

$$C = (1 + k_v(W_w\ell + P_AB \sin(\delta+\beta)$$

$$D = P_Ah_a\cos(\delta+\beta) + k_h\ W_wh$$

Introducing the numerical values of the geometry and the material parameters into the above expressions, it is found that

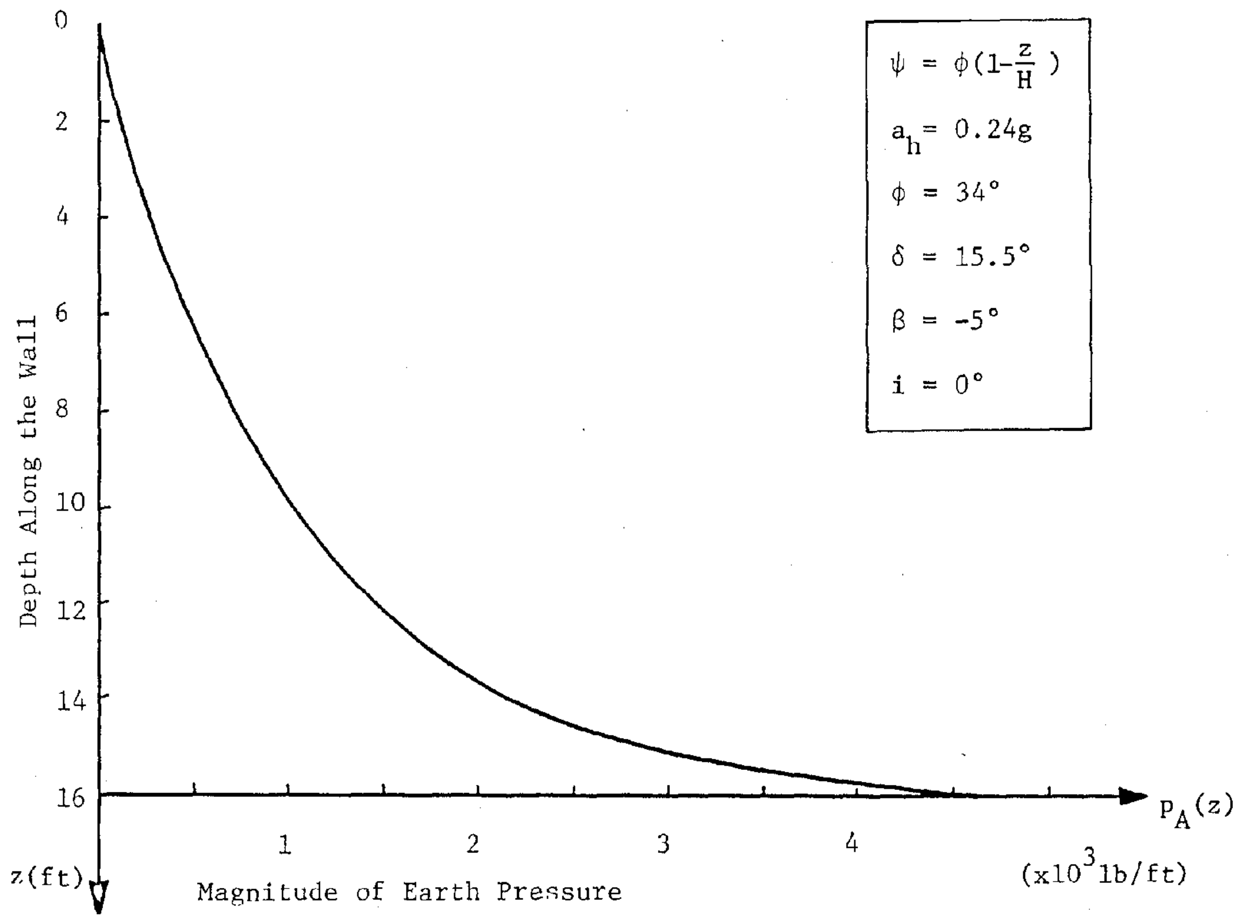

Figure 5.4 Pressure Distribution Along Wall in Accordance with the Extended Dubrova Method.

$$C = 126{,}224.37 \text{ lb-ft/ft } (568\text{kN-m/m})$$

$$D = 86{,}315.86 \text{ lb-ft/ft } (338\text{kN-m/m}).$$

Thus,

$$FS_o = \frac{126{,}224.37 \text{ lb-ft/ft}}{86{,}315.86 \text{ lb-ft/ft}} = 1.46$$

(b) Similarly, the factor of safety against sliding (FS_s) of the wall along its base is given by Eqn. (5-2a) in which the capacity C and the demand D are equal to

$$C = [P_A \sin(\delta+\beta) + W_w(1+k_v)] \tan\phi$$

$$D = P_A \cos(\delta+\beta) + W_w\ k_h$$

Introducing the numerical values of the geometry and the material parameter into the above expressions, it is found that

$$FS_s = \frac{12{,}780.37 \text{ lb-ft/ft } (57.51\text{kN-m/m})}{19{,}989.28 \text{ lb-ft/ft } (89.95\text{kN-m/m})} = 0.64$$

5.3 Comparison of Results

In Table 5.1 is given a summary of the values of the factors of safety found using each available procedure. It can be seen that the Dubrova (static) and the extended Dubrova (seismic) procedures resulted to more critical values for the factor of safety while, in

Table 5.1 Values of Factor of Safety for the Various Methods Examined

Conditions	Method	Factor of Safety	
		Overturning	Sliding
Static	Coulomb	5.9	3.39
	Dubrova	2.33	0.934
Seismic	Mononobe and Okabe	2.29	1.44
	Simplified M-O	2.167	1.35
	Prakash and Basavanna	2.31	1.46
	Richard and Elms	2.31	1.44
	Extended Dubrova	1.46	0.64

the case of the seismic conditions, the most critical value for the factor of safety correspond to the base sliding mode of failure.

5.4 Probabilistic Analysis.

The probabilistic approach described in Chapter 4 is applied to determine the safety of the retaining wall shown in Fig. 5.1. It is assumed that the wall is located in an earthquake area exhibiting the characteristics of Northeast United States, and that earthquakes are caused by a point source (Section 3.4.1).

The expressions for the mean value and variance of maximum horizontal ground acceleration are given in Eqns. (3-27) as

$$\bar{a}_{max} = \frac{b_1 e^{b_2 \bar{m}}}{(R + b_4)^{b_3}} \left[1 + \frac{1}{2} b_2^2 \, \mathrm{Var}(m) \right]$$

$$\mathrm{Var}(a_{max}) = \left[\frac{b_1 b_2 e^{b_2 \bar{m}}}{(R + b_4)^{b_3}} \right]^2 \mathrm{Var}(m)$$

in which b_1, b_2, b_3, b_4 are regional parameters. For the case of the Northeast U.S., these parameters may be assumed to be equal to (Donovan et al., 1973) $b_1 = 1,100$, $b_2 = 0.5$, $b_3 = 1.32$, and $b_4 = 25$.

Introducing these values into Eqns. (3-9), and letting $m_0 = 2$, $m_1 = 6.3$ and $\beta = 1.35$ (A-Grivas, et al., 1979), it is found that

$$\bar{m} = 2.72$$

and

$$Var(m) = 0.492$$

Substituting the above values for $\bar{m}$, Var(m), and regional parameters b_1, b_2, b_3, b_4 into Eqns. (3-27), and assuming that R = 1 km, one has that

$$\bar{a}_{max} = 0.63g$$

and

$$Var(a_{max}) = 0.426 \quad (\sigma_{a_{max}} = 0.0208g)$$

Furthermore, for the purposes of this example, it is assumed that the angle of internal friction ϕ and cohesion c of the backfill material are correlated random variables with mean values, standard deviations and correlation coefficient equal to

$$\bar{\phi} = 34.86° \quad , \quad \sigma_\phi = 9.13°$$

$$\bar{c} = 0.795 \text{ kips/ft}^2 (37.36 \text{kN/m}^2),$$

$$\sigma_c = 0.665 \text{ kips/ft}^2 (31.25\text{kN/m}^2)$$

$$\rho_{c,\phi} = -0.293$$

The active thrust P_A against the wall is found using the extended Dubrova Method for a rotation of the wall around its base. From Eqn. (2-25), one has

$$P_A = \frac{1}{2}\gamma H^2 \frac{(1+a_v)\cos^2(\psi-\lambda_1-\beta)}{\cos\lambda_1\cos^2\beta\cos(\delta+\beta+\lambda_1)} \left[\frac{1}{1+\left\{\frac{\sin(\psi+\delta)\sin(\psi-\lambda_1)}{\cos\beta\cos(\delta+\beta+\lambda_1)}\right\}^{1/2}} \right]^2$$

in which

$$\psi = \phi \left(1 - \frac{z}{H}\right)$$

5.4.1 Overturning. In the case of the overturning mode of failure of the retaining wall, capacity C and demand D are given by Eqns. (4-11) and (4-12), respectively, as

$$C = (1 + a_v)\, W_w\, \ell + P_A\, B \sin\delta'$$

$$D = P_A h_A \cos\delta' + a_h W_w h$$

in which $\delta' = \delta + \beta$ and all other parameters are shown in Fig. 5.1.

From the above expressions, it can be seen that C and D are functions of two random variables, namely, (a) the maximum horizontal ground acceleration a_h, and (b) the ϕ parameter of soil strength (both a_h and ϕ enter the expression for the total active thrust P_A). That is,

$$C = C\ (a_h, \phi)$$
$$D = D\ (a_h, \phi) \qquad (5\text{-}11)$$

The mean values and standard deviations of C and D can be found using the "point estimates method" presented for the first time by Rosenblueth (1975). In accordance with this method, the mean value of C is expressed in the form

$$\bar{C} = E[C] \simeq P_{++}C_{++} + P_{+-}C_{+-} + P_{-+}C_{-+} + P_{--}C_{--} \qquad (5\text{-}12)$$

in which C_{++} C_{+-}, C_{-+}, C_{--} are the point estimates of C, shown in Fig. 5.5, and P_{++}, P_{+-}, P_{-+}, P_{--} are the so-called "weights" of C. For the case of two uncorrelated random variables, the weights are all equal , i.e.,

$$P_{++} = P_{+-} = P_{-+} = P_{--} = \frac{1}{4}$$

The second moment of C, denoted as $E[C^2]$, is found from the following expression:

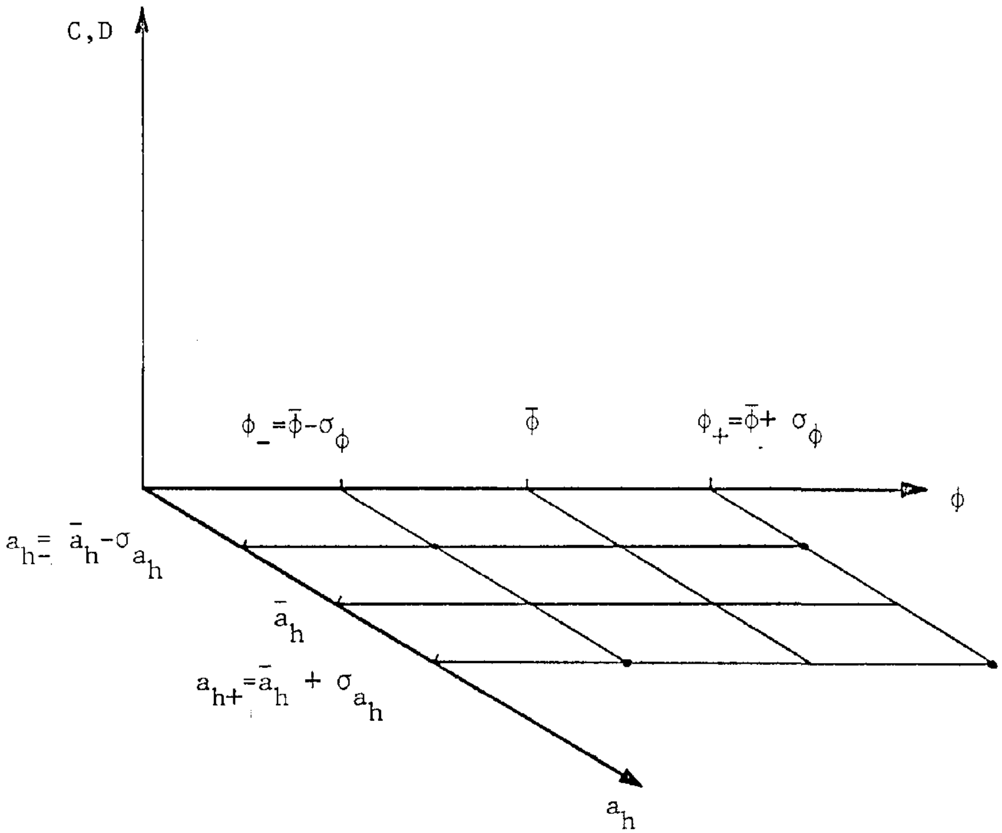

Point Estimates

ϕ	$\phi_+ = \bar{\phi} + \sigma_\phi$ $\phi_- = \bar{\phi} - \sigma_\phi$
a_h	$a_{h_+} = \bar{a}_h + \sigma_{a_h}$ $a_{h-} = \bar{a}_h - \sigma_{a_h}$
C	$C_{++} = C\ (\phi_+, a_{h+})$ $C_{+-} = C\ (\phi_+, a_{h-})$ $C_{-+} = C\ (\phi_-, a_{h+})$ $C_{--} = C\ (\phi_-, a_{h-})$
D	$D_{++} = D\ (\phi_+, a_{h+})$ $D_{+-} = D\ (\phi_+, a_{h-})$ $D_{-+} = D\ (\phi-, a_{h+})$ $D_{--} = D\ (\phi_-, a_{h-})$

Figure 5.5 Illustration of the Point Estimates of C and D.

$$E\,[C^2] = P_{++}\,C_{++}^{\;2} + P_{+-}\,C_{+-}^{\;2} + P_{-+}\,C_{-+}^{\;2} + P_{--}C_{--}^{\;2} \qquad (5\text{-}13)$$

The standard deviation σ_C of C is determined from the mean value and second moment of C as follows:

$$\sigma_C = \{E\,[C^2] - (E[C])^2\}^{1/2} \qquad (5\text{-}14)$$

Similarly, the mean value and standard deviation of the demand D are expressed as

$$\bar{D} = E[D] \simeq P_{++}\,D_{++} + P_{-+}\,D_{+-} + P_{-+}\,D_{-+} + P_{--}\,D_{--} \qquad (5\text{-}15)$$

$$\sigma_D = \{E[D^2] - (E[D])^2\}^{1/2} \qquad (5\text{-}16)$$

in which $E[D^2]$ is the second moment of D.

Introducing the numerical values of the mean values $(\bar{a}_h, \bar{\phi})$ and standard deviations $(\sigma_{a_h}, \sigma_\phi)$ of a_h and ϕ into the expressions for the point estimates of C and D, the latter are found to be equal to

C_{++} = 112,131.9 lb-ft/ft(504.6kN-m/m)

C_{+-} = 112,090.9 lb-ft/ft(504.4kN-m/m)

C_{-+} = 108,915.5 lb-ft/ft(490.1kN-m/m)

C_{--} = 108,902.0 lb-ft/ft(490 kN-m/m)

D_{++} = 56,438.3 lb-ft/ft (254 kN-m/m)

D_{+-} = 63,627.2 lb-ft/ft (286.3kN-m/m)

D_{-+} = 51,161.3 lb-ft/ft (230.2kN-m/m)

D_{--} = 58,276 lb-ft/ft (262.2kN-m/m)

After the above values of the point estimates and weights of C and D are introduced into Eqns. (5-12), (5-14), (5-15) and (5-16), it is found that

$\bar{C}$ = 110,510 lb-ft/ft (497.3kN-m/m)

σ_C = 1,601 lb-ft/ft (7.2 kN-m/m)

$\bar{D}$ = 57,376 lb-ft/ft (20. kN-m/m)

σ_D = 4,455 lb-ft/ft (20. kN-m/m)

The value of the central factor of safety in overturning is then equal to

$$\overline{FS}_o = \frac{\bar{C}}{\bar{D}} = \frac{110{,}501 \text{ lb-ft/ft}}{57{,}376 \text{ lb-ft/ft}} = 1.92$$

The mean value $\overline{SM}$ and standard deviation σ_{SM} of the safety margin SM are found from Eqn. (4-3) to be equal to

$\overline{SM} = \bar{C} - \bar{D}$ = 53,134.4 lb -ft/ft (239. kN-m/m)

$\sigma_{SM} = (\sigma_C^2 + \sigma_D^2)^{1/2}$ = 4,734.1 lb-ft/ft (21.3 kN-m/m)

Finally, assuming that the safety margin SM follows a normal distribution, the probability of failure p_{f_o} in overturing is found from Eqn. (4-5) to be equal to

$$p_{f_o} = P[SM \leq 0] = P\left[\frac{SM-\bar{SM}}{\sigma_{SM}} \leq \frac{0-5,313.4}{4,734.1}\right]$$

If $u = \frac{SM-\bar{SM}}{\sigma_{SM}}$ denotes the standardized normal variate, then the above expression can be written as

$$p_{f_o} = P\,[SM \leq 0] = P[u \leq -11.3]$$

From tables of the standard normal distribution (Harr, 1977), and has that $P\,[u \leq 11.3] \cong 0.0$ and, therefore,

$$p_{f_o} \simeq 0.0$$

5.4.2 Bearing Capacity. In the case of bearing capacity of the wall foundation, capacity C and demand D are given by Eqns. (4-13) and (4-14), respectively; i.e.,

$$C = \frac{1}{2}\gamma B'^2 N_\gamma + \gamma\, D_f\, B' N_q + N_c B' c$$

$$D = (D_v^{\;2} + D_H^{\;2})^{1/2}$$

in which

$$D_H = P_A \cos(\delta+\beta) + a_h\, W_w$$

$$D_v = P_a \sin(\delta+\beta) + (1 + a_v)\, W_w$$

and all other parameters are shown in Fig. 5.1. In this case, C is a function of two correlated random variables, namely, the cohesion c and angle of internal friction ϕ of the foundation material, or

$$C = C\ (c,\phi)$$

while demand D is a function of two uncorrelated random variables a_h and ϕ, or

$$D = D(a_h,\phi)$$

The numerical values of the point estimates of C and D are equal to

$$C_{++} = 1{,}108.4 \text{ lb } (5.0\text{kN})$$
$$C_{+-} = 393 \text{ lb } (1{,}8\text{kN})$$
$$C_{-+} = 163.3 \text{ lb } (0.1\text{kN})$$
$$C_{--} = 31.3 \text{ lb } (0.1\text{kN})$$
$$D_{++} = 22.4 \text{ lb } (0.1\text{kN})$$
$$D_{+-} = 22.4 \text{ lb } (0.1\text{kN})$$
$$D_{-+} = 21.4 \text{ lb } (0.1\text{kN})$$
$$D_{--} = 21.4 \text{ lb } (0.09\text{kN})$$

As the correlation coefficient ($\rho_{c,\phi}$) of c and is equal to -0.293 ($\rho_{c,\phi}$ = -0.293), the numerical values of the weights for the of the weights for the capacity C are

$$P_{++} = P_{--} = \frac{1 + \rho_{c,\phi}}{4} = \frac{1 - 0.293}{4} = 0.176$$

$$P_{+-} = P_{-+} = \frac{1 - \rho_{c,\phi}}{4} = \frac{1 + 0.293}{4} = 0.323$$

while the weights for demand D are all equal to $\frac{1}{4}$.

Introducing the above values of the point estimates and weights of C and D into Eqns. (5-12), (5-14), (5-15) and (5-16), it is found that

$$\bar{C} = 380.3 \text{ lb } (1.71\text{kN})$$

$$\sigma_C = 360.9 \text{ lb } (1.6 \text{ kN})$$

$$\bar{D} = 21.9 \text{ lb } (0.09\text{kN})$$

$$\sigma_D = 0.6 \text{ ln } (0.003\text{kN})$$

The value of the central factor of safety in bearing capacity is then equal to

$$\bar{FS}_{bc} = \frac{\bar{C}}{\bar{D}} = \frac{380.3 \text{ lb}}{21.9 \text{ lb}} = 17.38$$

From Eqn. (4-3), the mean value $\bar{SM}$ and standard deviation σ_{SM} of the safety margin SM are found to be equal to

$$\bar{SM} = \bar{C} - \bar{D} = 358.4 \text{ lb } (1.6\text{kN})$$

$$\sigma_{SM} = (\sigma_C^2 + \sigma_D^2)^{1/2} = 361.0 \text{ lb } (1.6\text{kN})$$

Assuming that the safety margin SM follows a normal distribution, the probability of failure $p_{f_{bc}}$ in bearing capacity is found from Eqn. (4-5) to be equal to

$$p_{f_{bc}} = P[SM \leq 0] = P[\frac{SM - \bar{SM}}{\sigma_{SM}} \leq \frac{0-358.4}{360.9}]$$

If $u = \frac{SM-\bar{SM}}{\sigma_{SM}}$ denotes the standardized normal variate, then the value of $p_{f_{bc}}$ may be determined using tables (Harr, 1977) as

$$p_{f_{bc}} = P[SM \leq 0] = P[u \leq -0.99] = 0.162$$

5.4.3 Base Sliding. In the case of failure of the retaining wall in base sliding, capacity C and demand D are given by Eqns. (4-15) and (4-16) in the form

$$C = [P_A \sin(\delta+\beta) + W_w(1 + a_v)] \tan\phi$$

$$D = P_A \cos(\delta+\beta) + a_h W_w$$

The geometry of the wall and the parameters of the backfill material are shown in Fig. 5.1. In this case, C and D are functions of the two uncorrelated random variables a_h and ϕ; i.e.,

$$C = C(a_h, \phi)$$

$$D = D(a_h, \phi)$$

The point estimates for C and D are

$$C_{++} = 16{,}360 \text{ lb } (73.6 \text{ kN})$$
$$C_{+-} = 8{,}169.4 \text{ lb } (36.8 \text{ kN})$$
$$C_{-+} = 15{,}900.2 \text{ lb } (71.6 \text{kN})$$
$$C_{--} = 7{,}941.1 \text{ lb } (35.7 \text{kN})$$

$$D_{++} = 14{,}690 \text{ lb } (66.105 \text{kN})$$
$$D_{+-} = 14{,}660 \text{ lb } (65.97 \text{kN})$$
$$D_{-+} = 13{,}610 \text{ lb } (61.24 \text{kN})$$
$$D_{--} = 13{,}600 \text{ lb } (61.2 \text{ kN})$$

while the values of the weights for both C and D are equal to $\frac{1}{4}$.

Introducing the above values of the point estimates and weights of C and D into Eqns. (5-12),(5-14), (5-15) and (5-16), it is found that

$$\bar{C} = 12{,}092.67 \text{ lb } (54.41 \text{ kN})$$

$$\sigma_C = 4{,}041.52 \text{ lb } (18.18 \text{ kN})$$

$$\bar{D} = 14{,}140 \text{ lb } (63.63 \text{ kN})$$

$$\sigma_D = 535.1 \text{ lb } (2.4 \text{ kN})$$

The value of the central factor of safety in base sliding is then equal to

$$FS_s = \frac{\bar{C}}{\bar{D}} = \frac{12{,}092.67 \text{ lb}}{14{,}140 \text{ lb}} = 0.85$$

From Eqn. (4-3), the mean value $\overline{SM}$ and standard deviation σ_{SM} of the safety margin SM are found to be equal to

$$\overline{SM} = \bar{C} - \bar{D} = -2{,}047.33 \text{ lb } (-9.21 \text{kN})$$

$$\sigma_{SM} = 4{,}076.79 \text{ lb } (18.34 \text{kN})$$

Assuming that the safety margin SM follows a normal distribution, the probability of failure p_{f_s} in base sliding is determined as

$$p_{f_s} = P[SM \leq 0] = P\left[\frac{SM-\overline{SM}}{\sigma_{SM}} \leq \frac{0 + 2{,}047.33}{4{,}076.79}\right]$$

If $u = \dfrac{SM-\overline{SM}}{\sigma_{SM}}$ in the standardized normal variate, then the value of p_{f_s} is found from tables to be

$$p_{f_s} = P[SM \leq 0] = P[u \leq 0.5] = 0.691$$

5.4.4 Overall Sliding. In the case of failure of the retaining wall in overall sliding, capacity C and demand D are given by Eqns. (4-17) and (4-18), in the form (Figs. 4.6 and 5.1)

$$C = c\ R\ \Sigma\Delta\ell_i + R\ (1+a_v)\ \tan\phi[\Sigma W_i\ \cos\theta_i]$$

$$D = R\ [\Sigma W_i \sin\theta_i]\ (1+a_v) + a_h(\Sigma W_i y_i) + P_A y_A$$

In this case, capacity C is a function of three random variables, namely, cohesion (c), angle of internal friction (ϕ), and maximum horizontal ground acceleration (a_h), two of which (i.e., c, ϕ) are correlated; or,

$$C = C(a_h, \phi, c)$$

Demand D is a function of two random variables (ϕ and a_h); i.e.,

$$D = D\ (a_h, \phi)$$

Using the numerical point estimates method, one has that the mean values and standard deviations for C and D are equal to

$$\bar{C} = P_{+++}\ C_{+++} + P_{++-}\ C_{++-} + P_{+-+}\ C_{+-+} +$$

$$+ P_{-++}\ C_{-++} + P_{+--}\ C_{+--} + P_{-+-}\ C_{-+-} +$$

$$+ P_{--+}\ C_{--+} + P_{---}\ C_{---}$$

$$\sigma_C = \{ \ E[C^2] - (E[C])^2 \ \}^{1/2}$$

$$\bar{D} = P_{++}\ C_{++} + P_{+-}\ C_{+-} + P_{-+}\ C_{-+} + P_{--}\ C_{--}$$

$$\sigma_D = \{E[D^2] - (E[D^2])^2 \}^{1/2}$$

Introducing the numerical values of the mean values ($\bar{a}_h$, $\bar{\phi}$, $\bar{c}$) and standard deviations (σ_{a_h}, σ_ϕ, σ_c) of a_h, ϕ and c, the corresponding values of the point estimates of C are

C_{+++} = 2,208.0 lb - ft/ft (9.9 kN-m/m)

C_{++-} = 2,188.7 lb - ft/ft (9.8 kN-m/m)

C_{+-+} = 869.0 lb - ft/ft (3.9 kN-m/m)

C_{-++} = 1,828.4 lb - ft/ft (8.2 kN-m/m)

C_{+--} = 869.0 lb - ft/ft (2.9 kN-m/m)

C_{-+-} = 1,818.3 lb - ft/ft (8.2 kN-m/m)

C_{--+} = 889.2 lb - ft/ft (4.0 kN-m/m)

C_{---} = 498.6 lb - ft/ft (2.2 kN-m/m)

while those of D are

$$D_{++} = 485.6 \text{ lb-ft/ft } (2.2 \text{ kN-m/m})$$

$$D_{+-} = 477.7 \text{ lb-ft/ft } (2.2 \text{ kN-m/m})$$

$$D_{-+} = 460.9 \text{ lb-ft/ft } (2.0 \text{ kN-m/m})$$

$$D_{--} = 453.3 \text{ lb-ft/ft } (2.0 \text{ kN-m/m})$$

The numerical values of the weights for capacity C are equal to

$$P_{+++} = P_{---} = P_{++-} = P_{--+} = \frac{1 + \rho_{c,\phi}}{8} = \frac{1-0.293}{8} = 0.088$$

$$P_{+-+} = P_{-++} = P_{+--} = P_{-+-} = \frac{1 - \rho_{c,\phi}}{8} = \frac{1+0.293}{8} = 0.161$$

while those of D are

$$P_{++} + P_{+-} = P_{-+} = P_{--} = \frac{1}{4}$$

Introducing the above values of the point estimates and weights of C and D into Eqns. (5-12), (5-14), (5-15) and (5-16), it is found that

$$\bar{C} = 1{,}375.99 \text{ lb-ft/ft } (6.19 \text{kN-m/m})$$

$$\sigma_c = 602.01 \text{ lb-ft/ft } (2.70 \text{kN-m/m})$$

and

$$\bar{D} = 469.35 \text{ lb-ft/ft } (211 \text{kN-m/m})$$

$$\sigma_D = 13.03 \text{ lb-ft/ft } (0.058 \text{kN-m/m})$$

The value of the central factor of safety in overall sliding is then equal to

$$\overline{FS}_{os} = \frac{\bar{C}}{\bar{D}} = \frac{1{,}375.99 \text{ lb - ft/ft}}{469.35 \text{ lb - ft/ft}} = 2.93$$

From Eqn. (4-3), one has that the mean value $\bar{SM}$ and standard deviation σ_{SM} of the safety margin SM are equal to

$$\bar{SM} = \bar{C} - \bar{D} = 906.6 \text{ lb-ft/ft } (4.1 \text{ kN-m/m})$$

$$\sigma_{SM} = (\sigma_C^2 + \sigma_D^2)^{1/2} = 602.2 \text{ lb - ft/ft } (2.7 \text{ kN-m/m})$$

Assuming that the safety margin SM follows a normal distribution, the probability of failure $p_{f_{bs}}$ in overall sliding is found from from Eqn. (4-5) to be equal to

$$p_{f_{os}} = P\ [SM \leq 0\ ] = P\ [\frac{SM-\bar{SM}}{\sigma_{SM}} \leq \frac{0-906.64}{602.15}\ ]$$

If $u = \frac{SM-\bar{SM}}{\sigma_{SM}}$ is the standardized normal variate, then the value of $p_{f_{os}}$ is found from tables to be

$$p_{f_{os}} = P\ [SM \leq 0\ ] = P\ [u \leq -\ 1.5] = 0.067$$

5.4.5 Summary of Results. In Table 5.2 is given a summary of the obtained results, including the statistical values of capacity and demand, the values of the central factor of safety, and the corresponding values of the probability of failure for each mode of failure examined.

Table 5.2 Summary of Results of Probabilistic Analysis

Mode of Failure	Capacity		Demand		Central Factor of Safety	Probability of Failure
	$\bar{C}$	σ_C	$\bar{D}$	σ_D	$\bar{FS}$	P_f
Overturning [lb-ft/ft)	110,510.1	1,601.4	57,375.7	4,455.0	1.9	0.0
Bearing Capacity [lb/ft]	380.3	361.0	21.9	0.6	17.38	0.162
Base Sliding [lb/ft]	12,092.7	4,041.5	14,140.0	535.1	0.86	0.691
Overall Sliding [lb-ft/ft]	1,376.0	602.0	469.4	13.0	2.9	0.067

The value of the total probability of failure p_f is found using Eqn. (4-10) to be equal to $p_f = 0.758$.

CHAPTER 6

PARAMETRIC STUDY

The purpose of the present parametric study is to examine the effect on the factor of safety and the pressure distribution along a retaining wall of (a) the magnitude of the maximum horizontal ground acceleration, (b) the ϕ-parameter of strength, and (c) the inclination of the backfill material.

The retaining wall used for the purposes of this parametric study is shown schematically in Fig. 6.1. It has a height H = 16 ft (4.88m) and an average thickness of 6 ft (1.83m). The angle β between the back side of the wall and the vertical is equal to $\beta = 15°$. The backfill material has a unit weight equal to γ = 100 pcf (15.7 kN/m^3) while the unit weight of the concrete is γ_c = 150 pcf (23.55 kN/m^3).

The method employed in the parametric study is the extended Dubrova procedure, described in Section 2.2.5. It is assumed that the wall rotates around its top and, therefore, the expression for the ψ function is (Table 2.1)

$$\psi(z) = \phi \frac{z}{H}$$

The total active thrust on the wall is given by Eqn. (2-25) as

$$P_A = \frac{1}{2}\gamma H^2 \frac{(1+a_v)\cos^2(\psi-\lambda_1-\beta)}{\cos\lambda_1 \cos^2\beta(\delta+\beta+\lambda_1)} \left[\frac{1}{1+\left\{\frac{\sin(\psi+\delta)\sin(\psi-i-\lambda_1)}{\cos(\beta-i)\cos(\delta+\beta+\lambda_1)}\right\}^{1/2}}\right]^2 \qquad (6\text{-}1)$$

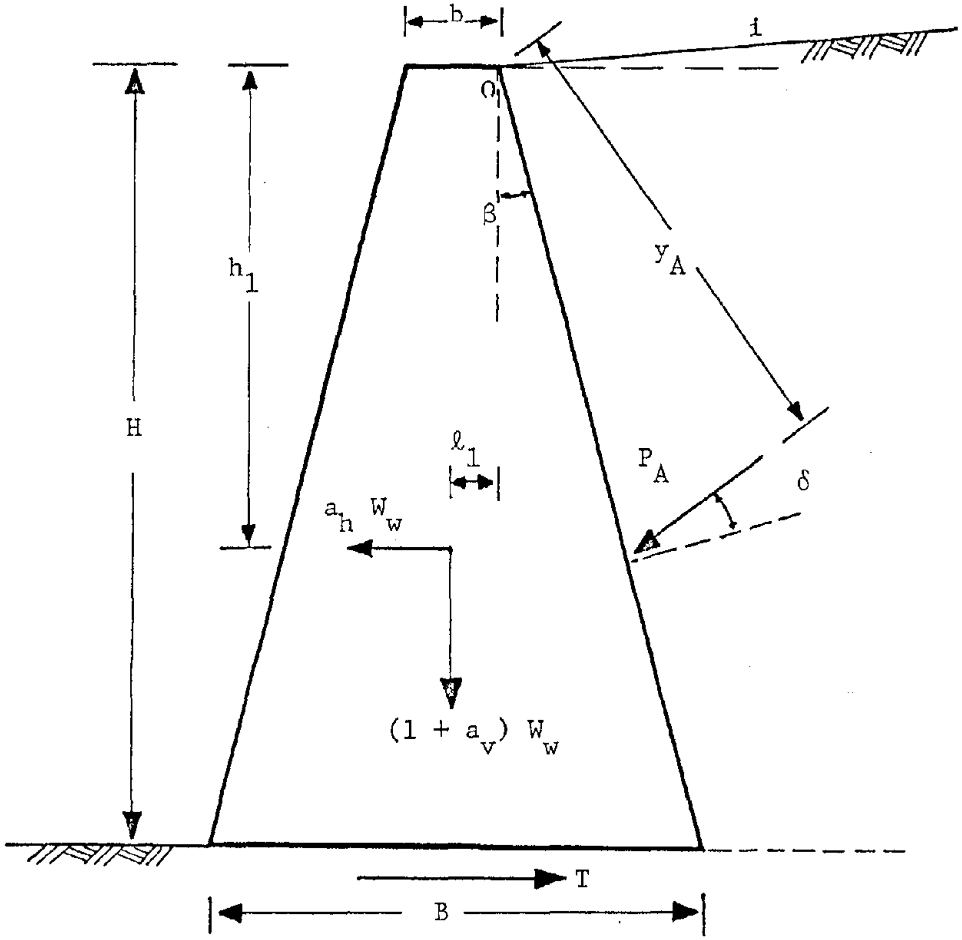

Geometry and Material Parameters:

$H = 16$ ft (4.8m)

$B = 10$ ft (3m)

$b = 2$ ft (0.6m)

$h_1 = 9.8$ ft (2.9m)

$\ell_1 = 1$ ft (0.3m)

$\gamma = 100$ lb/ft^3 (15.7kN/m^3)

$\gamma_c = 150$ lb/ft^3 (23.5kN/m^3)

$\psi = \frac{\phi z}{H}$

Figure 6.1 Geometry and Material Parameters of the Retaining Wall Used in the Parametric Study.

in which the geometry and material parameters are shown in Fig. 6.1.

The expression for the pressure distribution $P_A(z)$ along the wall is obtained by forming the derivative of P_A with respect to z (Appendix A).

6.1 Effect of the Maximum Horizontal Ground Acceleration

In Fig. 6.2 is shown the resulting pressure distribution $p_A(z)$ along the retaining wall for various values of the maximum horizontal ground acceleration a_h. It can be seen that the magnitude of $p_A(z)$ increases considerably for increasing values of a_h. The vertical component of the acceleration a_v is assumed to be equal to $a_v = \frac{2}{3} a_h$ while the other geometry and material parameters are given in Fig. 6.1 ($\phi = 30°$, $\beta = 15°$ and $i = 5°$).

6.2 Effect of the ϕ - Parameter of Strength.

The effect of the ϕ-parameter of strength on the pressure distribution $p_A(z)$ is shown in Fig. 6.3. The results were obtained for $a_h = 0.3g$, $a_v = \frac{2}{3} a_h$, $\beta = 15°$ and, and $i = 5°$ (Fig. 6.1). From Fig. 6.3, it is seen that the magnitude of the pressure $p_A(z)$ decreases considerably as the value of ϕ increases.

6.3 Effect of the Inclination of the Backfill.

In Fig. 6.4 is shown the effect on the $p_A(z)$ of the backfill slope i for $a_h = 0.3g$, $a_v = \frac{2}{3} a_h$, $\phi = 30°$, and $\beta = 15°$ (Fig. 6.1). It

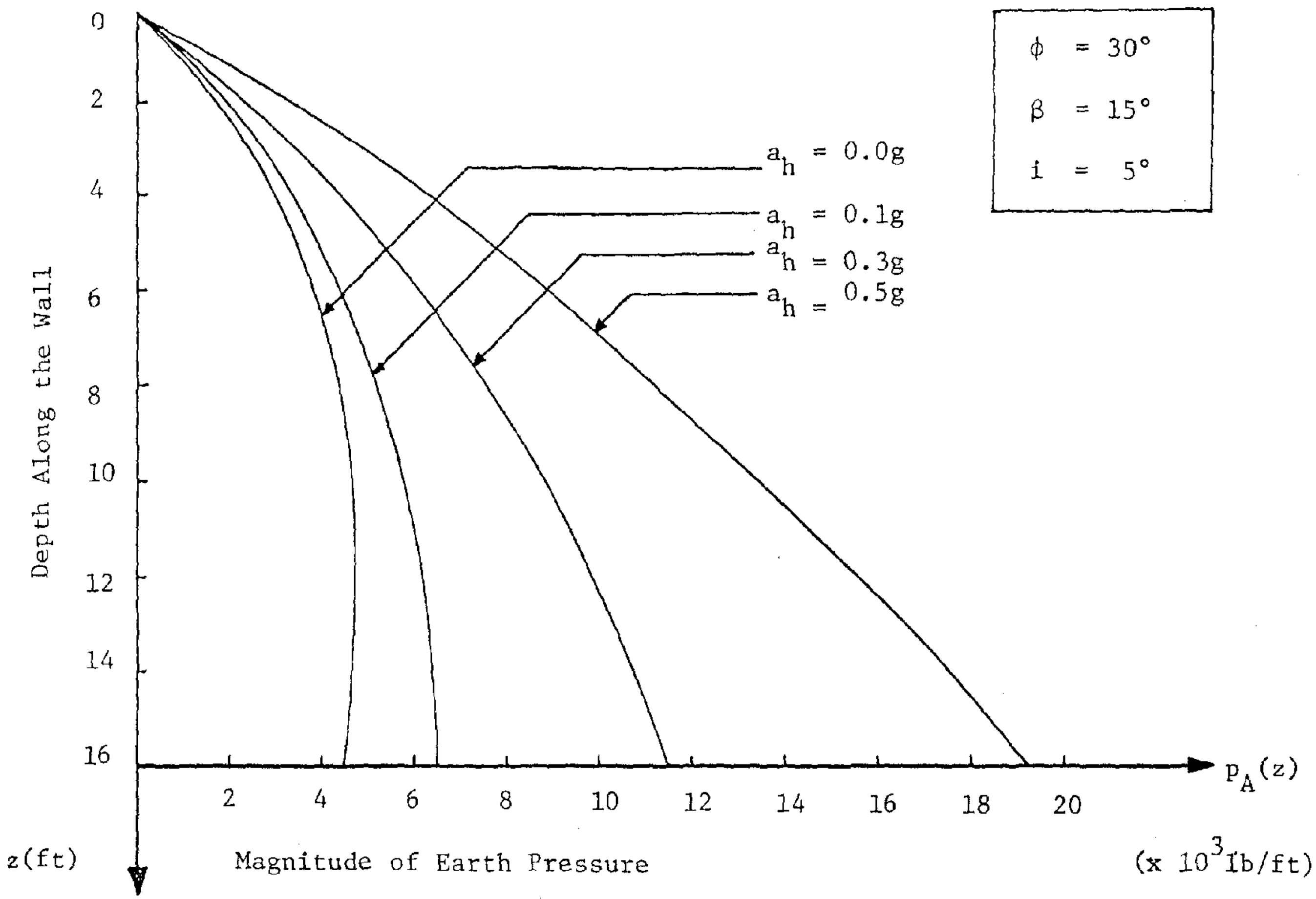

Figure 6.2 Dependence of Pressure Distribution Along the Wall on the Maximum Horizontal Ground Acceleration.

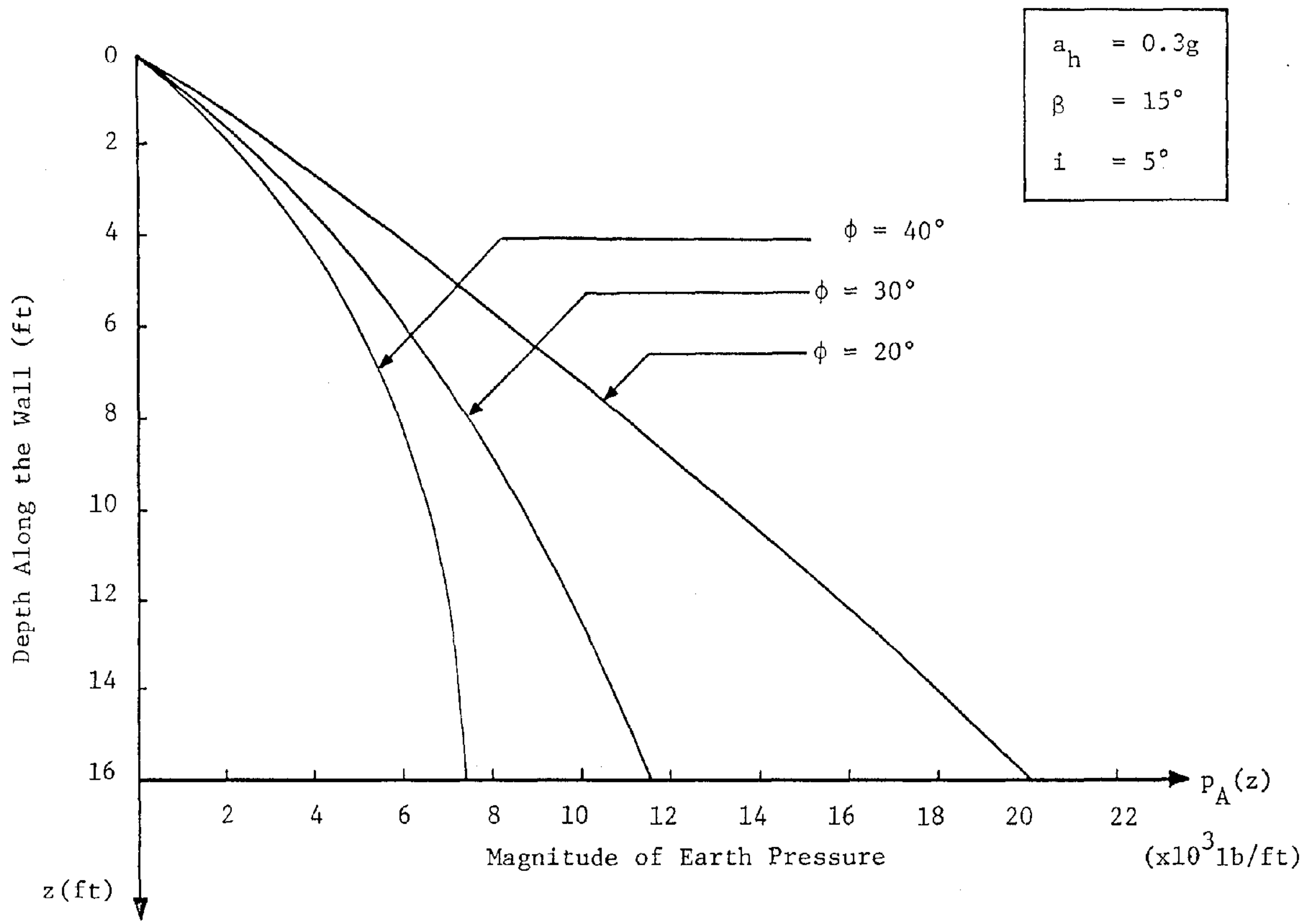

Figure 6.3 Dependence of the Pressure Distribution along the Wall on the ϕ Parameter of Strength.

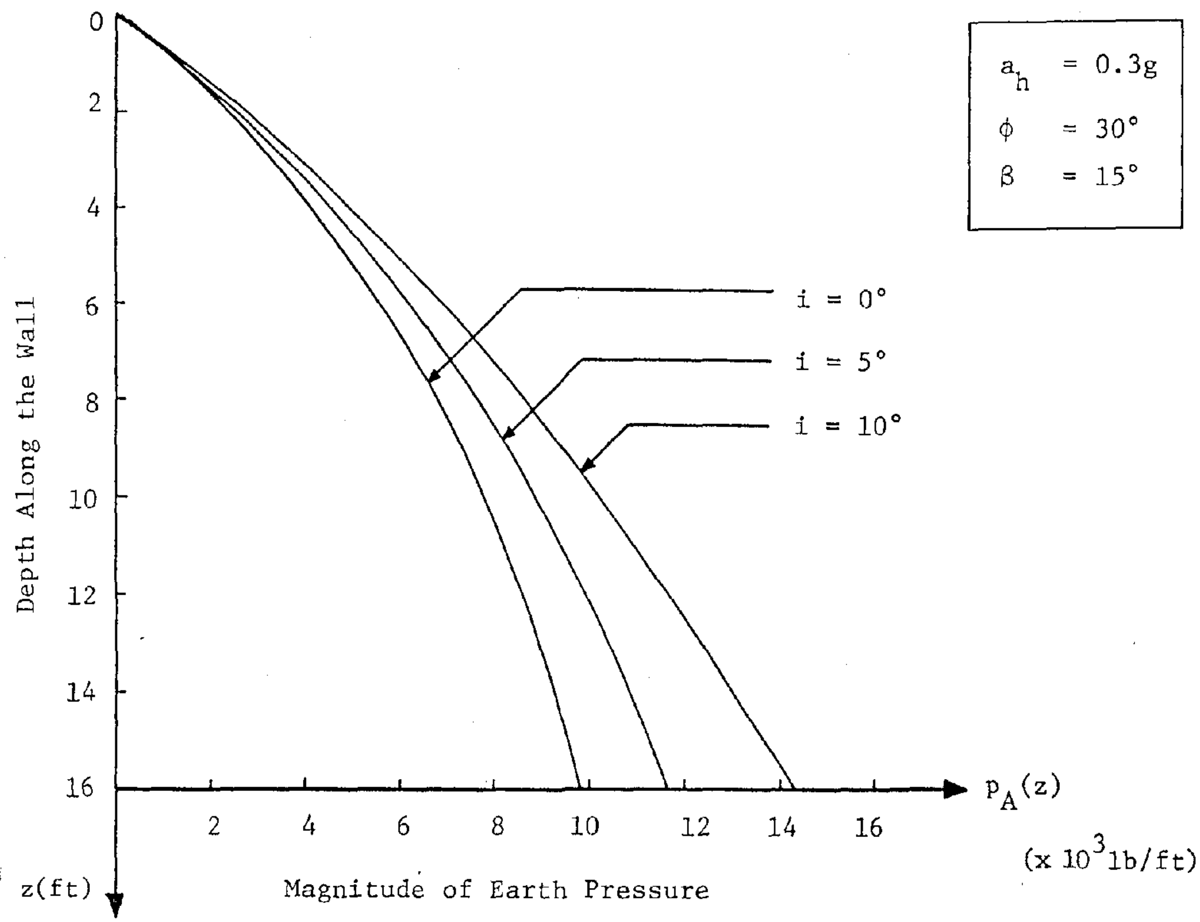

Figure 6.4 Dependence of the Pressure Distribution Along the Wall on the Inclination of the Backfill i.

can be seen that the dependence of $p_A(z)$ on the inclination of the backfill i is not as important as that of the maximum horizontal ground acceleration a_h and the strength parameter ϕ.

6.4 The Effect on the Factor of Safety of a_h, ϕ, and i.

Fig. 6.5 shows the dependence of the factor of safety FS of the retaining wall in overturning around its top (Fig. 6.1) of (a) the maximum horizontal ground acceleration, (b) the ϕ parameter of strength and (c) the slope i of the backfill material. In its present form, Fig. 6.5 constitutes a nomograph associated with the retaining wall shown in Fig. 6.1 which can be used to determine the value of the factor of safety FS for combinations of values of the design parameters, a_h, ϕ, and i.

From Fig. 6.5, it is seen that as ϕ decreases and/or a_h and i increase, the corresponding values of the factor of safety FS decrease.

The analytical expression for the factor of safety FS of the retaining wall in overturning is given in Appendix B.

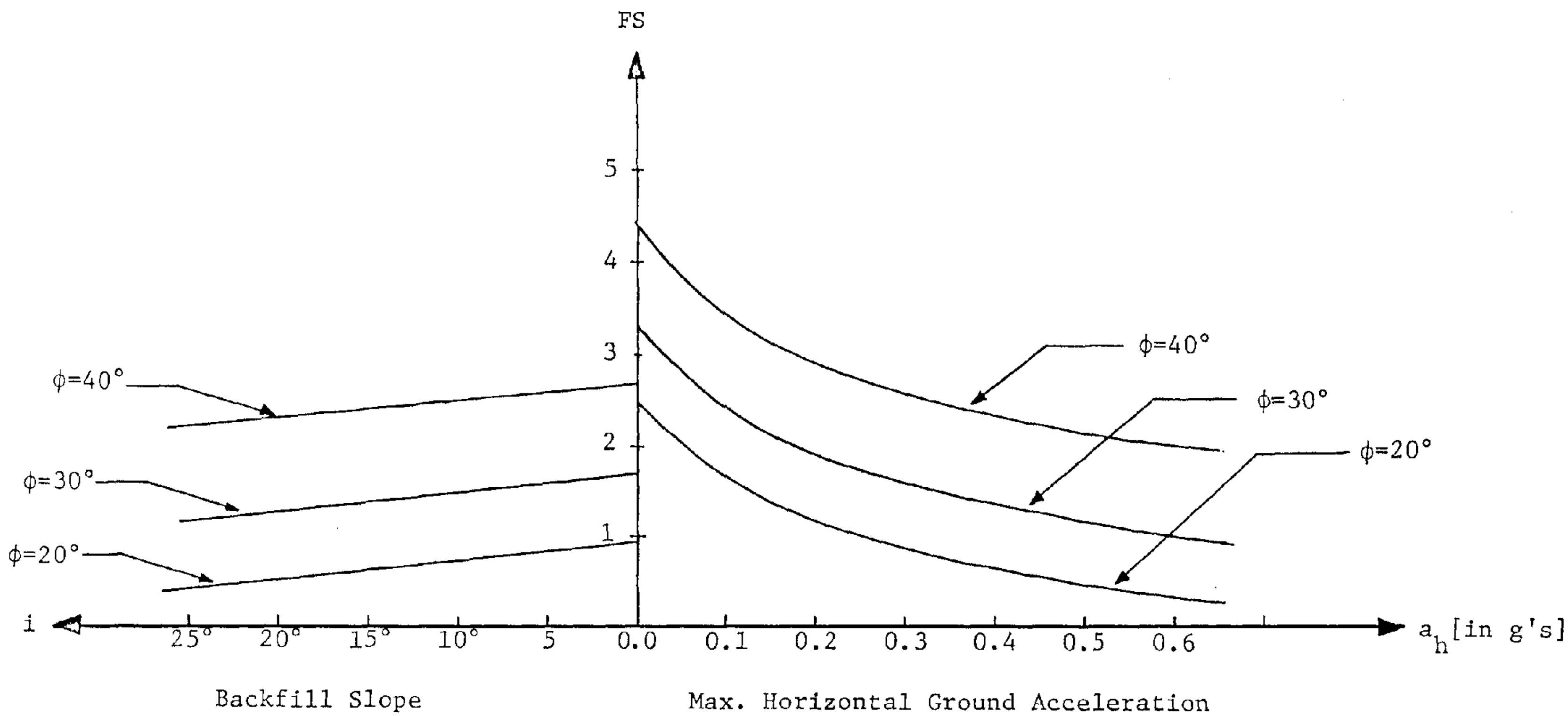

Figure 6.5 Dependence of the Factor of Safety FS in Overturning Around the Top of the Wall of a_h, ϕ and i.

CHAPTER 7

DISCUSSION

Experience with the performance of retaining walls indicates that the pressure distribution along such structures depends on the type and magnitude of the movement they are subjected to during loading. From among all the procedures reviewed in this study (Chapter 2), only one is capable of accounting for the occurring movement in order to arrive at an expression for the magnitude of the pressure and its distribution along the wall. This is the Dubrova method, initially developed for static conditions (Dubrova, 1963) and later extended in order to include seismic loading (Saran and Prakash, 1977; A-Grivas, 1978).

In accordance with the Dubrova method, the pressure distribution along a wall is expressed in terms of the ψ function which depends on two quantities: (a) the magnitude of the soil strength mobilized in the backfill material, and (b) the type of movement the wall experiences during loading. The wall is allowed to rotate around any point along its vertical axis and the resulting limiting state of the backfill material can be either active or passive or partially active and partially passive. For example, a rotation of the wall around its mid-point, with the top moving towards the backfill, will produce a passive state for the upper half of the soil medium while the lower half will be in an active state. This is shown schematically in Fig. 2.4(e). Moreover, the method assumes that all soil strength available is mobilized at the extreme points of the backfill medium (i.e., behind the top and bottom of the wall).

While the Dubrova method considers the type of movement the wall undergoes during loading, it does not account explicitly for the magnitude of this movement. That is, for a rotation of the wall around a given point, the resulting pressure distribution is independent of the magnitude of the rotation.

The method by Richard and Elms (Section 2.2.4) takes into consideration the magnitude of the permanent displacement experienced by the wall during the ground shaking. This is achieved by employing a previously developed empirical relationship between the maximum permanent ground displacement and the effective peak ground acceleration and velocity. In addition, this method considers the change in the inertia of the wall that occurs during the seismic loading, a novel concept that leads to an improved measure for the factor of safety.

In a comparative study, the safety of a retaining wall (Fig. 5.1) was examined using the various procedures presented in Chapter 2. Two modes of wall failur were considered, namely, overturning and base sliding. From Table 5.1, it can be seen that there is a rather wide scatter in the resulting numerical values of the factor of safety. Under static conditions, the Dubrova method produced a more critical value for FS than did the Coulomb method. The extended version of the Dubrova method also resulted to the most critical value for FS under seismic loading.

In the presented probabilistic procedure, the seismic load

(Section 5.4) was expressed in terms of the maximum horizontal ground acceleration (a_h) experienced by the retaining wall during an earthquake. It was assumed that the vertical component of the maximum ground acceleration has a value equal to two thirds that of the horizontal component, and that both components act on the retaining wall and backfill material simultaneously.

The statistical values of the capacity C and demand D of each mode of failure were determined using the point estimates method provided by Rosenblueth (1975). This is an approximate procedure capable of providing estimates for the statistical values of C and D on the basis of the mean values and standard deviations of the material and seismic parameters.

Finally, from the results obtained during the parametric study (Chapter 6), it is seen that the maximum horizontal ground acceleration and the ϕ parameter of strength of the backfill material have a considerable effect on the pressure distribution along the wall and the corresponding value of its factor of safety. The effect of the slope of the backfill material on these two quantities was found to be considerably smaller.

CHAPTER 8

SUMMARY AND CONCLUSIONS

The two main objectives of the present study were: (a) to review and compare the various methods that have been developed to describe the force system behind earth retaining structures under seismic loading; and (b) to provide a probabilistic analysis of the safety of such structures. The latter objective was achieved using the method of redistribution of pressure (Dubrova's method) and by exploring the variability of important material and loading parameters. Safety was measured in terms of the probability of failure of the structure rather than the customary factor of safety. Four possible modes of failure of a retaining wall were considered (i.e., overturning, base sliding, bearing capacity, and overall sliding) and the procedure required for the determination of the probability of failure in each mode was described.

The developed probabilistic approach and the available conventional methods were applied in a case study and the obtained results were compared and discussed. In a parametric study, the effect on the pressure distribution and the safety measure of important material and loading parameters was investigated and the results were presented in a series of charts.

On the basis of the analysis and results obtained in this study, the following conclusions can be drawn:

1. The extended Dubrova method can account for the movement experienced by a retaining wall during an earthquake and, therefore,

it provides a more realistic pressure distribution along the wall.

2. A probabilistic formulation of the safety of retaining walls during earthquakes is an improved approach over conventional methods of analysis as it can account for important material and loading uncertainties.

3. The value of the ϕ-parameter of soil strength and the magnitude of the ground acceleration have an important effect on the pressure distribution and the factor of safety of the retaining walls located in an earthquake environment.

CHAPTER 9

REFERENCES

1. A-Grivas, D. (1977), "Probability Theory and Reliability Analysis in Geotechnical Engineering," Proceedings of a special conference, Rensselaer Polytechnic Institute, Troy, NY.

2. A-Grivas, D. (1978), "Seismic Analysis of Slopes in the Northeast U.S.A.," VI Symposium on Earthquake Engineering, University of Roorkee, India, Vol. 1, pp. 157-161.

3. A-Grivas, D. (1978), "Reliability of Retaining Structures During Earthquakes," VI Symposium on Earthquake Engineering, University of Roorkee, India, Vol. 1, pp. 265-269.

4. A-Grivas, D. (1979), "Reliability Analysis of Retaining Structures," Proceedings of 2rd International Conference on Application of Statistics and Probability in Soil and Structural Engineering, Sydney, Australia, pp. 632-641.

5. A-Grivas, D. and Harrop-Williams, K. (1979), "Joint Distribution of the Components of Soil Strength," Proceedings of 3rd International Conference on Application of Statistics and Probability in Soil and STructural Engineering, Sydney, Australia, pp. 189-197.

6. A-Grivas, D., Howland, J.D., and Tolcser, F.P. (1979), "A Probabilistic Model for Seismic Slope Stability Analysis," Report No. CE-78-5, Department of Civil Engineering, Rensselaer Polytechnic Institute, Troy, N.Y.

7. ATC 3-06 (1978), Tentative Provisions for the Development of Seismic Regulations for Buildings, NSF Publication 78-8.

8. Cornell, A.C. (1968), "Engineering Seismic Risk Analysis," Bulletin of the Seismilogical Society of America, Vol. 58, No. 5, pp. 1583-1606.

9. Coulomb, A.A. (1976), "Essaie sur une Application des Regles de Maximis et Minimis ā Quelques Problemes de Statique Relatif on L'Architecture," Mem. Acad. Roy. Pres. Divers Savanats, Vol. 7, Paris, France.

10. Donovan, N.C. and Valera, J.E. (1973), "Incorporation of Uncertainties In the Seismic Response of Soils," Proceedings of 5th World Conference on EQ. Engineering, Rome, Vol. 1, pp. 370-375.

11. Dubrova, G.A. (1963), Interaction of Soil and Structures, Izd. "Rechnoy Transport," Moscow.

12. Franklin, A.G., and Chang, F.K. (1977), "Earthquake Resistance of Earth and Rock-Fill Dams." Report 5: Permanent Displacement of Earth Embankments by Newmark Sliding Block Analysis," Miscellaneous Paper S-71-17, Soils and Pavements Laboratory, U.S. Army Engineer Waterways Experiment Station, Vicksburg.

13. Freudenthal, A.M. (1956), "Safety and the Probability of Structural Failure," Transactions, ASCE, Vol. 121, pp. 1337-1375.

14. Harr, M.E. (1966), Foundations of Theoretical Soil Mechanics, McGraw-Hill Book Company, N.Y.

15. Harr, M.E. (1977), Mechanics of Particulate Media - A Probabilistic Approach, McGraw-Hill Book Company, N.Y.

16. Harrop-Williams, K. (1980), "Reliability of Geotechnical Systems", Ph.D. Dissertation, Department of Civil Engineering, Rensselaer Polytechnic Institute, Troy, N.Y.

17. Höeg, K. and Murarka, R. (1974), "Probabilistic Analysis and Design of a Retaining Wall," Journal of Geotechnical Engineering Division, ASCE, GT 3, March, pp. 349-366.

18. Howland, J.D. (1981), "A Simplified Procedure for Reliability Analysis in Geotechnical Engineering," Ph.D. Dissertation, Department of Civil Engineering, Rensselaer Polytechnic Institute, Troy, N.Y.

19. Ishii, Y., Arai, H. and Tsuchiba, H. (1960), "Material Earth Pressure in an Earthquake," Proceedings of 2nd World Conference on Earthquake Engineering, Tokyo, Japan, Vol. 1, pp. 165-181.

20. Kapila, J.P. (1962), "Earthquake Resistant Design of Retaining Walls," 2nd Earthquake Symposium University of Roorkee, Roorkee, India, pp. 97-107.

21. Lambe, T.W. and Whitman, R.V. (1969), Soil Mechanics, John Wiley and Sons Book Company, N.Y.

22. Lumb. P. (1970), "Safety Factors and Probability Distribution of Soil Strength", Canadian Geot. Journal, Vol. 7, No. 3, pp. 225-242.

23. McGuffey, V., Iori, J., Kyfor, Z. and A-Grivas, D. (1981), "The Use of Point Estimate for Probability Moments in Geotechnical Engineering," Transportation Research Record 809, "Frost Action and Risk Assessment in Soil Mechanics."

24. McGuire, R.K. (1978), "Seismic Ground Motion Parameter Relations," Journal of the Geotechnical Division, ASCE, Vol. 104, No. GT4, April, pp. 481-490.

25. Meem, J.C. (1910), "Pressure Resistance and Stability of Earth," Transactions of American Society of Civil Engineers, New York, 70, pp. 352-411.

26. Meyerhof, G.G. (1953), "The Bearing Capacity of Foundation under Eccentric and Inclined Loads," Proceedings of 3rd International Conference on Soil Mechanics and Foundation Engineering, Zürich, Vol. 1.

27. Mononobe, N. (1929), "Earthquake-Proof Construction of Masonry Dams," Proceedings of World Engineering Conference, Vol. 9, p. 275.

28. Newmark, N.M. and Hall, W.J. (1969), "Seismic Design Criteria for Nuclear Reactor Facilities," Proceedings of 4th World Conference on Earthquake Engineering, Santiago, Chile, Vol. 2, pp. B-4-37-B4-50.

29. Ohde, J. (1938), Zur Theorie des Erddruckes unter besonderer Berucksichtigung der Erddruchverteilung, Bautechnik, 16, pp. 150-159, 176-180, 241-245, 331-335, 480-487, 570-571, 753 and 761.

30. Okabe, S. (1926), "General Theory of Earth Pressure," Journal of Japanese Society of Civil Engineers, Vol. 12, No. 1.

31. Prakash, S. and Basavanna, B.M. (1969), "Earth Pressure Distribution Behind Retaining Walls During Earthquakes," Proceedings of 4th World Conference on Earthquake Engineering, Santiago, Chile, Vol. A.5, pp. 133-148.

32. Richards, R.M. and Elms, D.G. (1979), "Seismic Behavior of Gravity Retaining Walls," Journal of Geot. Eng. Division, ASCE, GT4, April, pp. 349-366.

33. Rosenblueth, E. (1975), "Point Estimates for Probability Moments," Proceedings of Nat. Acad. Sci., U.S.A., Vol. 72, No. 10, October, pp. 3812-3814.

34. Saran, S. and Prakash, S. (1977), "Effect of Wall Movement on Lateral Earth Pressure," 6th World Conference on Earthquake Engineering, India, pp. 2371-2372.

35. Scott, J.D., Wilson, N.E. and Bauer, G.E. (1972), "Analysis and Performance of a Braced Cut in Sand with Large Deformations," Canadian Geotechnical Journal, Vol. 9, pp. 384-406.

36. Seed, H.B. (1969), "Dynamic Lateral Pressures on Retaining Structures," Lecture presented at University of California, Berkeley.

37. Seed, H.B. and Whitman, R.V. (1970), "Design of Earth Retaining Structures for Dynamic Loads," Proceedings, Special Conference on Lateral Stresses and Earth-Retaining Structures, Cornell University, pp. 103-147.

38. Tang, W.H., Yuceman, M.S. and Ang, A.H-S. (1971), "Reliability Analysis and Design of Braced Excavations," Proceedings of 1st International Conference, Applic. of Stat. and Probab. in Soil and Struct. Engin., Hong Kong, pp. 187-202.

39. Terzaghi, K. (1936), "Distribution of the Lateral Pressure of and on the Timbering of Cuts," Proceedings of 1st International Conference on Soil Mechanics.

40. Terzaghi, K. (1936), "A Fundamental Fallacy in Earth Pressure Computations," Journal of Boston Society of Civil Engieers, April pp. 78-79.

41. Terzaghi, K. (1941), "General Wedge Theory of Earth Pressure," Transactions of American Society of Civil Engineers paper No. 20099, 106, pp. 68-97.

42. Terzaghi, K. (1943), Theoretical Soil Mechanics, John Wiley and Sons Book Company, N.Y.

43. Tong, W.H. (1975), "Seismic Risk Analysis for Two-Sites Case," SDDA Report No. 18, Department of Civil Engineering, Massachusetts Institute of Technology.

44. Tschebotarioff, G.P. (1951), Soil Mechanics, Foundations and Earth Structures, McGraw-Hill Book Company, N.Y.

45. Vanmarcke, E. (1977), "Reliability of Earth Slopes," Journal of Geot. Engin. Div. ASCE, Vol. 103, GT 11, November, pp. 1247- 1266.

46. Wu, T.H. and Kraft, L.M. (1970), "Safety Analysis of Slopes," Journal of Soil Mech. and Found. Engin., Div., ASCE, pp. 609-630.

APPENDICES

APPENDIX A

EXPRESSION FOR THE PRESSURE DISTRIBUTION USED IN PARAMETRIC STUDY

The expression for the active force on a retaining wall is given in Eqn. (2-25) as

$$P_A = \frac{\gamma z^2(1+a_v)\cos^2(\psi-\lambda_1-\beta)}{2\cos\lambda_1\cos^2\beta\cos(\delta+\beta+\lambda_1)}\left[\frac{1}{1+\left\{\frac{\sin(\psi+\delta)\sin(\psi-i-\lambda_1)}{\cos(\beta-i)\cos(\delta+\beta+\lambda_1)}\right\}^{1/2}}\right] \quad \text{(A-1)}$$

in which,

i = inclination of backfill,

β = angle between the back side of the wall and the vertical direction,

γ = unit weight of the soil,

$\lambda_1 = \tan^{-1}\left(\frac{a_h}{1+a_v}\right)$,

a_h = maximum horizontal ground acceleration in g's,

a_v = maximum vertical ground accelerations in g's,

ψ = amount of strength mobilized as a result of the movement experienced by the wall during loading,

δ = angle of wall-soil friction.

Forming the derivative of Eqn. (A-1) with respect to depth z, one has that the expression of the pressure distribution $p_A(z)$ is equal to

$$p_A(z) = \frac{dP_A}{dz} = 2D\ C\ E_1\ z + D\ E_1\ z^2\ \frac{dC}{dz} + D\ C\ z^2\ \frac{dE_1}{dz} \qquad \text{(A-2)}$$

in which,

$$C = \cos^2(\psi-\lambda_1-\beta)$$

$$D = \frac{\gamma(1 + a_v)}{2\cos\lambda_1\cos^2\beta\cos(\delta+\beta+\lambda_1)}$$

$$D_1 = \cos(\delta+\beta+\lambda_1)$$

$$E = \frac{\sin(\psi+\delta)\sin(\psi-i-\lambda_1)}{\cos(\beta-i)\cos(\delta+\beta+\lambda_1)}$$

$$E_1 = \left(\frac{1}{1 + (E)^{1/2}}\right)^2$$

$$E_2 = \sin(\psi+\delta)$$

$$E_3 = \sin(\psi-i-\lambda_1)$$

$$\frac{dc}{dz} = 2\ \cos(\psi-\lambda_1-\beta)\ \sin(\psi-\lambda_1-\beta)\ \frac{d\psi}{dz}$$

$$\frac{dE_1}{dz} = -\frac{1}{[1 + (E)^{1/2}]^3}\ E^{-1/2}\ \frac{dE}{dz}$$

$$\frac{dE}{dz} = \frac{1}{D_1}\left(E_3\ \frac{dE_2}{dz} + E_2\ \frac{dE_3}{dz}\right) - \frac{E_2E_3}{D_1^{\,2}}\ \frac{dD_1}{dz}$$

$$\frac{dE_2}{dz} = \cos(\psi+\delta)\ \frac{d(\psi+\delta)}{dz}$$

$$\frac{dE_3}{dz} = \cos(\psi - i - \lambda_1)\,\frac{d\psi}{dz}$$

$$\frac{dD_1}{dz} = -\sin(\delta + \beta + \lambda_1)\,\frac{d\delta}{dz}$$

APPENDIX B

FACTOR OF SAFETY OF A WALL

IN OVERTURNING AROUND ITS TOP

The expression for the factor of safety in overturning FS_o may be obtained using Eqn. (5-1); i.e.,

$$FS_o = \frac{C}{D} \tag{B-1}$$

in which,

C = moment of resisting forces around center of rotation, and

D = moment of driving forces around same point.

For the given wall geometry, one has that the capacity C and demand D for a rotation around point 0 (Fig. 6.1) are equal to

$$\begin{aligned} C &= (1 + a_v)\, W_w\, \ell_1 + T \\ D &= P_A\, y_A + a_h\, W_w\, h_1 \end{aligned} \tag{B-2}$$

in which,

$$T = [(1 + a_v)\, W_w + P_A \sin(\delta+\beta)]\tan\phi$$

Combining Eqns. (B-1) and (B-2), the expression for FS_o is found as

$$FS_o = \frac{(1 + a_v)W_w\, \ell_1 + [1 + a_v)W_w + P_A \sin(\delta+\beta)]\tan\phi}{P_A y_A + a_h\, W_w\, h_1}$$